2014

Determination of the factors that affect the gas-phase reactivity of metal-centered cyclopropanation catalysts and examination of the properties of their reaction products

Jamal Aldajaei
Virginia Commonwealth University

College of Humanities and Sciences

Virginia Commonwealth University

This is to certify that the Dissertation prepared by Jamal Talaat Musa Aldajani Aldajaei entitled "Determination of the factors that affect the gas-phase reactivity of metal-centered cyclopropanation catalysts and examination of the properties of their reaction products" has been approved by his committee as satisfactory completion of the dissertation requirement for the degree of Doctor of Philosophy

Dr. Scott Gronert, Research Director, College of Humanities and Science

_____

Dr. Suzanne Ruder, Committee Chairman, College of Humanities and Science

_____

Dr. James Terner, Committee Member, College of Humanities and Science

_____

Dr. Hani M. El-Kaderi, Committee Member, College of Humanities and Science

_____

Dr. Stephen S. Fong, Committee Member, College of Chemical and Life Science Engineering

_____

Dr. Scott Gronert, Department Chairman, College of Humanities and Science

_____

Dr. Jim Coleman, Dean, College of Humanities and Science

_____

Dr. Douglas F. Boudinot, Dean of Graduate Studies

_____

Determination of the factors that affect the gas-phase reactivity of metal-centered cyclopropanation catalysts and examination of the properties of their reaction products

A dissertation submitted in partial fulfillment of the requirements for the degree of Doctor of Philosophy at Virginia Commonwealth University

By

Jamal Talaat Musa Aldajani Aldajaei

B.S., Basrah University

Basrah, Iraq

Jan, 1983

Director: Dr. Scott Gronert

Professor Department of Chemistry

Virginia Commonwealth University

Richmond, Virginia

May 2014

Seek knowledge from the cradle to the grave

Muhammad (Peace be upon him)

Prophet of Islam

DEDICATION

This dissertation is dedicated to my late parents' souls; my son, Ali; my daughter, Manar; and to the woman who has always supported me throughout all the hardships, and has shared my happiness, my wonderfully loving wife Kifah. I would like to thank all of them for their encouragement and support at every stage of my life and for supporting my decision to attend graduate school. All my life they have made sacrifices to ensure I was given every opportunity to succeed, and they have celebrated my accomplishments with me.

Also I would like to thank my adviser Dr. Scott Gronert for his support and continued motivation, which has helped me achieve my dreams. You have done everything you could to make this journey easier.

Acknowledgments

I would like to thank my advisor, Dr. Scott Gronert, for his assistance and support during my graduate research. I am especially grateful that he took the time to listen to many research ideas, no matter how far off course they might have taken me. His dedication in the field of gas-phase reaction research is motivational and inspiring to scientists everywhere. Without him, this endeavor would not have been possible.

I would like to thank the members of my committee: Dr. Suzanne Ruder, Dr. Hani El-Kaderi, Dr. James Terner, and Dr. Stephen S. Fong, for their continued support and helpful insights in guiding me along in my research hardships. I would also like to express my sincere heartfelt gratitude to Dr. David Simpson for his support and friendship.

A very special thank you is needed for the entire office staff, especially Monica Atkinson.

Thanks to Dr. Maryanne M. Collinson for her support, and her help towards my acceptance to graduate school.

I gratefully acknowledge my parents late souls. I would also like to thank my son, Ali, and my daughter, Manar, for their support.

Last, but definitely not least, I would like to thank my sweetheart, my wife, Kifah, and as I told her before:

The life without wife like fifty without five

Table of Contents

Chapter 3 Determine the factors that affect the gas-phase reactivity of porphyrin-based cyclopropanation catalysts with diazo reagents and examine the fragmentation behavior of the reaction products

Chapter 4 Determine the factors that affect the gas-phase reactivity of copper bis-oxazoloine-based cyclopropanation catalysts with diazo reagents and examine the fragmentation behavior of the reaction products

Chapter 5 Gas-phase synthesis of copper 1, 10-phenanthroline carbene complexes and evaluation of their structure and reactivity

List of Tables

List of Figures

List of Schemes

Abstract

Determination of the factors that affect the gas-phase reactivity of metal-centered cyclopropanation catalysts and examination of the properties of their reaction products

By

Jamal Talaat Musa Aldajani Aldajaei, Ph.D.

A dissertation submitted in partial fulfillment of the requirements for the degree of Doctor of Philosophy at Virginia Commonwealth University

Virginia Commonwealth University, 2014

Director: Dr. Scott Gronert

Professor Department of Chemistry

Gas phase studies of organometallic systems have provided deep insight into reaction mechanisms and reaction intermediates. In this thesis, several metal/ligand systems were

examined in an effort to form metal carbenes in the gas phase. With cobalt and iron porphyrins, the carbene undergoes metal-ligand insertion. With copper bis-oxazolines, metal carbenes tend to undergo metal-ligand insertion and a Wolff rearrangement. To avoid insertions, we turned to a rigid ligand, 1, 10-phenanthroline. Under ESI conditions, a copper (I) complex with phenanthroline can be formed. When treated with diazoacetate esters, the dominant product results from addition with loss of nitrogen followed by loss of CO. This appears to be the result of a Wolff rearrangement of the metal carbene to give a metal ketene complex that spontaneously loses CO. There is no evidence of any stable metal carbenes in this reaction system. Trimethylsilyldiazomethane was also used as a carbene precursor, and its reaction with the copper phenanthroline complex gives addition with loss of nitrogen; but the product exhibits no carbene reactivity with alkenes. Here computational modeling suggests that the metal carbene undergoes a 1, 2 methyl migration, giving an exceptionally stable sila-alkene complex with the copper. As an alternative path to a metal carbene, we have used ESI to form a complex between the copper (I) phenanthroline and betaine (N, N, N-trimethylglycine). Under CID, this complex wills decarboxylates to give a copper ylide complex. Further CID leads to loss of trimethylamine and the formation of a complex between methylene and the copper phenanthroline. Depending on the CID conditions, two isobaric products are formed. One exhibits no carbene reactivity and the other readily gives carbene behavior with alkenes. The former is likely a metal-ligand insertion product, and the latter is the true metal carbene species. We explored the reactions of the carbene with electron-rich alkenes, such as ethyl vinyl ether and 3, 4-dihydro-2H-pyran, and electron-deficient alkenes, such as trichloroethylene.

Abbreviation

CID ..... Collision Introduced Dissociation

rf .....Radio frequency

m/z ..... Mass/Charge

MS ..... Mass Spectrometer

ESI ..... Electrospray Ionization

EI ..... Electron Ionization

CI ..... Chemical Ionization

ESI-MS ..... Electrospray Ionization- Mass Spectrometer

MALDI ..... Matrix-Assisted Laser Desorption Ionization

CAD ..... Collision Activation Dissociation

IMR ..... Ion-Molecule Reaction

QIT ..... Quadrupole Ion Traps

3D ..... Three Dimensions

MS/MS ..... Mass Spectrometer/ Mass Spectrometer

R- ..... Substituent

Cp- ..... Cyclopentadienyl Group (C_5H_5)

$M=CR_2$ ..... Matel Carbene

LCQ ..... Liquid Chromatography Quadrupole

M ..... Metal

Et ..... Ethyl

tBu ..... *ter*-butyl

Std.dev ..... Standard deviation

Ph ..... Phenyl

Bz ..... Benzyl

ipr ..... Isopropyl

EWG ..... Electron-Withdrawing Group

cc/molecule/sec ..... $cm^3\ molecule^{-1}\ sec^{-1}$

QIT ..... Quadrupole Ion Trap

DFT ..... Density Functional Theory

EDA ..... Ethyl Diazo-Acetate

L_nM ..... Transition Metal Catalyst

Chapter 1- Carbenes and Metal carbenes

1-1 Carbene

Carbenes (R_2C:) are reactive 6-electron, divalent carbon fragments with two non-bonding electrons. Carbenes are generated thermally or photochemically. Carbenes are present in two electronic configurations, triplet and singlet. A singlet carbene has electrophilic and nucleophilic character with two non-bonding electrons in one orbital with anti-parallel spins. A triplet carbene has radical-like character with two non-bonding electrons with parallel spins in different orbitals (Figure 1).

Singlet carbene

Carbene center sp^2-hybridized

Triplet carbene

Carbene center sp^2- hybridized

Figure 1: Triplet and singlet carbenes.

The R-substituents have a deep effect on the electronics of carbenes and their reactions. R-substituents with electron donating properties will stabilize the carbenes and become less reactive than the carbenes with R-substituents with electron withdrawing properties, because

carbenes are 6-electron species and are electron deficient. Singlet carbenes react by concerted mechanisms, whereas triplet carbenes react via step-wise; radical pathways.

1-2 Metal carbene

The most famous carbene precursors are diazo-compounds. The diazo-compounds react with transition metals by two mechanistic steps, (see Figure 2) forming metal carbenes with the loss of N_2[1].

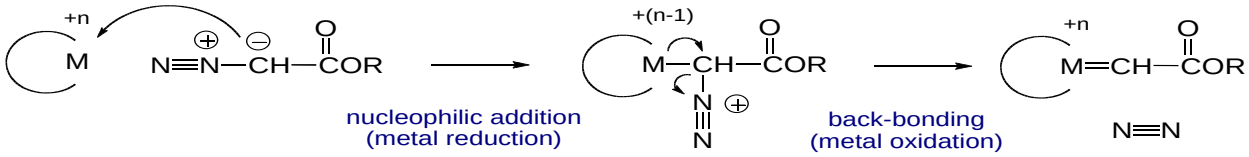

Figure 2: General mechanism to form metal carbene

Metal carbenes are organometallic compounds ($M=CR_2$) that are described as having a double bond between the carbon and the transition metal. Carbenes are an unstable species, but by forming a metal carbene, ($L_nM=CR_2$) they can become stable. Carbenoids ($M=CR_2$) react like carbenes but they are not a true divalent carbon species. Carbenoids are molecules in which all carbons are tetravalent but still have properties resembling those of a carbenes. The first transition-metal carbene complex was isolated by Fischer in 1964, $[(CO)_5 W=C(OR)(R)]$,[2-6]and it was later known as a Fischer carbene. In 1975, Schrock prepared a carbene with very different electronic states [Bis (cyclopentadienyl) methyl methylene tantalum],[7] and it was later known as the Schrock carbene. Each type of carbene has different properties such as: The Schrock carbine which occurs with early transition metals with a high oxidation state, the carbene carbon is

nucleophilic, and it has non π-acceptor ligands (Cp, alkyl), and non π-donor substituents (R=H, alkyl). The Fischer carbene is found with late and middle transition metals with low oxidation states, the carbene carbon is electrophilic, and it has π-electron acceptor metal ligands such as (CO), and π-donor substituents such as (R= -OR). In Fischer metal carbenes there is lone pair donation from carbon to the empty orbital in the transition metal and back donation from the non- bonding orbital of the transition metal to the empty orbital of the carbon. In the Schrock carbene, there are two (covalent) bonds formed (Figure 3-A). Fischer and Schrock carbenes can be described by the resonance forms in Figure 3B.

3-A Carbenoids

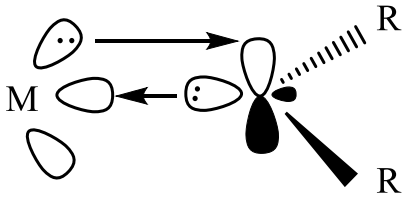

Fischer-type (electrophilic)

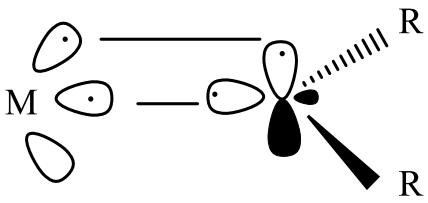

Schrock-type (nucleophilic)

3-B Resonance structures

$$L_nM\text{-}CR_2 \longleftrightarrow L_nM{=}CR_2 \longleftrightarrow L_nM\text{-}CR_2$$

Figure 3: Fischer and Schrock carbenes.

Carbenoids reactivity depends on the transition metals properties and the R-substituents at the carbon carbene. Fischer-type carbenes are found with low oxidation states, middle and late transition metal centers, and with π-donor R-substituents on the carbene carbon; there is electron donation from the full carbene carbon p-orbital to the metal empty orbital, and there is electron back donation from the metal full d-orbital to the empty p-orbital at the carbene carbon. The carbon tends to be positively charged (see Figure 3A, B left side). Schrock type carbenes are found with high oxidation states, early transition metal centers, and with hydrogen and electron donating R-substituents on the carbene carbon. Two covalent bonds are formed due to the triplet state of the carbine; each bond polarized toward the carbene carbon giving it a negative charge (see Figure 3A, B right side).

1-3 Applications of metal carbenes

Metal carbenes are useful synthetic intermediates. Two key reactions involving metal carbenes are C-H insertions and cyclopronanations (see Figure 4).

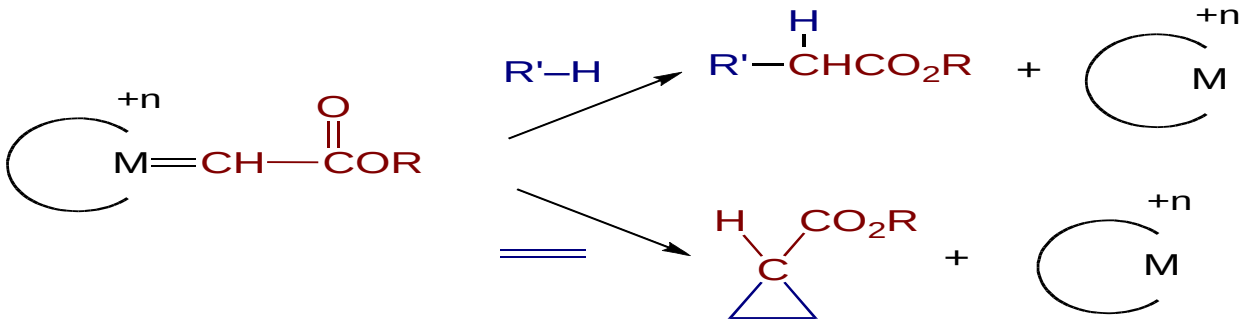

Figure 4: Applications of Metal Carbenes

1-4 Metal carbene insertion in to olefins

This thesis focuses on the development of metal-centered catalysts to yield cyclopropanation from the reaction of the metal carbene with olefins. We have completed extensive screening of the reaction pathways of transition metal carbene intermediates and their interactions with alkenes in the gas phase. I will first review some condensed phase chemistry of metal carbenes.

In 1862, Anton Geuther investigated dichlorocarbene as a reactive intermediate.[8] Doering introduced carbenes to organic chemistry by inserting carbenes into olefins forming cyclopropanes.[9]Organometallic carbene chemistry was begun by Fischer and Maasbol in 1964, when they succeeded in synthesizing a $(CO)_5$ W=C (Ph)(OMe) complex.[10,11] The first cyclopropanation metal (chromium) carbene process was described by Dötz and Fischer.[12-14] In the 1970s, Schrock prepared many tantalum carbene complexes such as $(Np)_3$ Ta=CH (CMe_3) and $(\eta^5$ - Cp$)_2$ MeTa=CH_2.[15,16]

Doyle studied the selectivity in cyclopropanation formation by the carbenoid addition to the olefin using a copper catalyst and EDA as carbene source[17] as shown below:

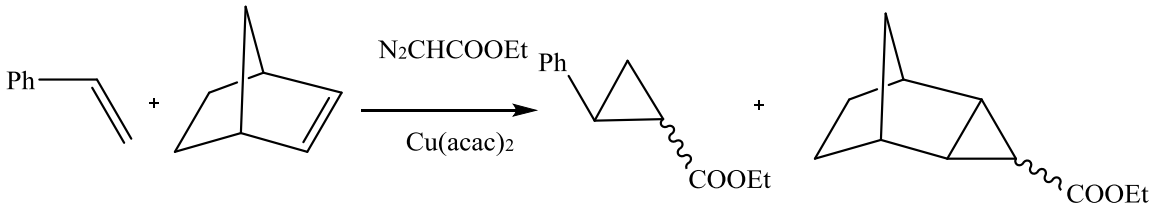

81% 19%

Perez studied cyclopropane formation by using EDA as a carbene precursor and a copper

catalyst. He found that EDA remained in the absence of styrene, but EDA consumption occurs with styrene addition, as described in the equation below.[18]

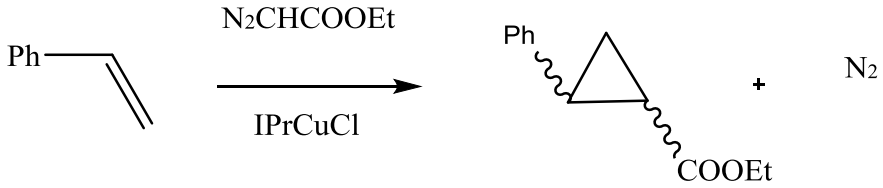

According to the catalytic cycle shown in Figure 5, the first step is the metal carbene formation. The second step is the reaction of the transition metal carbene intermediate with an alkene, reforming the metal catalyst and releasing the cyclopropane species.

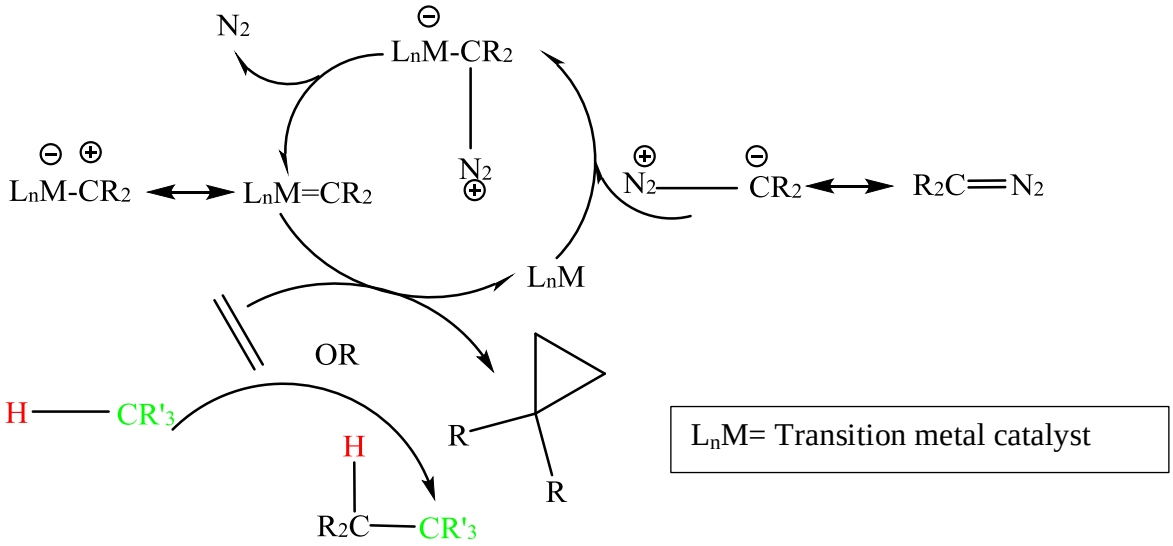

Figure 5: Generic catalytic cycle of metal-catalyzed reactions of diazo-compounds.

The alkene addition mechanism to the metal carbene, [this is the 2nd step in the catalytic cycle (Figure 5)], depends on the alkene electron density; both electron-rich and electron-

deficient alkenes react and produce metal complexes along with cyclopropanes (see Figure 6A-B).[19]

The cyclopropanation mechanism of electron rich alkenes (nucleophilic alkenes) involves an attack at the carbene carbon giving a zwitterion intermediate, which undergoes rearrangement to a cyclopropane (see Figure 6-A).[19]

A reasonable mechanism of cyclopropanation for electron poor alkenes involves coordination of the alkene to the electrophilic metal, and the coordination complex may rearrange to a metal cyclobutane. The cyclic intermediate undergoes a reductive elimination to give cyclopropane species (see Figure 6-B).[19]

6-A: Electron-rich alkene reacts with metal carbene

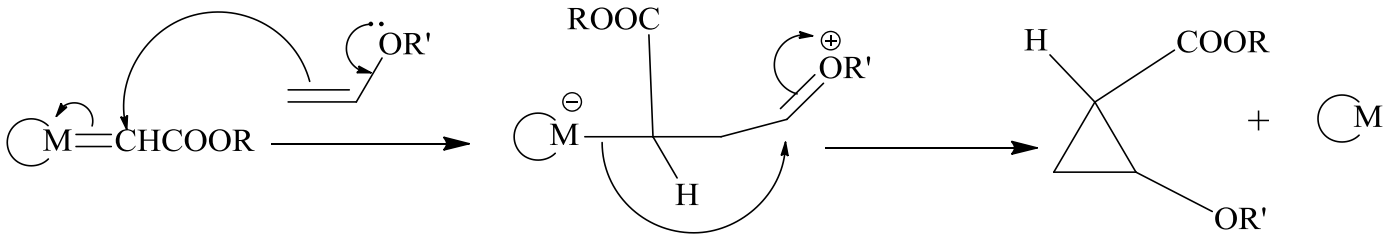

6-B: Alkene with electron-withdrawing group (EWG) reacts with metal carbene

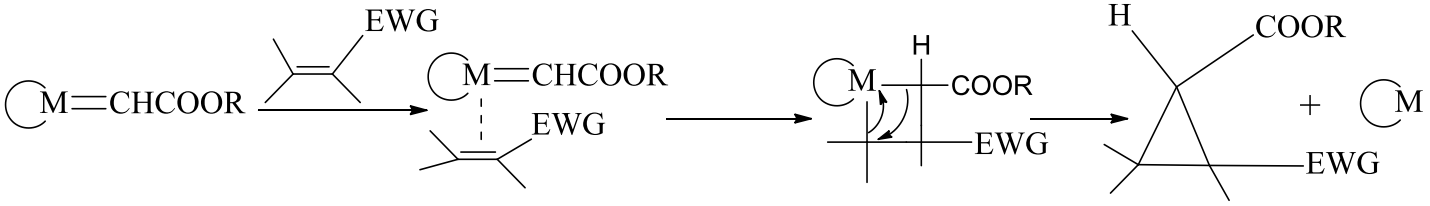

Figure 6: Alkenes addition to the metal carbenoids.

Substituents attached to the diazo compounds affect the reactivity of diazo decomposition.[20] Electron withdrawing groups increase the diazo species stability by delocalization of the π-system, while electron donating groups destabilize the diazo and make it more reactive (see Figure 7).

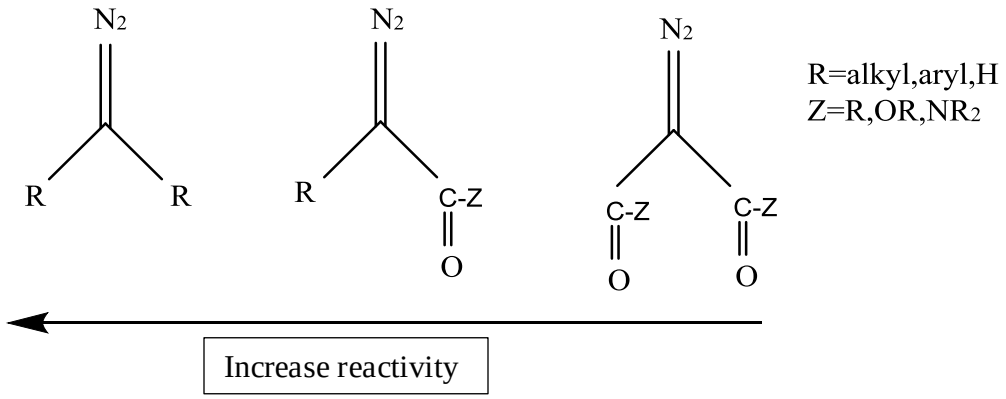

Figure 7: Carbene precursors.

1-5 C-H Insertion

The mechanism is not well understood. Two possible path way mechanisms have been suggested. Davies[21] suggests a concerted mechanism while, Pirrung[22] suggests a stepwise mechanism for dirhodium catalysts (Figure 8A, & 8B).

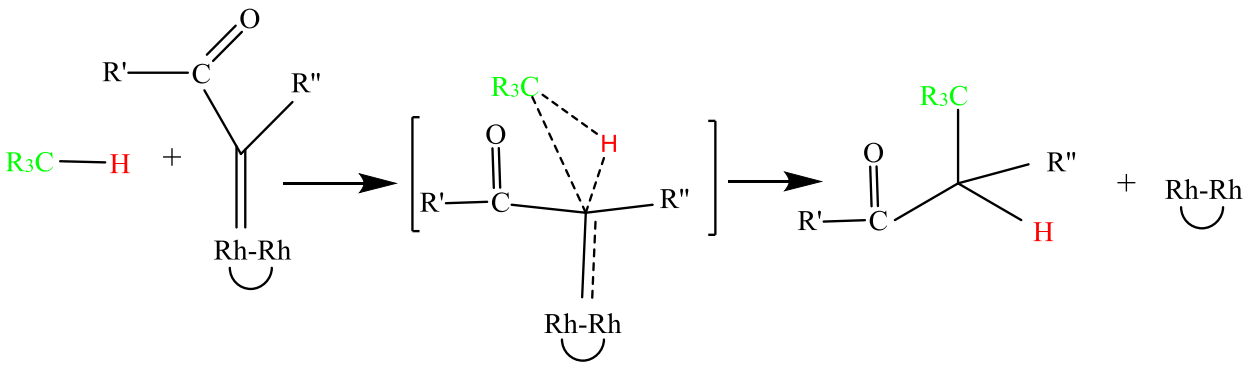

8-A Davie's suggested mechanism.

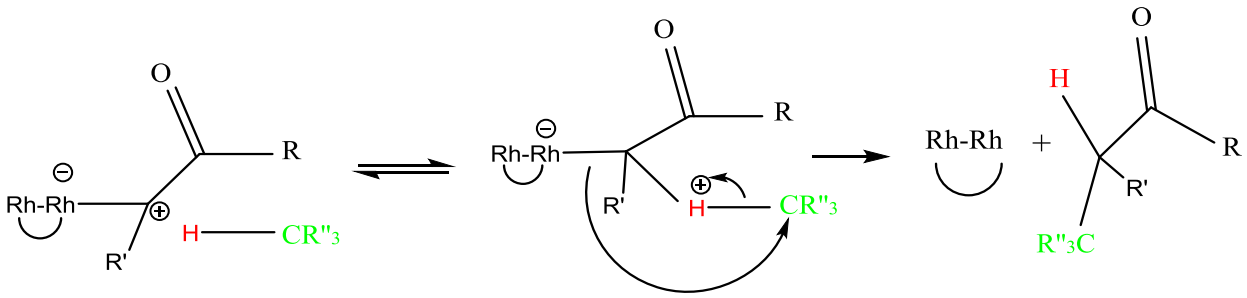

8-B Pirrung's suggested mechanism.

Figure 8: C-H insertion suggested mechanisms.

Transition metal complexes react with diazo compounds by two steps to form carbenoids $M=CR_2$ (see Figure 2).

With a suitable selection of transition metal salts e.g Cu, Rh, pd….etc and carbenoid precursors; carbenoids can react with alkenes leading to mainly C-H insertion rather than cyclopropanation.

Carbenoids used for C-H insertion can be divided into three groups as described by Davies (Figure 9).[23]

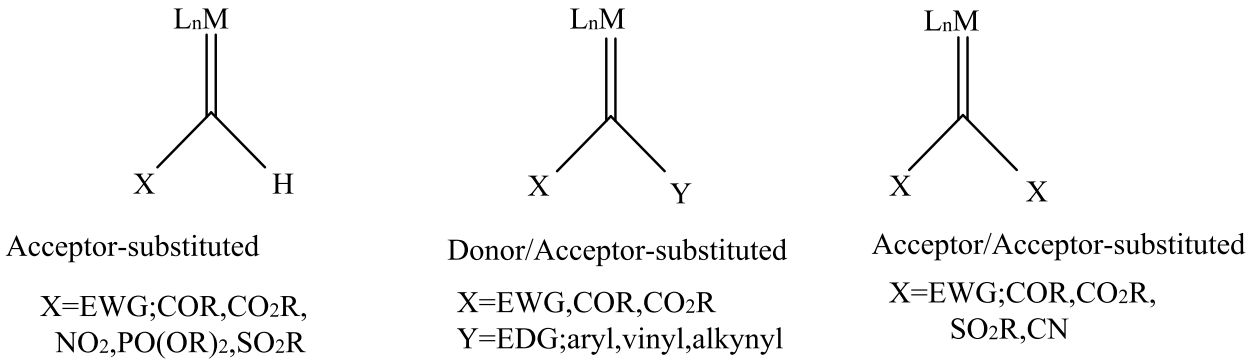

Figure 9: Metal carbenoids.

All three groups go through intermolecular C-H activation pathways. Acceptor-substituted carbenoids were investigated by Davies[24], Doyle[25], and Muller.[26] They used metal catalysts with diazoesters. The donor/acceptor substituted carbenoids was investigated by Davies and the acceptor/acceptor substituted carbenoids was investigated by Muller. Pirrung and his co-workers found that metal complexes with an electron withdrawing group were more reactive toward the C-H insertion.[27] The C-H insertion pathway is favored over the cyclopropanation product by design; a metal complex is allowed to react with specific carbenoid precursors, typically diazo compounds listed in Figure 7, to form the carbenoids represented in Figure 9. The C-H bond for the insertion should be activated by radical stabilizing groups attached to the carbon to decrease the C-H bond strength.

Although C-H insertion pathways is thermodynamically favored over C-C insertion pathways (cyclopropanation). The efficient C-H insertion requires a suitable design of a carbeniod as a Schrock-type carbenoid by choosing an early transition metal with a high oxidation state. Schrock carbenoids tend to react with C-H bonds by radical type mechanisms. In general, carbenoids designed as Schrock-type carbenoids tend to follow C-H insertion pathways while carbenoids designed as Fischer-type carbenoids tend to follow cyclopropanation pathways.

Chapter 2- Mass Spectrometric Studies of Gas-Phase Reactions

2-1 Introduction

In this study we investigated the formation of carbene complexes of four metals (Mn, Fe, Co, and Cu) bearing a variety of polydentate ligands including porphyrins, bis-oxazolines and 1, 10- phenanthroline. Reaction pathways with alkenes leading to the formation of cyclopropanes were also investigated in the gas phase using mass spectrometry as a tool. By isolating and studying the short-lived intermediates, which is very hard to do in the condensed phase, mass spectrometry gives us the opportunity and the ability to understand reaction mechanisms.

Mass spectrometry is an analytical tool used for the identification of molecules and compounds based on a mass-to-charge ratio. It's been proven that mass spectrometers are good instruments for studying the kinetics, mechanisms, product distributions of gas-phase, and bimolecular organic reactions. For example, "*ion chemistry in the condensed phase is often dominated by ion pairing and solvation interactions which can mask the intrinsic reactivity of the reaction partners*. *Moreover, comparison of gas phase and condensed phase data provides a powerful means for understanding the role that solvation and ion pairing play in determining the outcomes of ionic reactions*".[28] In this chapter, we present the advantages of mass spectrometric methodologies to the study of catalytic cycles and their reactive intermediates.

Our mass spectrometer (MS), a Finnigan LCQ Deca quadrupole ion trap mass spectrometer equipped with electrospray ionization (ESI) (see Figure 10), has been modified to allow for the study of ion/molecule reactions in the mass analyzer (see Figure 11). Before

describing the results of the studies, it is very important to introduce a brief description of the technique.

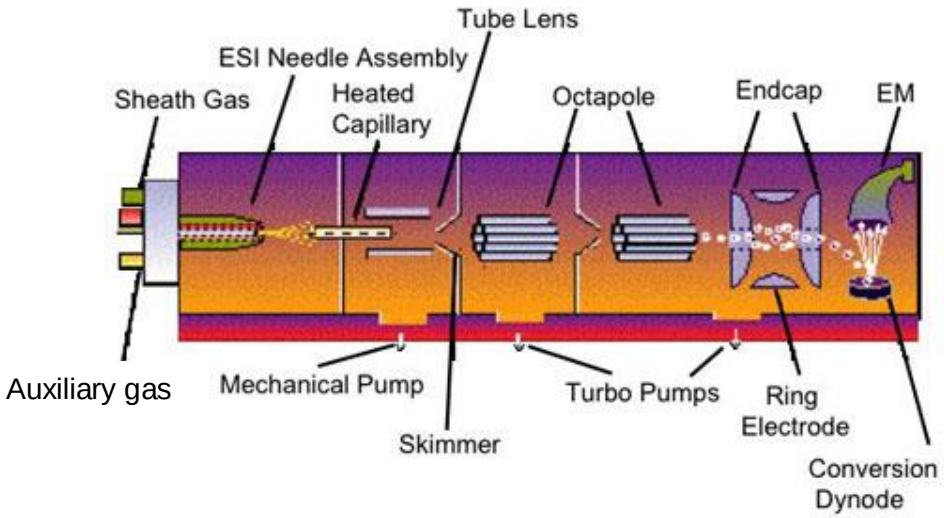

Figure 10: Mass spectrometer.

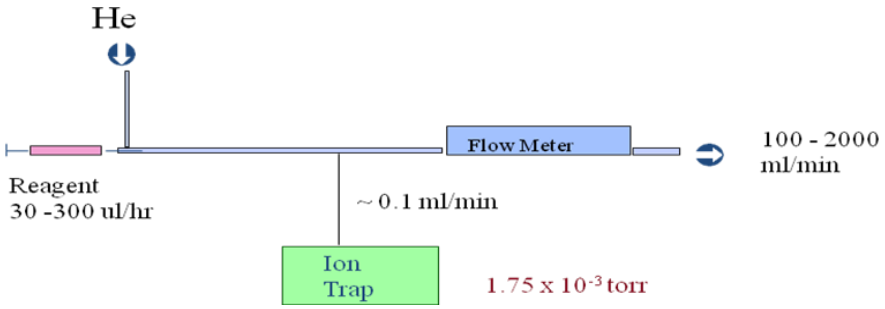

Figure 11: Gas handling manifold.

2-2 Method

Our mass spectrometer, a Finnigan LCQ Deca quadrupole ion trap mass spectrometer equipped with electrospray ionization (ESI), has been modified to allow the study of ion/molecule reactions in the mass analyzer. The LCQ Deca consists of an atmospheric pressure source where ESI is used to

produce gas-phase ions. Ions enter the mass spectrometer through a heated capillary tube and are then transported using an octapole ion guide, to the ion trap mass analyzer. The 3D quadrupole ion trap consists of two end cap electrodes (inlet and outlet), held at a static potential, and a ring electrode to which an rf potential is applied. For obtaining a mass spectrum, the rf amplitude is scanned so that m/z ratios become progressively unstable and are ejected from the ion trap towards the detector.

Fragmentation of a selected ion within the ion trap occurs by a process called collision-induced dissociation (CID), in which the ion of interest is accelerated by an rf field to high kinetic energy and then undergoes multiple collisions with a neutral gas (helium). Part of the energy transferred on collision is converted to internal energy, which leads to bond breakage and hence fragmentation of the selected ion into fragments. In our experiments, the ionic reagent enters through the atmospheric pressure interface while the neutral reagent enters the trap with the helium stream. Ionic precursors are dissolved in methanol (10^{-4}M) and injected into ESI interface at a measured flow rate (3-5 µl/min).

The cation of interest is isolated in the ion trap by the application of a notched waveform. The neutral reagent is introduced into a stream of helium gas, (30-300 µl/hr), via a syringe pump (see Figure 11); this allows fast vaporization at mixing ratios from 100 - 10,000 (He/reagent) which gives a reagent pressure of 10^{-5} - 10^{-7} torr in the ion trap. This reaction condition allows us to measure rate constants from approximately $4 \times 10^{-9} - 1 \times 10^{-12}$ cm^3 $molecule^{-1}$ sec^{-1}. A flow meter is used to establish and maintain the helium flow.

The concentration of the neutral reagent in the ion trap is calculated in the following way: Regularly the mass spectrometer is calibrated against the known rate constant of bromide reacting with iodomethane,[29] obtaining a calibration factor that we use to calculate the actual ion trap pressure according to the equation below:

$$\text{Resulting pressure} = \text{Neutral reagent fraction} \times \frac{\text{Standard pressure of the instrument (torr)}}{\text{Calibration factor}}$$

The neutral reagent fraction is calculated by using the equation below:

$$\text{The neutral reagent fraction} = \frac{\text{Neutral reagent flow rate (mol/min)}}{[\text{He-flow}(\frac{\text{L}}{\text{min}}) / 22.4\text{L (volume of 1 mole He-gas)}]}$$

Neutral reagent flow rate is dependent on the molecular weight, density, and the speed of the syringe pump. The unit's conversion to calculate the actual neutral reagent flow rate is shown below:

$$\text{Neutral reagent flow rate (mol/min)} = \frac{\text{Neutral reagent flow rate (µl/hr)} \times \text{density of neutral reagent g/ml}}{[\text{Neutral reagent m.wt. (g/mol)}/1000(\mu\text{l}/\text{ml})/60(\text{min}/\text{hr})]}$$

Finally, the equation below represents the neutral reagent pressure (torr).

$$\text{The neutral reagent pressure} = \text{Resulting pressure} \times \sqrt{\text{Neutral reagent m.wt./4}}$$

Since we have two species mixed together (the neutral reagent and the He-gas), the mixing ratio must be corrected for differential effusion. Helium atoms effuse faster due to their lower atomic weight than the neutral reagent molecules. They have the same kinetic energy, so the helium must have a higher velocity. So for two molecules:

$$1/2m_1(v_1)^2 = 1/2m_2(v_2)^2$$

where m = mass of the object and v = velocity of the object. Using the mass of helium=4, we get the following equation which accounts for the differential effusion.

$$V_1 / V_2 = \sqrt{\text{Neutral reagent m.wt.}/4}$$

The isolated ion is allowed to react with the neutral reagent for a pre-determined time delay, and a mass spectrum is collected. This time delay allows us to monitor the kinetics of the process. The densities of the ions are extremely small compared to concentrations of the neutral reagents, so we assume the neutral reagent concentration to be constant. This assumption leads us to a pseudo first-order equation. We determine absolute rates by collecting data at three different reagent pressures and monitoring reactions for at least 3 half-lives.

A simple scheme of a mass spectrometer can be drawn as shown in scheme 1:

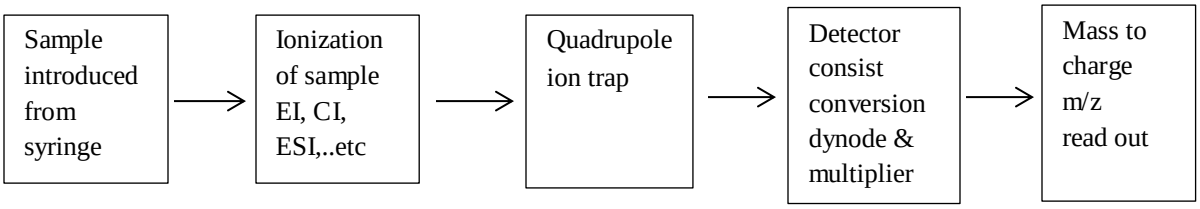

Scheme 1: General scheme of mass spectrometer.

2-3 Why ESI-MS to study organometallic catalysis

ESI-MS is very appropriate to study organometallic catalysis for many reasons:

- We can maintain weak bonding interactions from solution by using a soft technique ESI-MS.

- Only the charged species in the solution can be detected. Common solvents are invisible.
- Rapid analysis.
- Very low concentrations of intermediates can be detected.
- It is easy to get information from complex mixtures, because each charge species in the solution is represented by a single peak in the mass spectrum.

Reactive intermediates can be stable under these conditions and can be probed. Canty, in his study of many palladium and platinum organometallic complexes, used ESI-MS and tandem MS.[30] This general technique has been used to study hydrosilylation,[31] catalytic oxidation,[32-35] hydrogenation[36-38], and C-C bond formation.[39-41] Many authors have used this ESI-MS technique to study organometallic reaction intermediates.[42-44]

2-4 Components of Mass Spectrometry Experiment

2-4-1 Electrospray

In 2002, the Nobel Prize in chemistry was awarded to three recipients. John B. Fenn was one of recipients for his development of the electrospray ionization (ESI) mass spectrometry technique. There are many ionization methods, such as electron ionization (EI), chemical ionization (CI), electrospray ionization (ESI), and matrix-assisted laser desorption ionization (MALDI). All are ionization techniques assigned to the domain of the mass spectrometer. In this

thesis, the work is interested with the application of ESI/MS to understand the metal complexes and their reactivity in the gas phase.

Electrospray ionization (ESI) can be used to generate either positive or negative ions. In this thesis, we worked with the positive ion mode. The ESI process is described in many papers.[45-48] In short, at atmospheric pressure, the analyte solution passes through an electrically charged metal capillary. The electric field is used to generate a spray of highly charged droplets. Positive ions accumulate at the surface of the liquid, while the negative ions flow back to the inside of the capillary. When the surface tension of the liquid become less than the repulsion forces between the positive charges at the surface of the liquid, the liquid breaks into a fine spray of droplets. Evaporation of the solvent from the droplets leads to contraction and shrinks the size of the droplets, increasing the charge density at the surface of the droplets. At the Rayleigh limit (when there is no more decreasing in the droplets size), the repulsion force of the like charges becomes more than the surface tension that holds the droplet together. At this point the droplets will pass through a coulombic cleavage to smaller droplets.[28]

2-4-2 Collision induced dissociation (CID)

In 1913, Thomson used an accelerated ion beam deflected by electric and magnetic fields. He noted unusual "fragments" corresponding to the H_2 molecule breaking up into two atoms. In the 1970s, Yost and Enke used a triple quadrupole for MS/MS, the first quadrupole was used to isolate the ion of interest, the second quadrupole was used to fragment the ion and the third quadrupole was used to identify the product.

Collision induced dissociation (CID) is widely used to identify the structural fragmentation reactions in mass spectrometry. Collision induced dissociation (CID) is also known as collision activated dissociation (CAD).[49,50]

The collision between the ion of interest and the target neutral species (He or N_2) is the first step of collision induced dissociation. The ion will be excited due to this collision, which converts some of the translational energy of the ion into internal energy. The excited ion will fragment, as a second step.

2-4-3 Ion-molecule reaction (IMR)

An ion-molecule reaction (IMR) is the reaction between the ion of interest and a neutral reagent.

IMR is a useful method to study the structure of ions and their reactivity in the gas phase, and can be used in conjunction with CID.[51] Ion-molecule reactions (IMR) have been used by my adviser, Dr. Gronert, to study organic chemistry,[52] inorganic chemistry,[53,54] organometallic chemistry,[36,55-57] and hydrogen/ deuterium exchange of biomolecules.[58-61]

2-4-4 Quadrupole Ion traps (QIT)

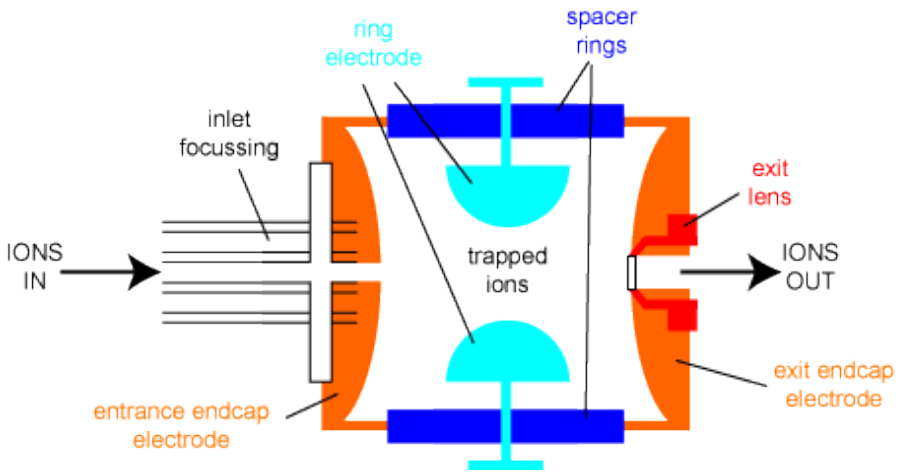

Figure 12: Quadrupole ion trap (source University of Bristol).

Wolfgang Paul developed the foundation for Quadrupole Ion Trap (QIT) mass spectrometry with his Nobel Prize winning work.[62]Sharing the Nobel Prize in Physics in 1989, Wolfgang Paul developed and invented the 3-D quadrupole ion trap.[63] There are many advantages to using a quadrupole ion trap such as: very fast scan speed, high sensitivity, low maintenance costs, robust system, ion/molecule reactions, and tandam mass spectrometry MS/MS, as well as other uses.[64,65]

A 3-D quadrupole ion trap has electrodes enfolded into a circle like a single quadrupole. The figure shows that there are two end-cap electrodes and one ring electrode. The ions enter and exit through the end-cap electrodes. The ions inside the trap will find themselves in a potential well when we apply various voltages between the ring electrode and the two end-caps. A cavity is formed in which ions are trapped (see Figure 12). The ring electrode RF potential, an A.C. potential of constant frequency but variable amplitude, produces a 3-D quadrupolar potential

field within the trap. Altered potentials allow for the manipulation of the ions. Ions are ejected through the exit end-cap electrode to the detector plate and multiplier.

2-4-5 Detection (electron multiplier)

The detection of the ions ejected through the exit end-cap electrode occurs at the detector plate and multiplier. The ions are ejected from the ion trap and hit the high potential conversion dynode to convert ions into electrons. Secondary electrons emitted from the conversion dynode strike the first dynode surface causing an emission of more secondary electrons. Due to the potential differences between the dynodes, the secondary electrons are accelerated continuously as the electrons travel towards the ground potential. The electron cascade is created and the final electron flow affords an electric current.

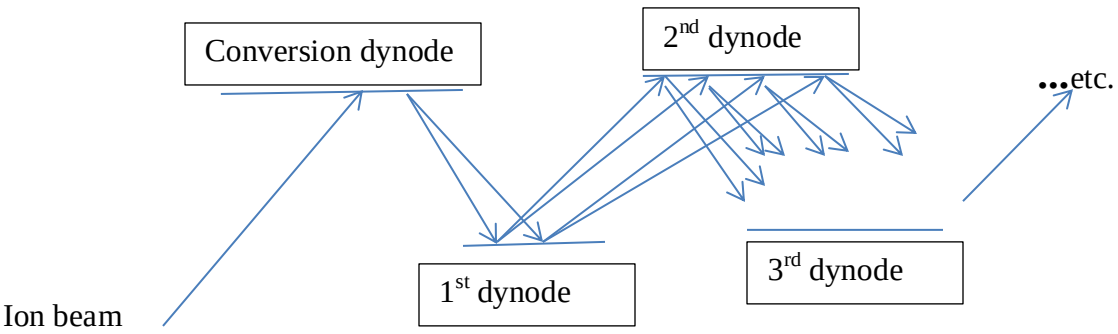

Figure 13: Detector.

Chapter 3- Factors that affect the gas-phase reactivity of porphyrin-based cyclopropanation catalysts with diazo reagents and examine the fragmentation behavior of their reaction products.

3-1 Introduction

Biological processes such as the photosynthesis of plants, bacteria, and the oxygen transport in the cardiovascular systems of humans and animals are based on porphyrins and related macrocycles. It is clearly of ultimate importance to all living beings on our planet. Life as we know it would cease to exist without the porphyrin components in these processes. Thus they have attracted great interest from researchers of varied scientific backgrounds. For many investigators in the past century, porphyrins became the center of their research because of naturally occurring porphyrinoids like chlorophyll, hemes, and coenzyme B_{12}. The present project involves investigations of organometallic porphyrins in areas such as: the effect of the metal center on the kinetics and effectiveness of porphyrin metal carbene formation, the mechanism of porphyrin metal carbene formation, the fragmentation pathways of porphyrins metal carbenes, and the properties of the fragmentation products.

Hans Fischer, known as the godfather of modern porphyrin chemistry, is believed to have published the first monographs concerned with these macrocycles.[66-68] Porphyrin, as shown in

Figure 14, consists of four pyrrole rings connected by methylene units. *Meso*-positions are numbered 5, 10, 15, and 20. The β- Positions are 2, 3, 7, 8, 12, 13, 17, and 18. The rest of the carbon atoms positions are called α- positions (Figure 14). The *meso*-substituted porphyrins are popular to use due to their ease of synthesis and ability for synthetic modification. Tetraphenylporphyrin (TPP) was first synthesised by Rothemund in 1936,[69-71] using benzaldehyde and pyrrole under acidic conditions at high temperatures. Metals can be inserted into the center of the porphyrin system. Metal porphyrins in the condensed phase have been investigated by many scientists. They have used different metals as a core for the porphyrin system, such as cobalt,[72] iron,[73]manganese,[74]and many other metals.

In this chapter, we investigate three metallated porphyrins (Mn, Fe, Co) in the gas phase by using mass spectrometry as a tool to gain a better understanding of the reaction pathways of the metals porphyrins with ethyl diazoacetate and tert-butyl diazoacetate to form metals carbenes. The short lived carbene intermediates, which are very hard to isolate in the condensed phase, will be isolated in the gas phase and their properties will be probed.

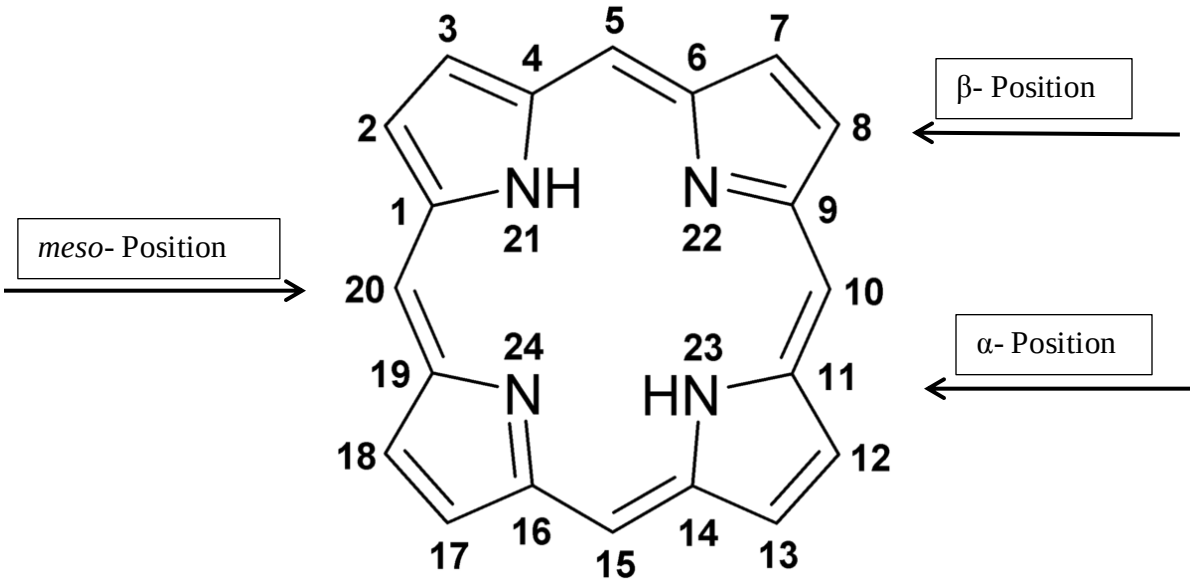

Figure 14: Porphyrin

Our mass spectrometer, a Finnigan LCQ Deca quadrupole ion trap mass spectrometer equipped with electrospray ionization (ESI) (see Figure 10), has been modified to allow the study of ion/molecule reactions in the mass analyzer (see Figure 11).

In the last decade, there have been many studies that employed gas phase techniques to examine the reaction mechanisms of organometallic catalysts. Using an ion trap mass spectrometer, O'Hair and his coworkers have examined each of the steps in a full catalytic cycle for converting methanol to formaldehyde on a vanadium oxide catalyst.[75] There have been several highly relevant studies examining the reactions of metal salen complexes with oxidants related to epoxidation processes. Plattner and co-workers have shown that a variety of ligated and oxidized Mn $(salen)^+$ ions can be produced by electrospray ionization, and the salen can detain ligands in gas-phase reactions.[76] Chen and Chisholm have examined the gas-phase reactivity of propylene oxide/M $(salen)^+$ complexes.[77] Our own group has studied the reactions of Co salens with ethyl diazoacetate and found

that salens react readily in the gas phase to give carbene species, through a mechanism that involves rate-determining addition followed by N_2 expulsion.[78]

Our goal here was to study cyclopropanation processes. Many catalytic studies involving metal carbenes have used diazocarbonyl compounds as the carbene source. We have used diazoacetates as our carbene precursors in these studies. Transition-metal-mediated cyclopropanation using metal carbenes has received attention because the cyclopropane ring can be found in thousands of natural isolated products[79] and many biologically active agents. Cyclopropyl derivatives operate as intermediates in a number of synthetic processes, such as complex molecule synthesis,[80] serve as synthetic building blocks,[81] and are used as a model for the assembly of structurally constrained amino acids and peptides.[82]

3-2 Method

In our experiments, the metal porphyrin cation enters through the atmospheric pressure interface while the diazoacetate compounds (10%) in cyclohexane enter the trap with the helium stream. The metal porphyrin cations are dissolved in methanol (10^{-4}M) and injected through ESI at a measured flow rate (3-5 µl/min). The metal porphyrin cation of interest is isolated in the ion trap by the application of notched waveform. The ethyl and tert-butyl diazoacetate are introduced into a stream of helium gas, (30-300 µl/hr), via a syringe pump (see Figure 11). The isolated metal prophyrin cation is allowed to react with the diazoacetate reagent for a pre-determined time delay, and a mass spectrum is collected (see Figure 11, 15). This time delay allows us to monitor the kinetics of the process. The densities of the ions are extremely small compared to concentrations of the neutral reagents, so we assume the concentration of the neutral reagent to be constant. This assumption leads

us to a pseudo first-order equation. We determine absolute rates by collecting data at three different reagent pressures and monitoring reactions for at least 3 half-lives. Using metal carbene intermediates to react with alkene to form cycpropanation species.

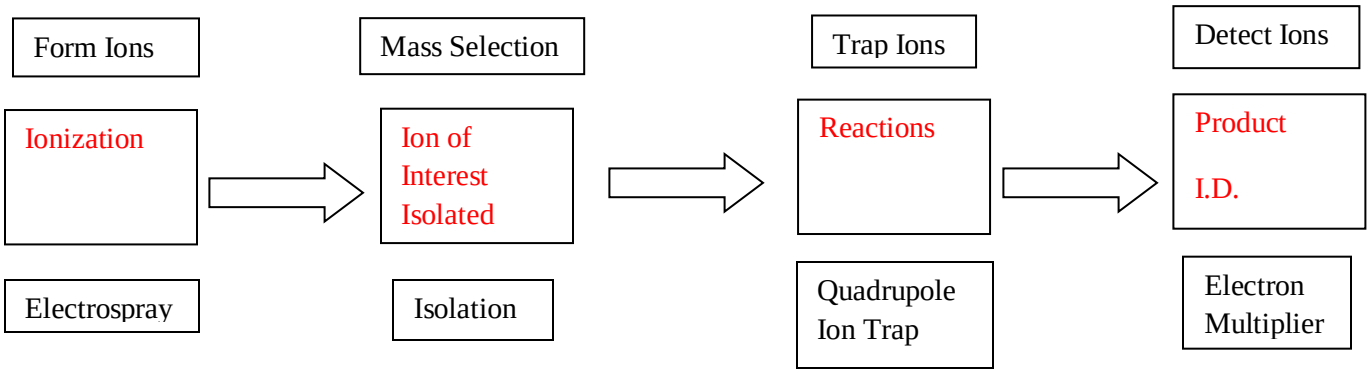

Figure 15: Ion/Molecule Reactions in the LCQ

3-3 Objectives

- Use metals porphyrins as models of cyclopropanation catalysts.
- Examine the reactivity of metal carbenes and their fragmentation products.

3-4 Background

In organic synthesis, ethyl diazoacetate (EDA) has been widely used as carbene sources in metal-mediated cyclopropanation reactions. Many metal porphyrin complexes can catalyze the cyclopropanation of alkenes using EDA. Examples are rhodium pophyrin,[83] cobalt porphyrin,[84] and iron porphyrin.[85,86] Transition metals bearing a wide variety of ligands react with diazoacetates to produce metal carbenes through a two-step reaction. The first step is the addition to the metal, and the second step involves the loss of N_2 (see Figure 16, 2).

Figure 16: Metal carbenes from diazoacetates.

There is mechanistic evidence that suggests a two-step process (see Figure 2). The initial nucleophilic addition is believed to be potentially reversible, followed by N_2 extrusion forming a metal carbene. Depending on the metal, either step could be the rate determining.[87]

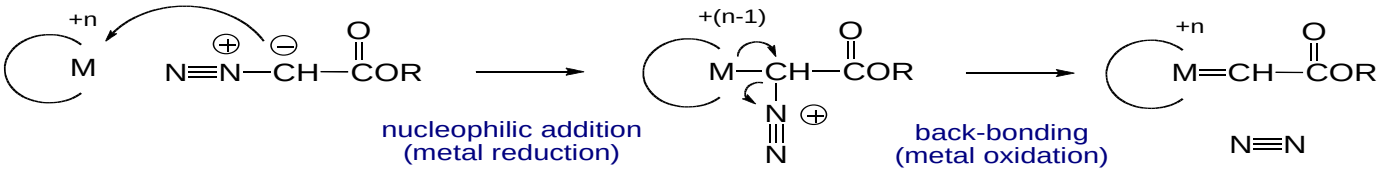

Figure 2: General mechanism to form metal carbene.

Metal carbenes are useful synthetic intermediates. Two key reactions involving metal carbenes are C-H Insertions and cyclopronanations (see Figure 17).

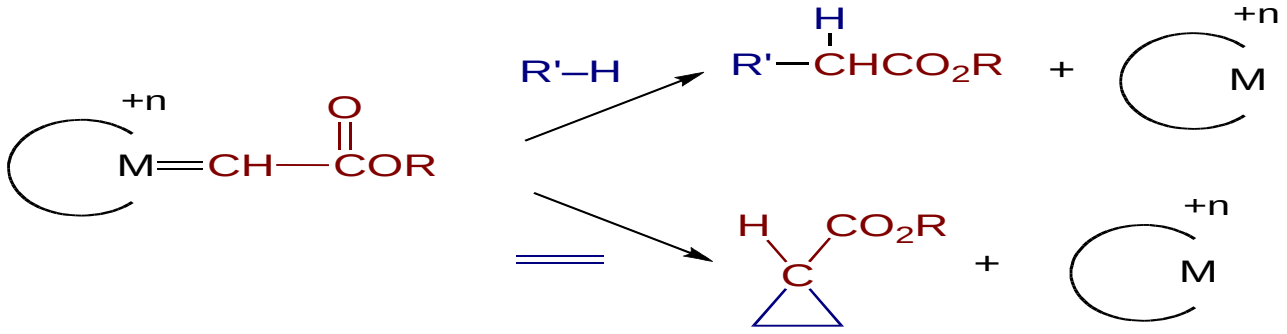

Figure 17: Applications of metal carbenes.

There are two key issues that drive research in this field, (i) the need for efficient catalysis under mild conditions, and (ii) the need for high diastereoselectivity and enantioselectivity (with chiral ligands).

To investigate the chemistry of metal carbenes and their formation, we examined three metal porphyrin systems (see Figure 18). All the metals are in roughly square planar coordination in the +3 oxidation state. The porphyrin ligands are doubly deprotonated. Scheidt and Reed investigated Fe^{+3} porphyrin using density functional theory (DFT) and they found that the quartet spin state, S=3/2, is lower in energy than the other spin states (low-spin S=1/2 doublet and high-spin S=5/2 sextet). They noted that *the nature of those intermediate spin state merits special attention because the pure S=3/2 ground state the [d-orbital population* $(d_{xy})^2 (d_{xz},d_{yz})^2(d_z^2)^1(d_x^2\text{-}d_y^2)^0$*] there is possibility of spin orbital coupling to a nearby S=5/2 state to give a new quantum mechanically admixed-intermediate state.*[88]

Hill and his coworkers established that Mn^{+3}porphyrin is in a quintet state (S=2) with the d-

orbital population $(d_{xy})^1 (d_{xz},d_{yz})^2(d_z^2)^1(d_x^2-d_y^2)^0$.[89] Because there is no spin data for the Co^{+3}porphyrin, we use the Co-corrole system as analogy to the Co^{+3} porphyrin system. Rovira and his coworkers found that the cobalt is in a triplet state (S=1) and they found a Co d-orbital configuration of $(d_{xy})^2 (d_{xz},d_{yz})^2(d_z^2)^2(d_x^2-d_y^2)^0$.[90] Each of the metal complexes in (Figure 18) was allowed to react with either ethyl or t-butyl diazoacetate in the gas phase and the rate constants were determined. Computational work was completed in the research group for all three porphyrins in the model reaction with the diazoacetic acid and has shown that there is agreement between the literature and the calculations of the spin states of the Mn^{+3}, Fe^{+3} and Co^{+3}-porphyrins.

3-5 Experimental Design

5,10,15,20-Tetraphenyl-21*H*,23*H*-porphine cobalt, 5,10,15,20-Tetraphenyl-21*H*,23*H*-porphine iron chloride, 5,10,15,20-Tetraphenyl-21*H*,23*H*-porphine manganese chloride, Ethyl diazoacetate, and tert-butyl diazoacetate purchased from Sigma-Aldrich, St. Louis, MO, USA.

The porphyrins were dissolved in methanol (10^{-4}M) for ESI. Ethyl and tert-butyl diazoacetate where dissolved in cyclohexane (10%) before introduction into the helium manifold.

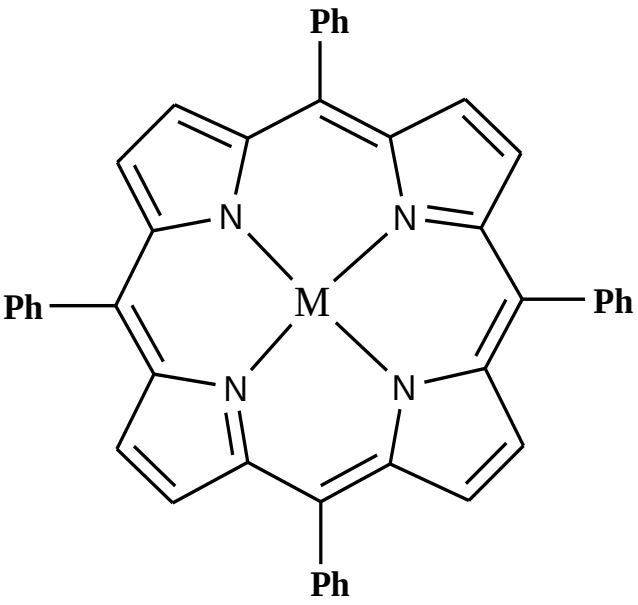

Reagents

1- tBu-$N_2CHCO_2C(CH_3)_3$ t-butyl diazoacetate

2-Et-$N_2CHCO_2C_2H_5$ ethyl diazoacetate

Porphyrins

M=Mn^{+3}, Fe^{+3}, Co^{+3}

Figure 18: Experimental design of the metal porphyrin systems.

3-6 Results

3-6-A: Porphyrins Fragmentation:

Collision induced dissociation (CID) fragmentation patterns for the bare metal porphyrin ions were collected to provide a foundation for understanding the fragmentation of the metal carbene. The ion to be fragmented is first accumulated in the ion trap and is then accelerated by the ring electrode rf field to a high kinetic energy. Frequent collisions with the inert collision gas, Helium, lead to a building up of internal energy that can result in bond breakages and hence, a fragmentation pattern. These patterns can often reveal the molecular structure. Using a normalized collision energy of 60% of maximum on the LCQ, the Mn-prophyrin exhibits limited fragmentation and produces a small amount of a species that has lost one (48%) or two (24%) of its phenyl groups. In Fe-porphyrin using the same normalized collision energy, the ion loses one

(66%) or two (27%) phenyl groups. Finally in Co-porphyrin at 60% of maximum in the LCQ, a first phenyl (76%) and second phenyl (22.5%) are lost (See Table 1).

Metal Porphyrin	**1st phenyl Loss**	**2nd phenyl Loss**
Mn (28%)	(48%)	(24%)
Fe (7%)	(67%)	(27%)
Co (1.5%)	(76%)	(22.5%)

Table 1: Ion intensities using collision-induced dissociation (CID) at 60% of maximum on LCQ

Percentage listed for metal porphyrins is unreacted porphyrin intensity.

Note: In fragmentation of Fe porphyrin, some complexation reactions with background methanol was observed.

3-6-B: Reactions of Metal/Porphyrins with Ethyl and t-Butyl Diazoacetate:

We allowed the Mn(III), Fe(III), and Co(III) porphyrins to react with ethyl and t-butyl diazoacetate. With Mn-porphyrin, only adducts are seen, and there is no evidence of metal carbene formation. While with Co-porphyrin, we can see the loss of N_2 to give a "metal carbene" and there is no adduct species formed. While with Fe-porphyrin, we see a first addition with loss of N_2 and a secondary addition of the diazoacetate with loss of N_2; as well as an adduct product, (see Figure 19).

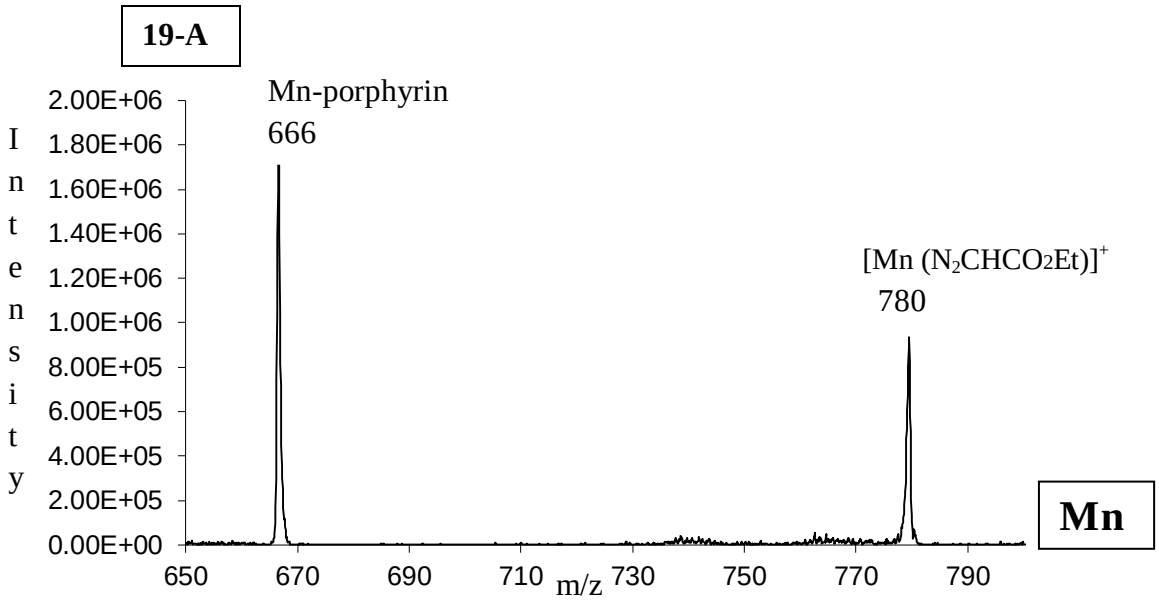

Figure 19-A: Mn-porphyrin reaction with ethyl diazoacetate.

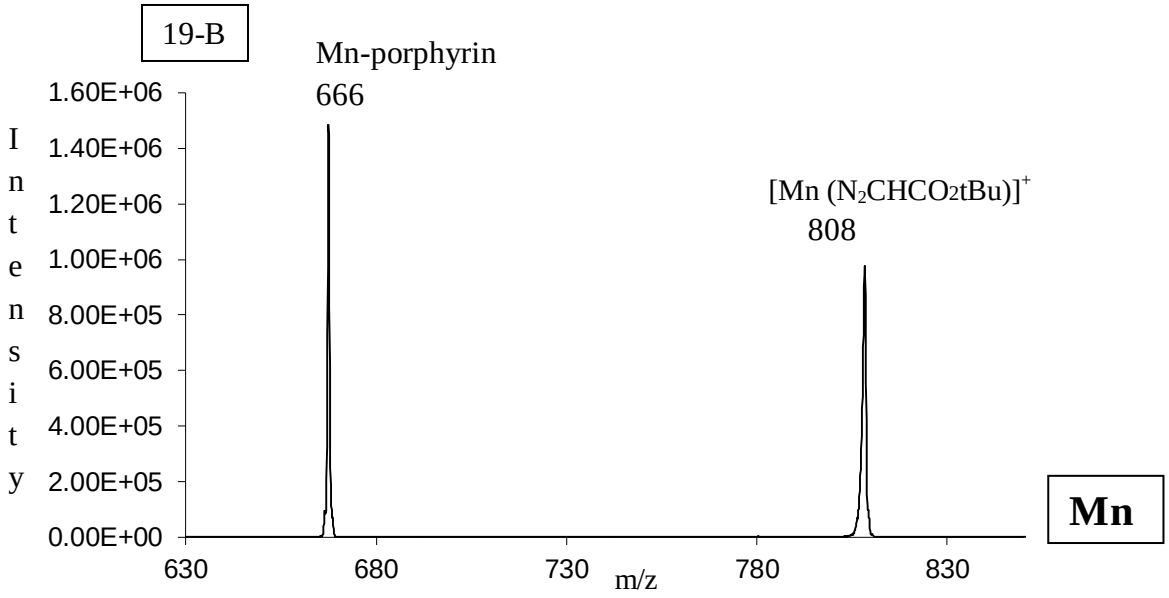

Figure 19-B: Mn-porphyrin reaction with tert-butyl diazoacetate.

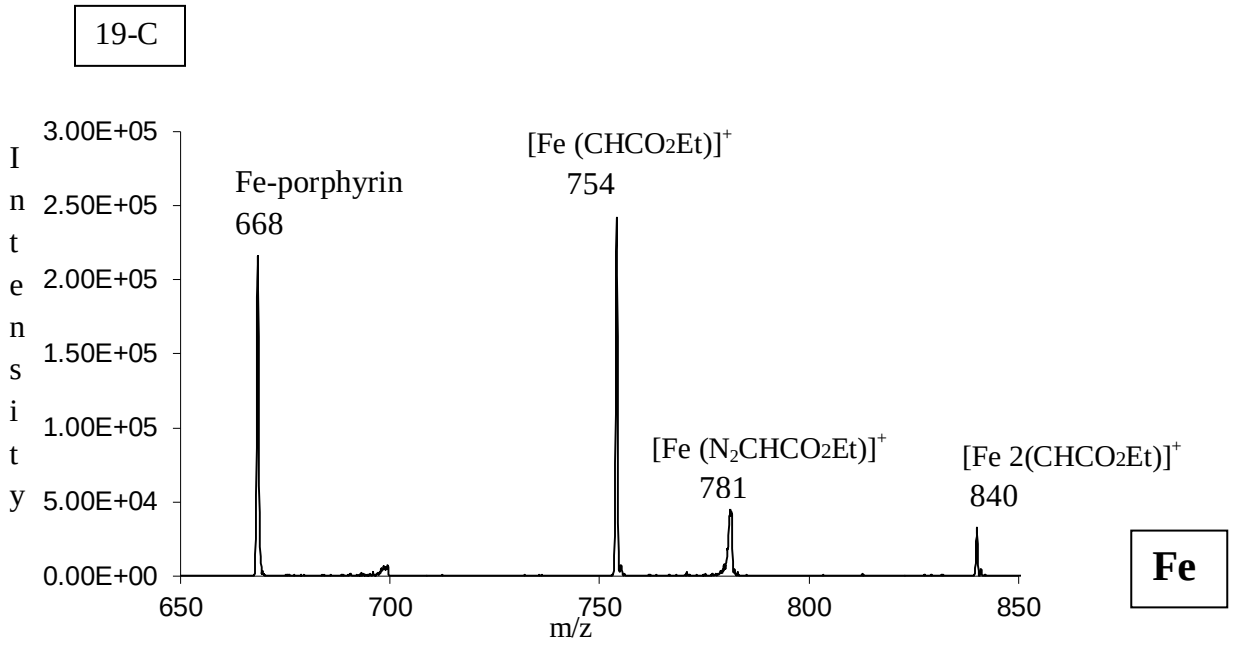

Figure 19-C: Fe-porphyrin reaction with ethyl diazoacetate.

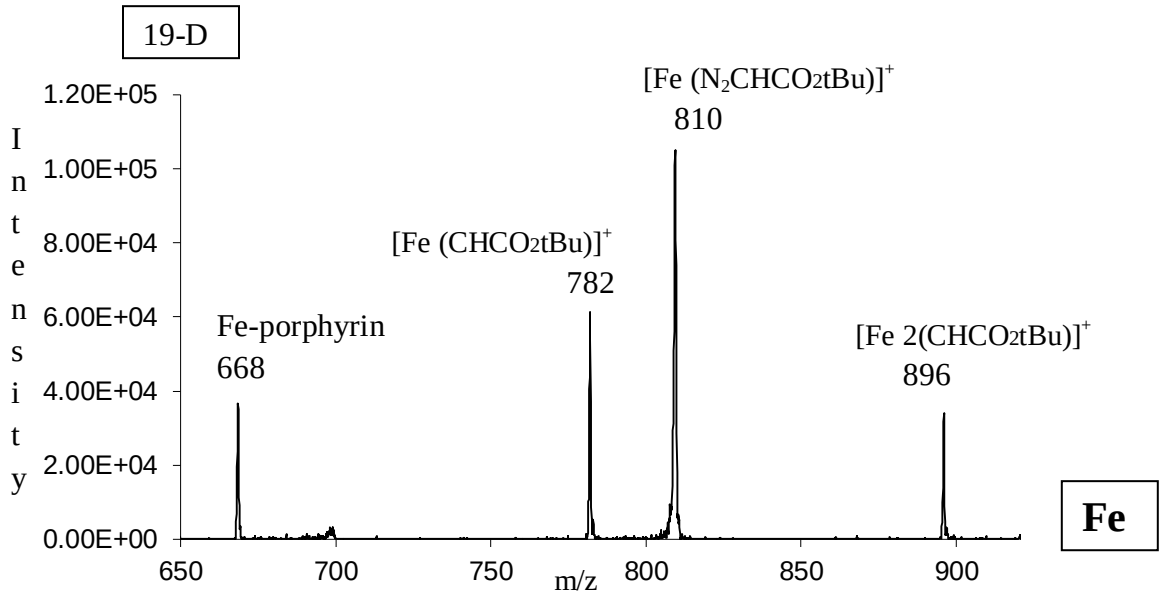

Figure 19-D: Fe-porphyrin reaction with tert-butyl diazoacetate.

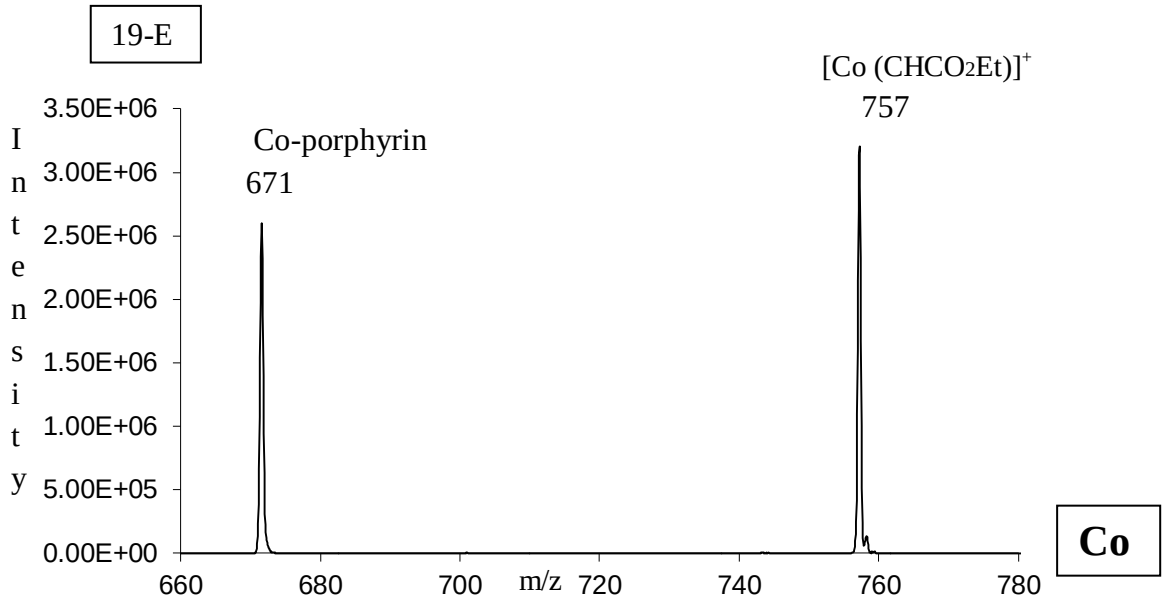

Figure 19-E: Co-porphyrin reaction with ethyl diazoacetate.

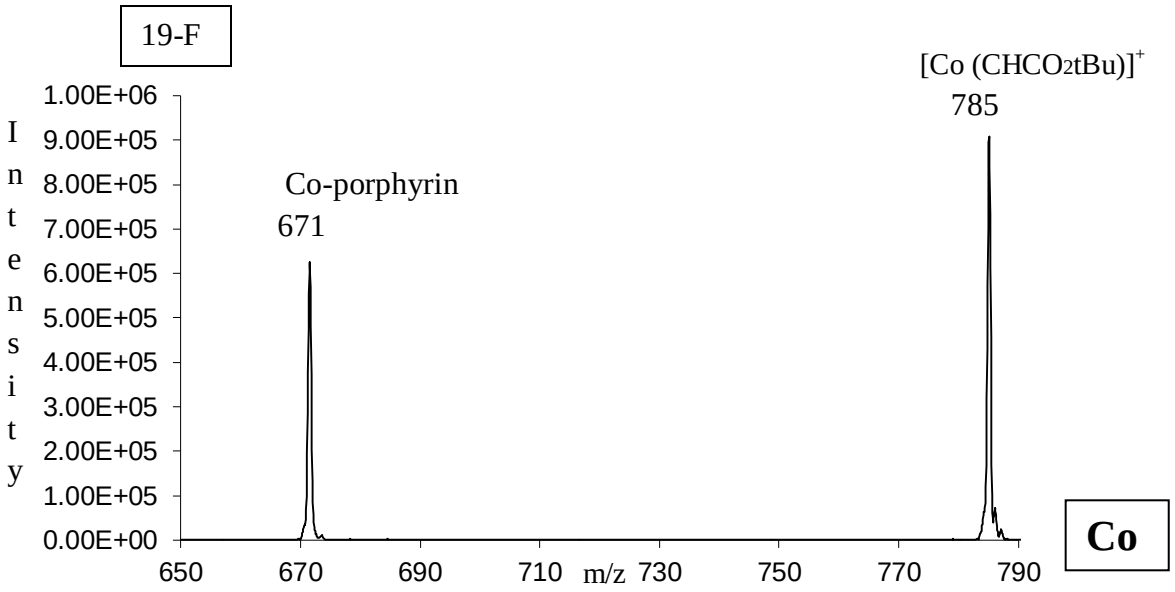

Figure 19-F: Co-porphyrin reaction with tert-butyl diazoacetate.

3-6-C: Rate Measurement:

Because the densities of the ions are extremely small compared to concentrations of the neutral reagents, we assume the neutral reagent concentration to be constant. This assumption leads us to apply pseudo first-order kinetics. We measure the absolute rates at three different reagent pressures, while monitoring reactions for at least three half-lives (see Figure 20). The rate constants parallel with the neutral reagent flow rates. In Figure 20, increasing the neutral reagent flow rate two-fold, which increases the neutral reagent concentrations two-fold, increases the rate constant two-fold. This behavior suggests that the flow rate is linearly proportional to the concentration in the ion trap and that our assumption of rapid evaporation is valid.

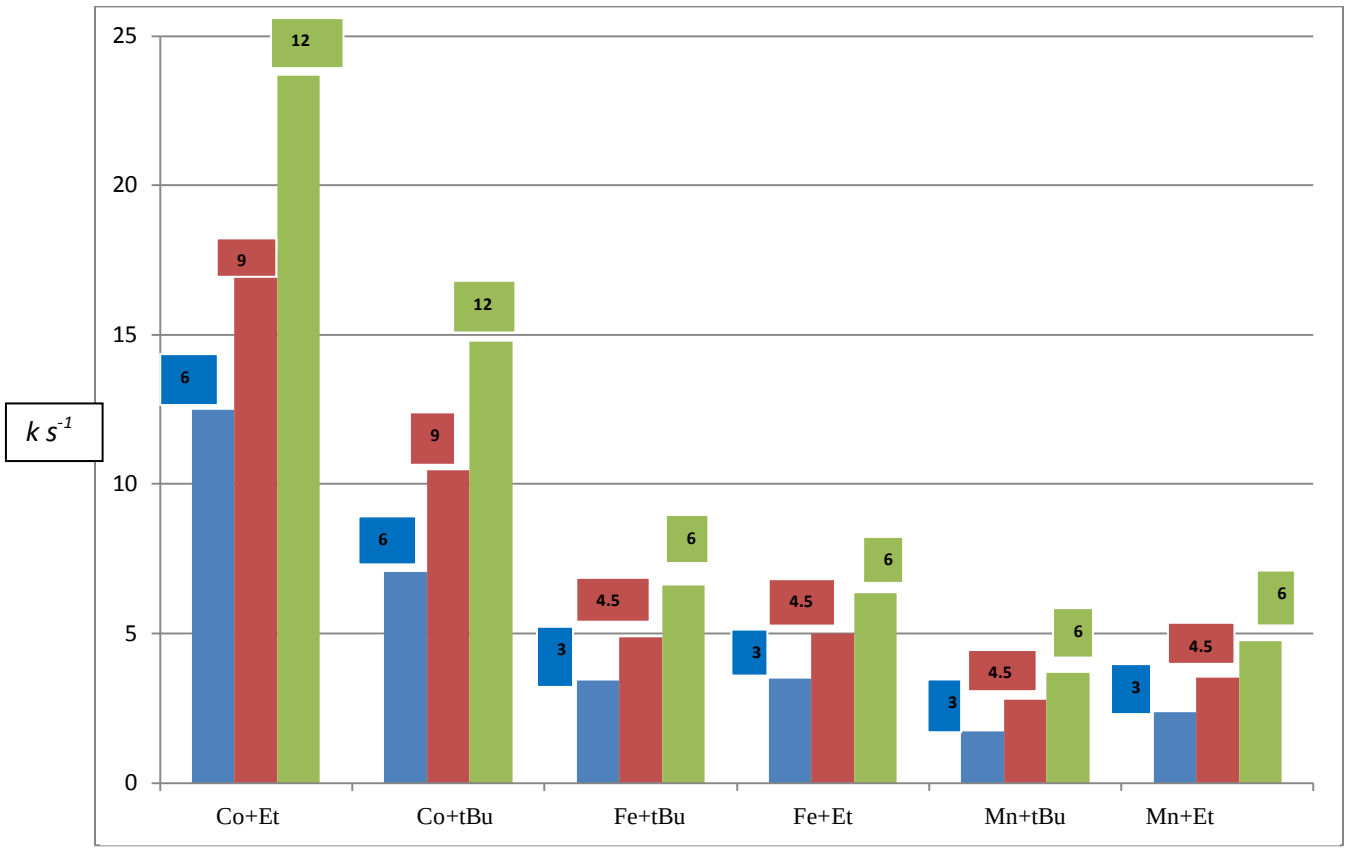

Figure 20: Pseudo first-order rate constants for reactions of metal porphyrins at different flow rates (µl/hr) of the neutral reagent.

3-6-D: Kinetics:

Looking at Table 2, we obtain precise results with standard deviations of less than 5%. Our reaction has two steps: addition to the metal, followed by N_2 expulsion (see Figure 2). Either one could be the rate determining step. We found that in Mn, the second step is rate determining, so only adduct products are formed. With the Co, only metal carbenes are formed as a product, which suggests that the first step is rate-determining.

With Fe, carbenes are formed, followed by a second addition forming a bis-carbene. Adducts were also seen, and it is unclear which step is rate-determining.

Metal+Reagent	Rate Constant cc/molecule/sec. ±std. dev. %	Metal+Reagent	Rate Constant cc/molecule/sec. ±std. dev. %
(Mn+Et-diazoacetate)	9.87E-10 ±0.4%	(Mn+tBu diazoacetate)	6.41E-10 ± 3.7%
(Fe+Et-diazoacetate)	1.39E-09 ±5.0%	(Fe+tBu diazoacetate)	1.18E-09 ±2.6%
(Co+Et-diazoacetate)	2.14E-09 ±2.9%	(Co+tBu diazoacetate)	1.49E-09 ±2.9%

Table 2: Measured rate constants for the reactions of metal porphyrins with the diazoacetates

All the reactions are fast and approach the collision-controlled limit. We can interpret the kinetic data in general as the Co systems are more reactive than Fe systems. This may suggest that

greater electron density on the metal enhances the 2nd step in the carbene formation process. The Mn systems are the slowest, which is consistent with a barrier to carbene formation.

3-6-E DFT Calculation

DFT calculations were completed in the research group by Dr. Scott Gronert and the results are listed in Table 3. Diazoacetic acid with an unsubstituted metal porphyrin was used for computational modeling. According to the computational data the results agree with the previous literatures [114-116] in that Mn is a quintet, Fe a quartet, and Co is a triplet in their ground states (Table 3).

The expected reaction pathway of the diazo compound with the metals, involves an interaction between the metal with the carbon of the diazo groups π-system. That is, the two reactants framework planes are aligned in parallel. This alignment cause, steric effects between the porphyrin and the alkyl group of the diazoacetate ester. This complexation of the diazo reagent with the metal porphyrin provides little energy to expel N_2.

After N_2 loss, the carbene framework is orthogonal to the plane of the metal porphyrin (shift from a π-type complex to an σ-type complex). The C-M bond is reduced from 2.4 Å (diazo adduct with metal porphyrin) to the 1.9-2.0 Å range.

A bridging carbene species appears to be more favorable than the formal carbene. Although conventional carbenes are not favored in the Mn and Fe systems, formation of the bridged product is favorable when the metal porphyrins react with diazoacetic acid (by at least 13 kcal/mol). In these structures, the replacement of a direct bond between one porphyrin nitrogen and the metal center with a bridging bond, via the carbene center, results in the metal becoming 4-coordinate. Such bridging

results in the bending of the porphyrin structure significantly for all metals. The bridged carbene is more about 30 kcal/mol stable than the conventional structure. Interestingly, the metal-carbon bond length is not greatly altered in going from 5-coordinate to 4-coordinate, even though π-bonding is no longer possible. At the carbene, the M-C-N angle is approximately 95°, but the carbon-nitrogen bond appears to be strong. Finally, the figure also includes a structure for the complex of CH with the iron porphyrin (Figure 21). The CH group adds an unpaired electron, so spin-pairing to give a triplet from the quartet iron porphyrin is assumed in the calculations. A pyramidal geometry was found for the CH group, with a much wider N-C-Fe angle and significantly shorter bonds to the bridging carbon.

As expected, the preferred reaction product depends on the metal. Mn-d^4 is the least reactive and does not produce the carbene product with the diazoacetate. This agrees with the DFT calculations which indicate that the Mn=C species is unfavorable; however this species can collapse, forming a stable bridging compound through the metal carbene (Mn=C), but this step cannot happen because the energy of the metal carbene is too high (15.5 kcal/mol). That is why the Mn system cannot lose nitrogen and stops the reaction at the adduct species. Fe-d^5 produces the formal metal carbene with loss of N_2 (Fe=C). The computational data indicates that this species requires less energy (9.3 kcal/mol) than needed for the formation of Mn=C (15.5 kcal/mol). That explains why the iron can react faster than the manganese and form the bridging carbene in an exothermic process. The Co-d^6 system reacts rapidly with the diazoacetate to give the metal carbene with loss of nitrogen. The high stability of the free carbene (-0.4 kcal/mol) indicated in the computational work suggests a fast reaction followed by collapse to give a bridging carbene which is more stable (-27.5 kcal/mol) than the iron system. According to the periodic trend, the rate constant increases from Mn to Co due to the increasing valence electron density on the metal (increasing the back-bonding from metal).

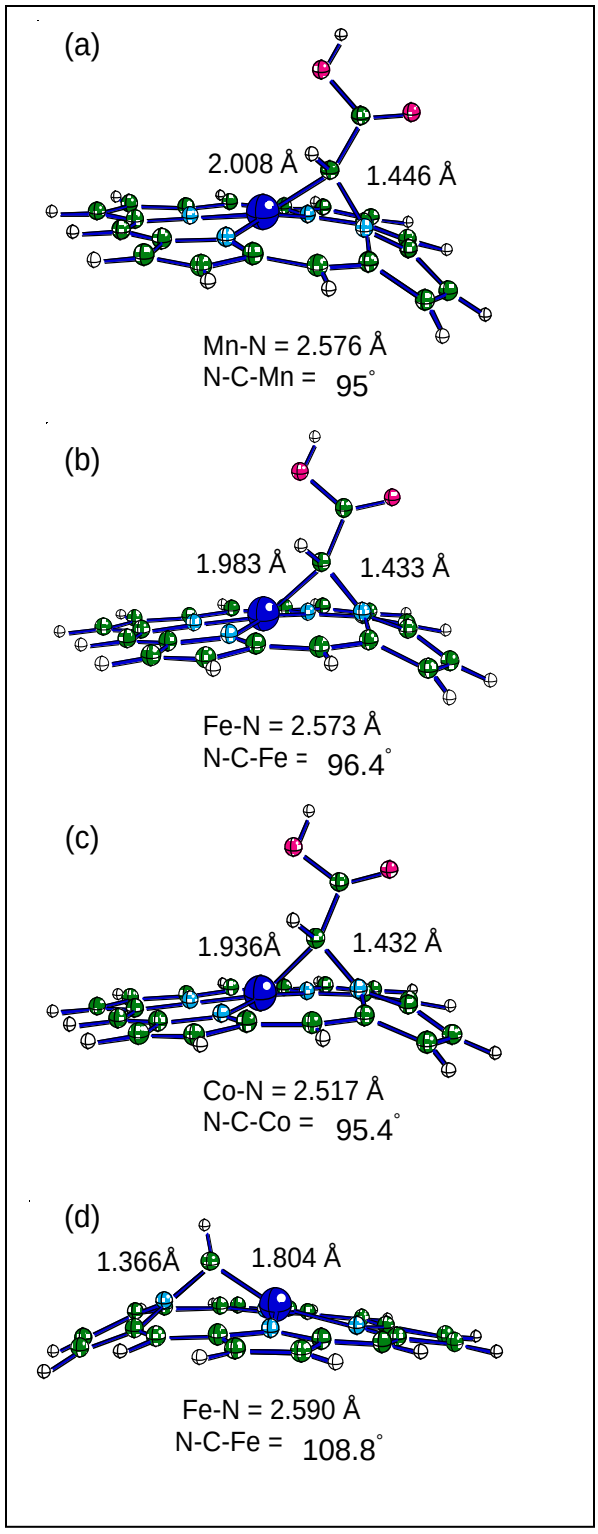

Mn (quintet) with diazoacetic acid carbene

Fe (quartet) with diazoacetic acid carbene

Co (triplet) with diazoacetic acid carbene

Iron (triplet) CH complex

Figure 21: Structures of bridged porphyrins are shown in (a,b,c,d) at B3LYP/6-311+G* level. Manganese is in quintet state, iron in quartet state, and cobalt in triplet state. Energies are relative to reactants in the same spin state.

	Co (triplet)	Fe (quartet)	Mn (quintet)
Porphyrin	0.0	0.0	0.0
Adduct	-2.3	-7.6	-4.5
Carbene	-0.4	9.3	15.5
Bridged Carbene	-27.5	-17.5	-13.6

Table 3: Relative Energies (kcal/mol) of Reactants and Products in Various Spin States (B3LYP/6-31+G*)

3-6-F: Product Fragmentation:

The fragmentation of the metal carbenes leads to new products with potentially remarkable chemistry. In this study, we have determined the fragment patterns of all the metal carbenes. There are additional secondary reaction products resulting for diazoacetate reactions with the reactants or fragmentation products. Iron porphyrins reacts with the ethyl diazoacetate and with tert-diazoacetate to give three products M=carbene, metal-biscarbene, and adduct product (see Figures 19C & 19D respectively). While cobalt porphyrins give only M=carbene in reaction with ethyl and tert-butyl diazoacetate (see Figures 19E & 19F respectively). Manganese porphyrin reacts with ethyl diazoacetate and with tert-diazoacetate to give only adducts products (see Figures 19A & 19B respectively).

Applying CID energy to the iron and cobalt "carbene" produced from the reaction of the iron and cobalt porphyrin with ethyl diazoacetate: the major product has a loss of $C_3H_5O_2$=73 units, which

is assumed to be a metal carbyne $[M (CH)]^+$; as well as a product with a loss of C_2H_5OH=46 units, assumed to be a metal cumulene $[M (C=C=O)]^+$; and very little of a product with loss of $C_3H_4O_2$=72 units, assumed to be $[M (CH_2)]^+$ (see Figures 22 &23 respectively and Table 4). All are expected to be bridged.

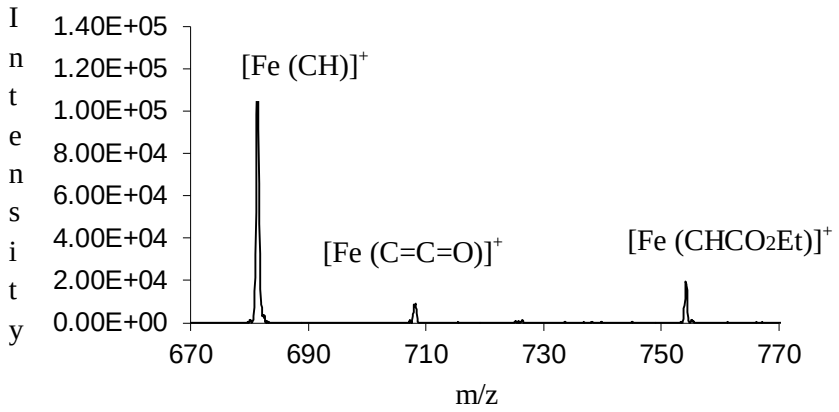

Figure 22: Fragmentation spectrum of $[Fe (CHCO_2Et)]^+$ complex produced from the reaction of iron porphyrin with ethyl diazoacetate.

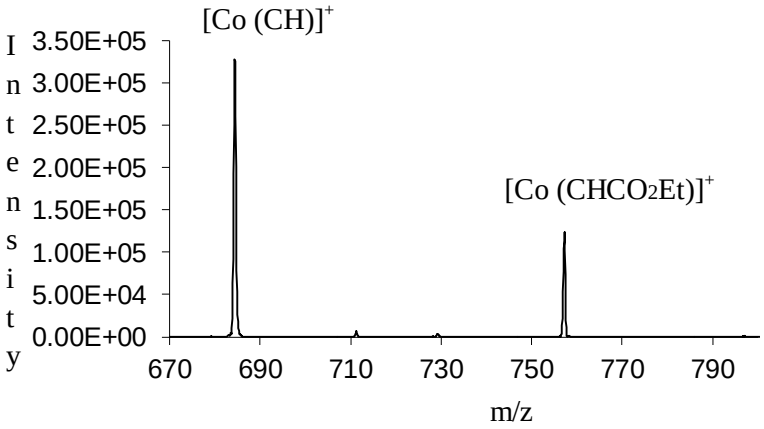

Figure 23: Fragmentation spectrum of $[Co (CHCO_2Et)]^+$ complex produced from the reaction of cobalt porphyrin with ethyl diazoacetate.

Applying CID energy to the iron and cobalt "carbene" produced from the reaction of the iron and cobalt porphyrin with t-butyl diazoacetate: the major product has loss of C_4H_8=56 units, which is

assumed to be a metal carboxylic acid $[M (CHCO_2H)]^+$ followed by a product with a loss of $C_5H_8O_2$=100 units, which is assumed to be $[M (CH_2)]^+$; as well as product with a loss of C_4H_9OH=74 units, which is assumed to be metal cumulene $[M (C=C=O)]^+$; and finally a product with a loss of $C_5H_7O_2$=99 units, which is assumed to be $[M (CH)]^+$. If we isolate and fragment $[M (CHCO_2H)]^+$, it decarboxylates to give $[M (CH_2)]^+$ (see Figures 22 &23 respectively and Table 4).

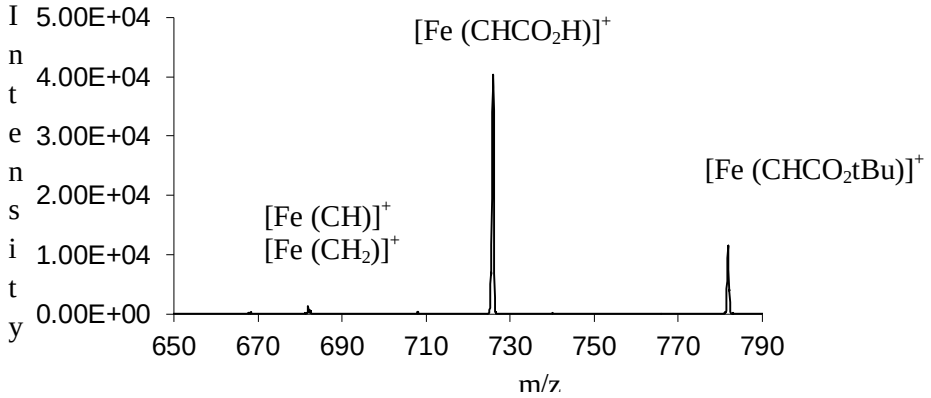

Figure 24: Fragmentation spectrum of $[Fe (CHCO_2tBu)]^+$ complex produced from the reaction of iron porphyrin with tert-butyl diazoacetate.

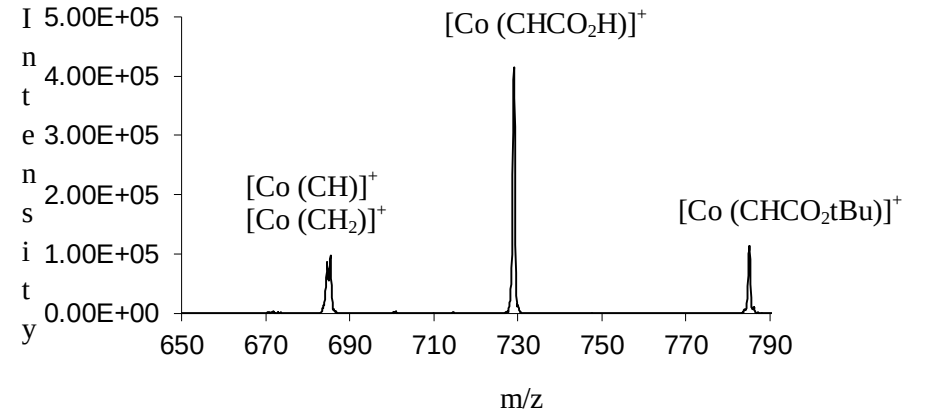

Figure 25: Fragmentation spectrum of $[Co (CHCO_2tBu)]^+$ complex produced from the reaction of cobalt porphyrin with tert-butyl diazoacetate.

3-6-G: Fragmentation Mechanisms:

The CID spectra show that the ester group has more effect than the metal on the fragmentation pathway, as shown in the fragmentation mechanism pathways below. The first pathway is a homolytic cleavage of the O-R (O-C) bond of the ester forming two radicals, followed by decarboxylation producing a metal carbyne $[M (CH)]^+$ (loss of 73 or 101, respectively, from the ethyl and *t*-butyl esters). This pathway is more favorable in the ethyl ester (scheme 2).The second pathway forms the metal carbene or metal carboxylic acid (loss of 28 or 56 and loss of 72 or 100, respectively, for the ethyl and t-butyl esters). This pathway is an alkene elimination of the ester to give a carboxylic acid.[91]

The metal porphyrin carboxylic acid undergoes decarboxylation under CID energy, producing the metal carbene $[M (CH_2)]^+$. This elimination is more favorable with a t-butyl than an ethyl group (scheme 3). Alcohol elimination from the ester is the less common pathway, giving a cumulene product $[M (C=C=O)]^+$ by two possible pathways. The first is metal oxidation (+1 to +2) with loss of an alkoxide anion, followed by a proton transfer giving the metal cumulene (see Scheme 4A). On the other hand, a concerted 1, 2 eliminations via a 4-center transition state are possible too (see Scheme 4B). We cannot make a distinction between these two possibilities.

M+R	Product	Activation Energy %	Loss	Fragmentation Product
Fe+Et	[Fe ($CHCO_2Et$)]$^+$	25	$C_3H_5O_2$ $C_3H_4O_2$ C_2H_5OH	[Fe (CH)]$^+$ 100% [Fe (CH_2)]$^+$ 20% [Fe (C=C=O)]$^+$ 20%
Fe+tBu	[Fe ($CHCO_2tBu$)]$^+$	15	C_4H_8	[Fe ($CHCO_2H$)]$^+$ 100%
		20	C_4H_8 $C_5H_8O_2$ $C_5H_7O_2$ C_4H_9OH	[Fe ($CHCO_2H$)]$^+$ 100% [Fe (CH_2)]$^+$ 50% [Fe (CH)]$^+$ 10% [Fe (C=C=O)]$^+$ 15%
	[Fe ($CHCO_2H$)]$^+$	25	CO_2	[Fe (CH_2)]$^+$ 100%
Co+Et	[Co ($CHCO_2Et$)]$^+$	15	———	[Co 2($CHCO_2Et$)]$^+$ 8%
		20	——— $C_3H_5O_2$	[Co 2($CHCO_2Et$)]$^+$18% [Co (CH)]$^+$ 10%
		25	$C_3H_5O_2$ C_2H_5OH $C_3H_4O_2$	[Co (CH)]$^+$ 100% [Co (C=C=O)]$^+$ 15% [Co (CH_2)]$^+$ 10%
Co+tBu	[Co ($CHCO_2tBu$)]$^+$	15	———	[Co 2($CHCO_2tBu$)]$^+$30%
		20	——— C_4H_8 $C_5H_8O_2$	[Co 2($CHCO_2tBu$)]$^+$15% [Co ($CHCO_2H$)]$^+$ 35% [Co (CH_2)]$^+$ 8% [Co ($CHCO_2tBu$)]$^+$ 6%
		25	C_4H_8 $C_5H_8O_2$ $C_5H_7O_2$ C_4H_9OH	[Co ($CHCO_2H$)]$^+$ 100% [Co (CH_2)]$^+$ 65% [Co (CH)]$^+$ 40% [Co (C=C=O)]$^+$ 10%
	[Co ($CHCO_2H$)]$^+$	20	CO_2	[Co (CH_2)]$^+$ 100%

Table 4: Products fragmentation using CID

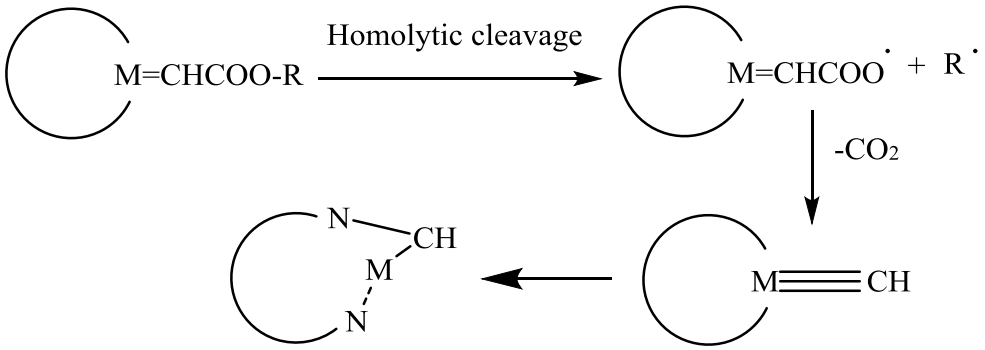

Scheme 2: Homolytic cleavage followed by decarboxylation to form metal carbyne

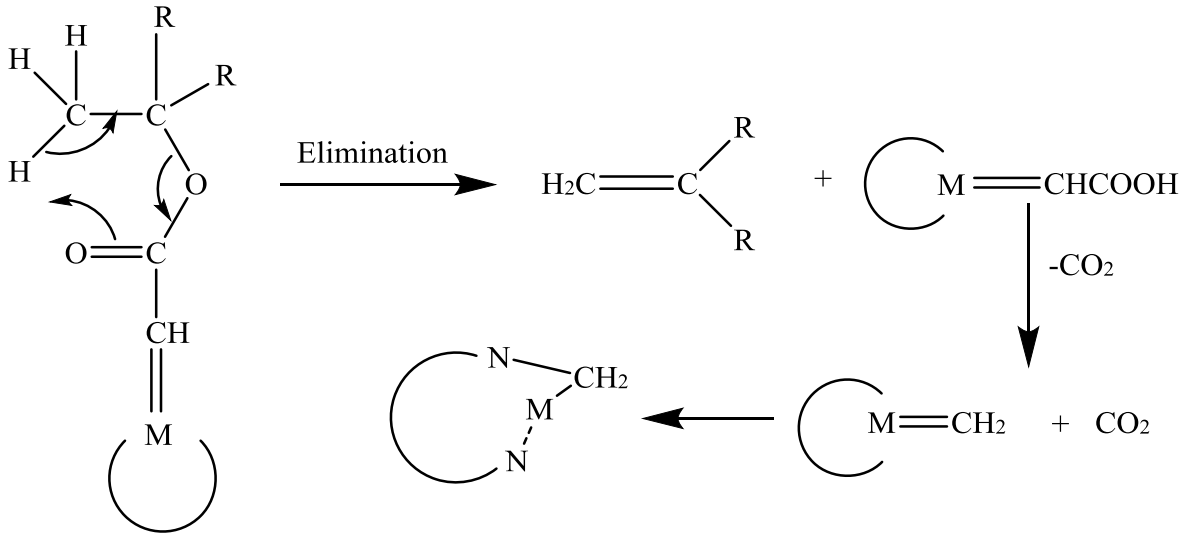

Scheme 3: Alkene elimination follows by decarboxylation to form metal carbene.

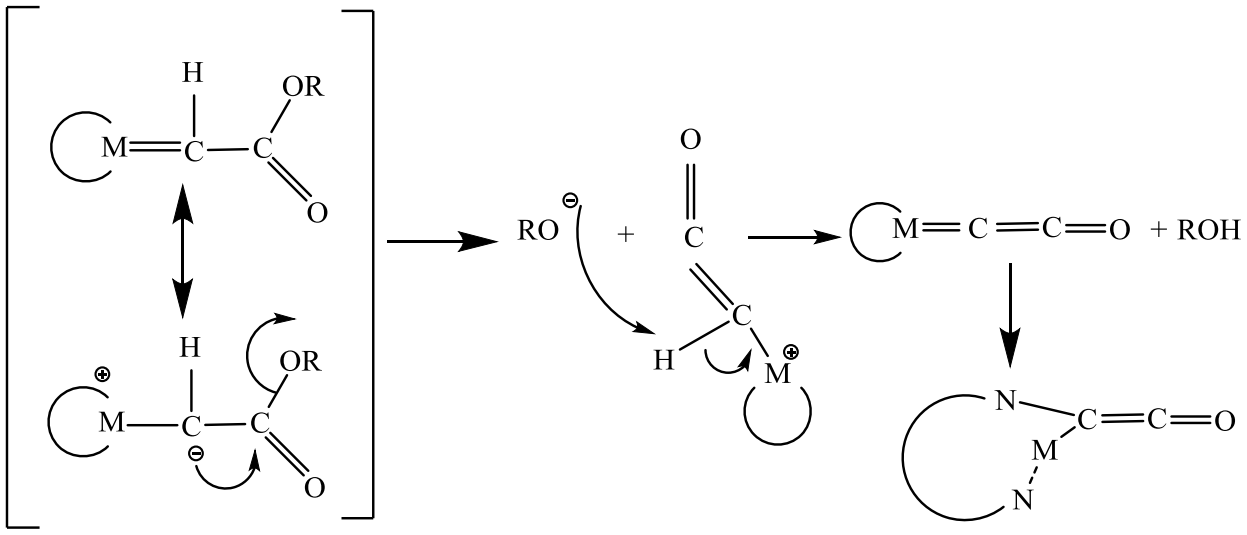

Scheme 4A: Alcohol elimination to form metal cumuelene

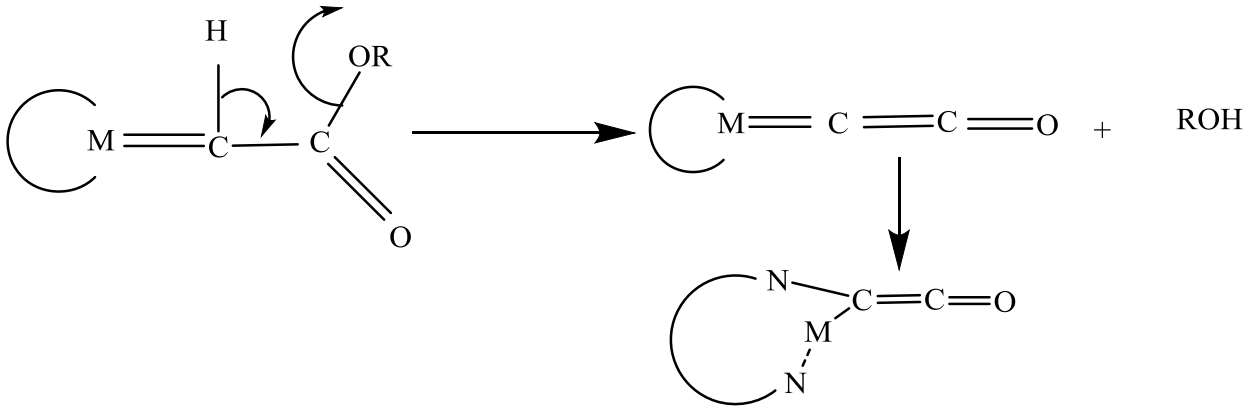

Scheme 4B: concerted 1, 2 elimination to form metal cumulene

3-6-H: Conclusions for chapter 3:

Mn, Fe and Co porphyrin complexes were allowed to react with ethyl and tert-butyl diazoacetate in an ion trap mass spectrometer. The manganese system produces only adducts, but the iron and cobalt systems give addition with loss of N_2 to produce metal carbene-like species. All the reactions are fast and approach the collision-controlled limit and the rate determining step varies among the metals; Mn-d^4, Fe-d^5 and Co-d^6. Co-porphyrin is the fastest reaction while the Mn-porphyrin is the slowest reaction. The metal has a major effect on the reaction pathway and the products obtained.

The porphyrin complexes prefer bridging (M-N insertion) over the formal carbene. In the insertion process, the metal goes from 5-coordinate to 4-coordinate. These results are supported by DFT calculation. This conclusion is supported by Dzik and coworkers using electron paramagnetic resonance (EPR) and complementary DFT calculations of EPR properties; found that the reaction of Co^{+2} porphyrin with ethyl diazoacetate resulted in a product, Co ($CHCO_2Et$),[92]that preferred the bridging form. Furthermore, Johnson and coworkers, using x-ray crystallography, found that the product of the reaction of Co^{+2} octaethyl porphyrin and ethyl diazoacetate preferred the bridging form.[93] There is another reason for us to believe that the insertion products are more favorable than the formal metal carbene $[M{=}CH_2]^+$ because, when we introduce alkenes to react with the putative metal carbene, there is no evidence to cyclopropanation formation because we reach a dead end.

The metal has only a modest effect on the fragmentation pathway, whereas the ester group has a large one. This is expected for bridging products because the carbene is stabilized and the ester is the most fragile functional group. Both iron and cobalt porphyrin system have the same fragmentation patterns for their products $[M\ (CHCO_2R)]^+$. For the t-butyl systems, alkene elimination dominates,

presumably leading to a carboxylic acid product [M ($CHCO_2H$)]$^+$. This is a common path for *t*-butyl esters in general. Secondary fragmentation of [M ($CHCO_2H$)]$^+$ give decarboxylation to form a [M (CH_2)]$^+$ species. For the ethyl diazoacetate system, the formation of the CH metal complex is more unusual and the loss of a CO_2R radical unit from simple esters is not common. In this case, it seems more likely, that the fragmentation process involves breakdown of the M-N insertion product and the intermediary of the true metal carbene species, [M ($CHCO_2R$)]$^+$.

We have found that, the metal porphyrins give carbenes that are unstable and lead to insertion products via unimolecular processes. Some factors in solution must be stabilizing them to allow the cyclopropanation processes seen in the condensed phase.

Chapter 4- Determine the factors that affect the gas-phase reactivity of copper bis-oxazoline-based cyclopropanation catalysts with diazo reagents and examine the fragmentation behavior of the reaction products.

4-1 Introduction

Nozaki opened the door in 1966 for the field of catalytic asymmetric cyclopropanation by the use of a salicylaldiminato copper (11) complex.[94,95]Aratani and co-workers designed many similar catalysts based on the Nozaki complex.[96,97]Pfaltz and his co-workers were the first to describe bis-oxazolines and related ligands.[98]Bis-oxazolines ligands have continued to be investigated because they are easy to prepare, they are effective in asymmetric catalysis, and bis-oxazolines ligand's chirality, a C_2-symmetric environment, offer an intrinsic simplicity.[99]

At Harvard University David Evans and coworkers used copper bis-oxazolines catalysts to synthesize beta lactams (biologically active) under mild conditions. They focused on the development of copper bis-oxazolines complexes as chiral Lewis acids for many highly enantioselective transformations such as Diels-Alder, cycloaddition, ene, Aldol, Michael and amination reactions.[100]Copper bis-oxazolines ligands also have been used by Pfaltz,[101,102]Masamune,[103,104] and Evans[105] to develop catalytic cyclopropanations using diazoacetic esters as carbene sources.

The Evans laboratory demonstrated the utility of chiral copper complexes in asymmetric catalysis (such as the copper bis-oxazolines), particularly in cyclopropanations, by using diazoacetate

reagents with alkenes in the presence of the copper catalyst.[106,107] In Japan Shuji Kanemasa and coworkers have had success in reacting styrene with diazoesters in the presence of copper catalysts to give 2-phenyl-1-cyclopropanecarboxylates in good yields.[108]

Previous work highlights the importance of catalytic cyclopropanations using metal porphyrin catalysts with diazoesters as carbene sources.[101-105] In our effort, we explore gas-phase metal carbene chemistry to develop a better understanding of the reaction pathways and mechanisms. Our previous work in Chapter 3 with carbenes of metal porphyrins indicates that the insertion product is more favorable than the formal carbene[109] and is inactive toward alkene addition to undergo cyclopropanations. We decided to test whether the copper carbene suffers the same fate with the bis-oxazolines ligands.

4-2 Objectives

- Use copper bis-oxazolines complexes as models of cyclopropanation catalysts.
- Examine the reactivity of copper bis-oxazoline carbenes and their fragmentation products.

4-3 Experimental Design

To investigate the chemistry of metal carbenes and their formation, we examined four copper bis-oxazolines systems with different groups attached to the oxazoline rings. (All ligands were purchased from Sigma-Aldrich St. Louis, MO, USA except the bis-oxazoline system with phenyl group was purchased from TCI America Portland, OR, USA). Each compound (A, B, C, and D), (see Figure 26), was allowed to react in a 1:1 ratio with the toluene complex of copper trifluoromethanesulfonate (purchased from Sigma-Aldrich St. Louis, MO, USA). The copper (I) complexes in Figure 26-A, B, C, and D were formed. It is assumed that the bis-oxazolines will be bidentate nitrogen ligands (see Figure 26).

In our experiments, the copper bis-oxazaoline cations enter through the atmospheric pressure ESI interface while the diazoacetate (purchased from Sigma-Aldrich St. Louis, MO, USA) compounds [10% in cyclohexane (purchased from Alfa-Aesar Ward Hill, MA, USA)] enter the trap with the helium stream. (Initially, methanol was used in place of cyclohexane, but it was found that methanol, when flowing directly into the ion trap, reacted with the copper complexes to give adducts). The copper bis-oxazolines cations are dissolved in methanol (purchased from Sigma-Aldrich St. Louis, MO, USA) (10^{-4}M) and injected through the ESI interface at a measured flow rate (3-5 µl/min). The copper bis-oxazolines cation of interest is isolated in the ion trap by the application of a notched waveform. The ethyl diazoacetate (10% in cyclohexane) is introduced into a stream of helium gas, (30-300 µl/hr), via a syringe pump (see Figure 11). The isolated copper bis-oxazoline cation is allowed to react with the ethyl diazoacetate reagent for a pre-determined time delay, and a mass spectrum is collected (see Figure 11). This time delay allows us to monitor the kinetics of the process.The densities of the ions are extremely small compared to concentrations of the neutral reagents, so we

assume the neutral reagent ion concentration to be constant. This assumption leads us to a pseudo first-order analysis. We determine absolute rates by collecting data at three different reagent pressures and monitoring reactions for at least 3 half-lives.

26-A

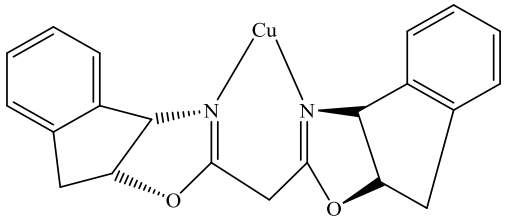

A=Ph

26-B

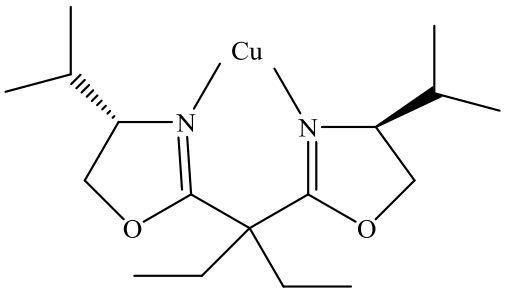

B=iPr

26-C

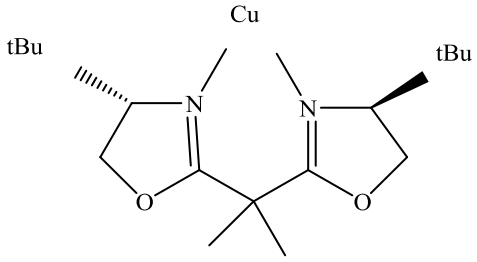

C=tBu

26-D

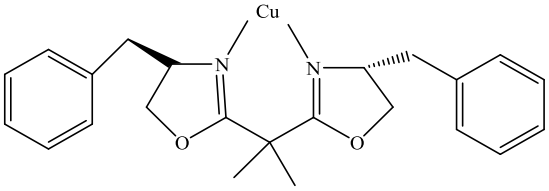

D=Bz

Figure 26: Copper bis-oxazolines complexes used in this study.

4-4 Results

4-4-A: Copper Complexes Fragmentation:

Using normalized collision energy of 35% of maximum in the LCQ, we obtained collision induced dissociation (CID) fragmentation patterns for the copper complexes to provide a foundation for understanding the fragmentation patterns of the metal carbenes that would result from these complexes. In this work we have two major fragments when we subject the Cu-complexes to CID (see Table 5).

Cu-Complexes	m/z of Cu complexes	m/z of fragment 1	m/z of fragment 2
A (Ph)	394(19%)	261(63%)	279(18%)
B (Iso)	357(28%)	271(28%)	289(44%)
C(tBu)	357(45%)	257(21%)	275(34%)
D(Bz)	425(60%)	291(40%)	0%

Table 5: Fragmentation of the copper complexes uses 35% CID of maximum energy.

Relative ion intensities are given parenthetically.

From the values shown in Table 5, we suggest a set of fragmentation mechanisms based on initial heterolytic cleavages. The first is step is N-C heterolytic bond cleavage forming a carbocation, from which we suggest three pathways. The 1st pathway involves proton transfer (green arrows) giving an amide and alkyne through an intramolecular elimination. The 2nd pathway is a direct rearrangement (black arrows) leading to an R-CN-Cu cation and epoxide. The 3rd pathway involves a hydride shift

(red arrows) to give an oxygen-stabilized cation followed by rearrangement forming the same R-CN-Cu cation and an aldehyde (see Scheme 5). We do not have sufficient data to distinguish between the two pathways leading to the R-CN-Cu cation.

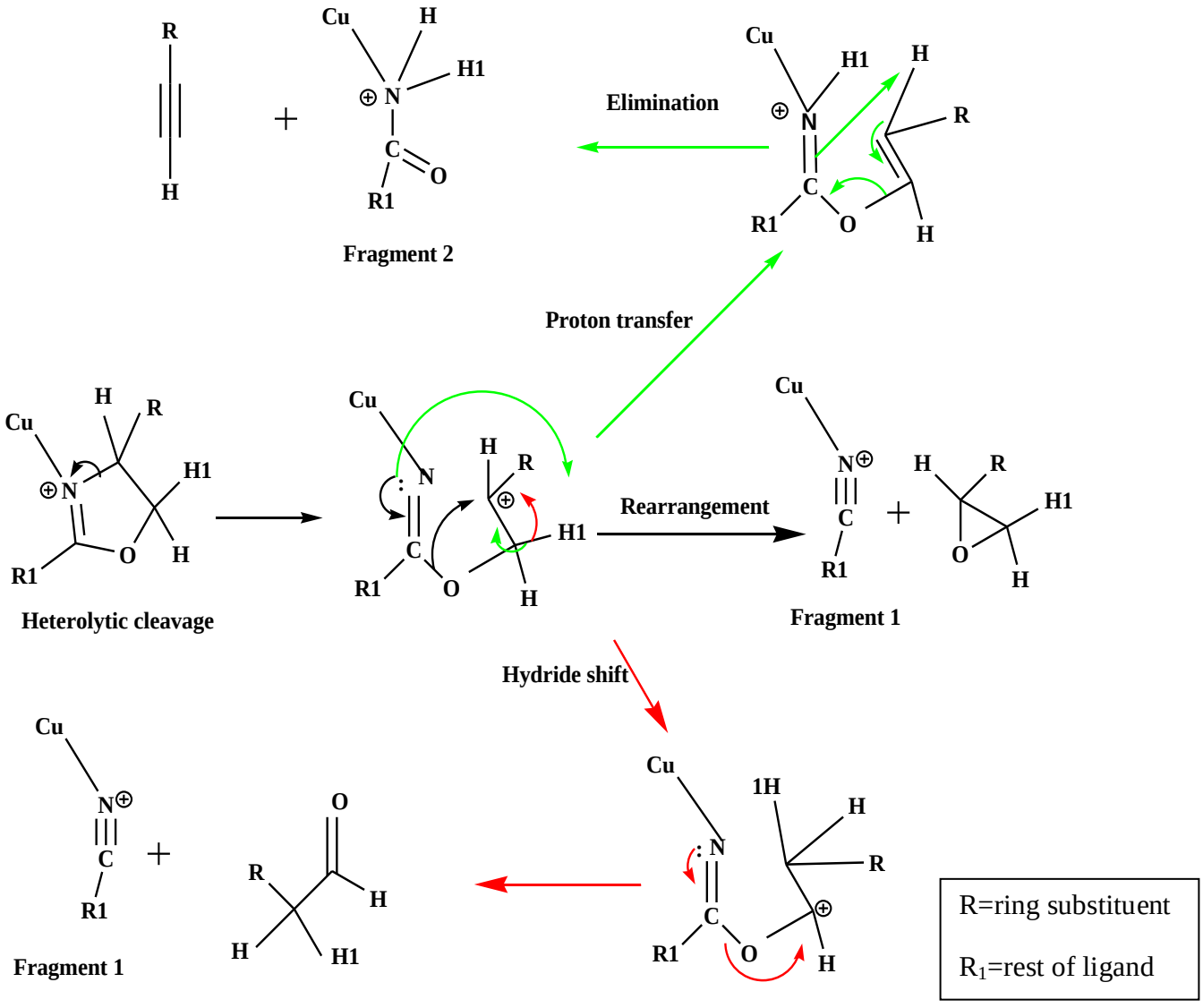

Scheme 5: Suggested mechanisms initiated by heterolytic cleavage of N-C bond in copper complexes.

4-4-B: Reaction of the copper bis-oxazolines with ethyl diazoacetate:

Mass spectra for the reactions of the copper complexes (A, B, C, and D) with ethyl diazoacetate (EDA) are shown as Figures 27-A, B, C, and D, respectively. Reactions were allowed to proceed without excitation and the ^{63}Cu-containing complexes were isolated prior to reaction to simplify the resulting mass spectra. At 5000 ms. reaction time for all the bis-oxazolines complexes reacting with ethyl diazoacetate, the main product was the single addition with loss of N_2, [M $(CHCO_2Et)]^+$, in all complexes (B, C and D) except for the A-complex, where the main product was double addition, possibly due to less steric hindrance in the cation. In addition, [M $(CHCO_2H)]^+$ or [M $(CHOEt)]^+$, m/z=415 fragmentation products were also formed in cases of the tert-butyl (C) and the isopropyl (B) complexes due to a loss of 28 mass units. (Note that both C and B bis-oxazolines complexes have the same m/z value). The first possible complex, [M $(CHCO_2H)]^+$, comes from alkene elimination (CH_2=CH_2) from the initial product [M $(CHCO_2Et)]^+$. The second possible complex, [M $(CHOEt)]^+$, comes from spontaneous CO elimination from an initial Wolff rearrangement product (see Scheme 6). With phenyl (A) and benzyl (D) copper bis-oxazolines complexes, no fragmentation is seen in the initial reaction.

Evidence was also seen for the formation of a metal cumulene, [M $(C=C=O)]^+$, for the tert-butyl (C) and the isopropyl (B) complexes (see Table 6). The metal cumulene [M $(C=C=O)]^+$comes from addition with loss of N_2 to give [M $(CHCO_2Et)]^+$, followed by two possible fragmentation pathways as described in Chapter 3, either alcohol elimination or a 1, 2 concerted elimination (see Schemes 4A and 4B respectively).

In summary, when we used the same reaction conditions for the four copper bis-oxazolines complexes A, B, C, and D, it appears that two possible additions with loss of N_2 products are formed; a Wolff rearrangement form and an ester insertion form (see Scheme 6).

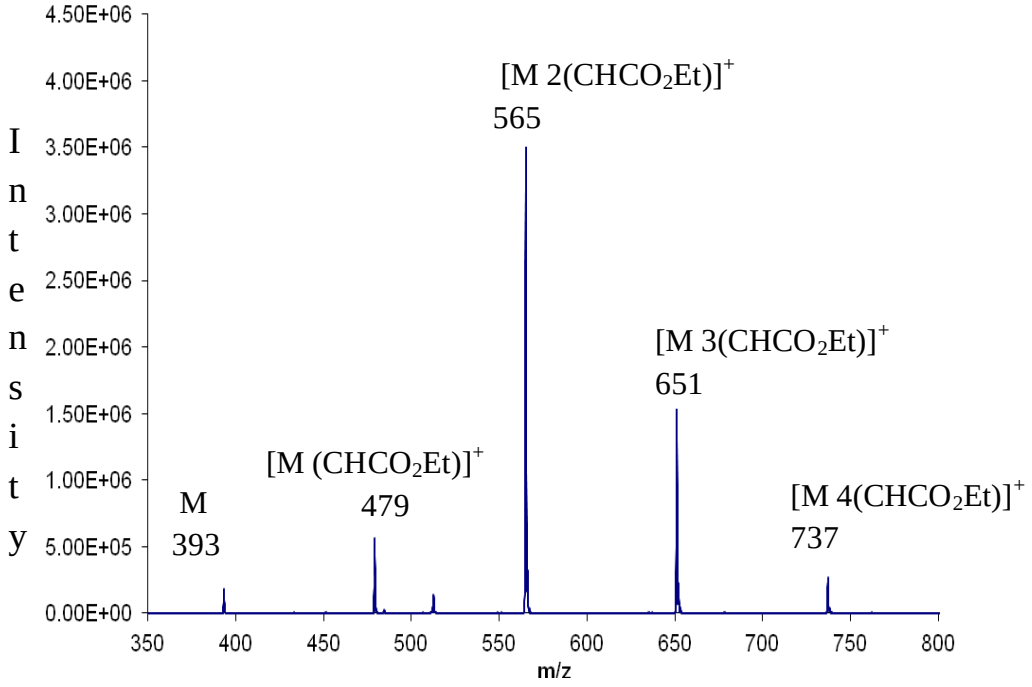

Figure 27-A: Reaction of ethyl diazoacetate with phenyl copper complex (A); this spectrum is dominated by multiple additions.

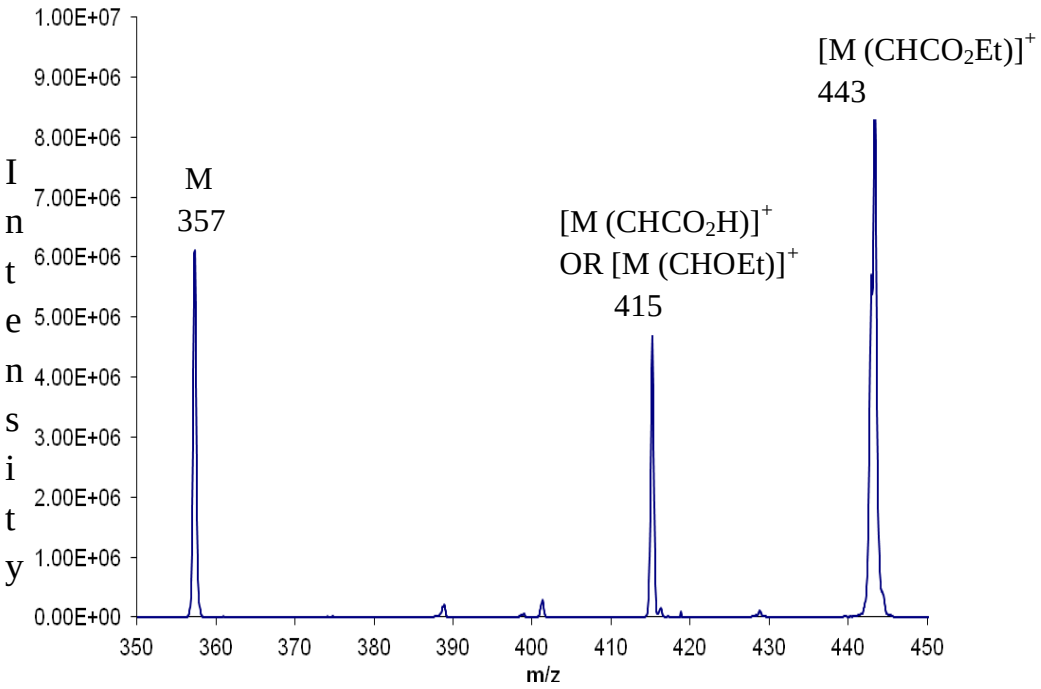

Figure 27-B: Reaction of ethyl diazoacetate with isopropyl-copper complex (B).

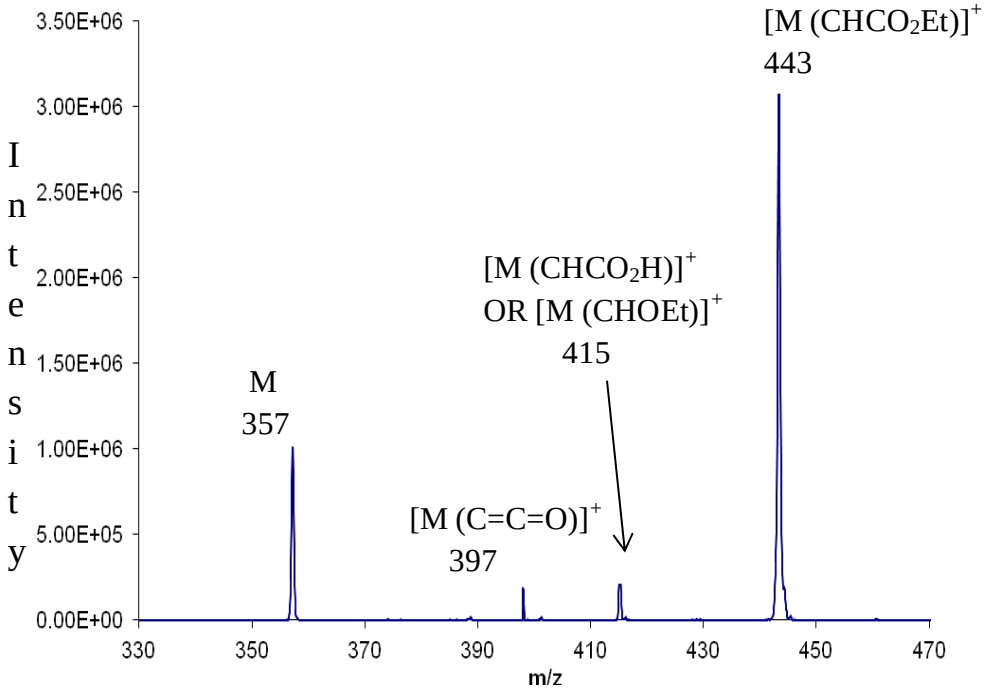

Figure 27-C: Reaction of ethyl diazoacetate with tBu-copper complex (C).

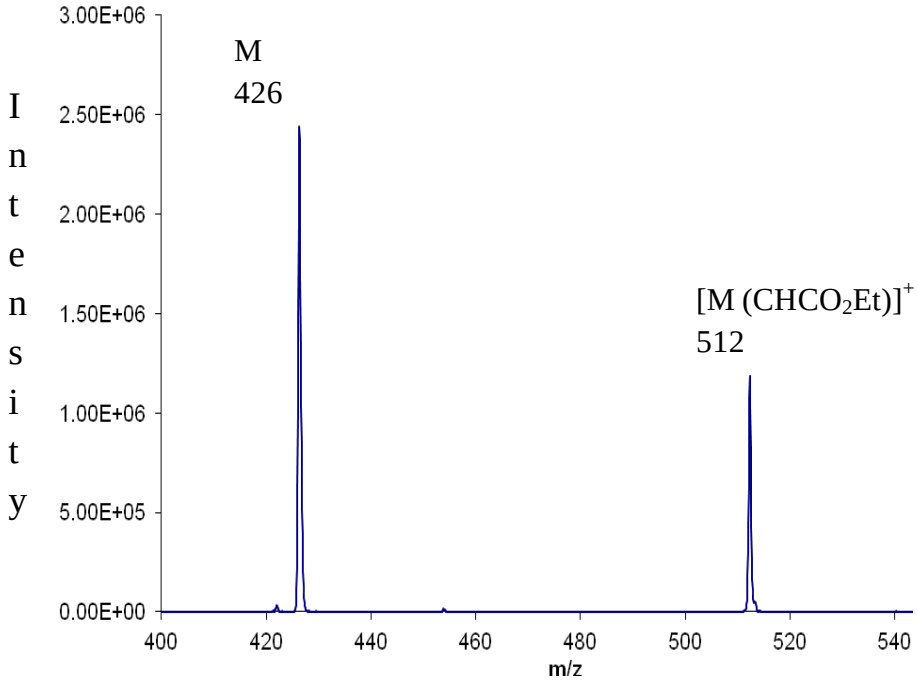

Figure 27-D: Reaction of ethyl diazoacetate with benzyl copper complex (D).

Beauchamp studied the gas-phase synthesis of copper and silver carbenes from diazomalonates.[110] She found that after losing N_2, the carbene can rearrange to a ketene form (Wolff rearrangement) which allows the metal to coordinate with an oxygen atom. Beauchamp used computational methods to estimate that the metal ketene form is favored by 27 kcal/mol over the metal carbene form, $M=C(CO_2R)_2$ (see Scheme 6). This paper supports our explanation of the results shown in Table 6 that there could be two kinds of products (covalent or coordination) obtained in the reaction of ethyl diazoacetate with copper bis-oxazolines complexes. Computational modeling in the group indicates that there is a more favorable product. This product is a bridging carbene; exactly the same as was seen in the porphyrin system (see Scheme 7).

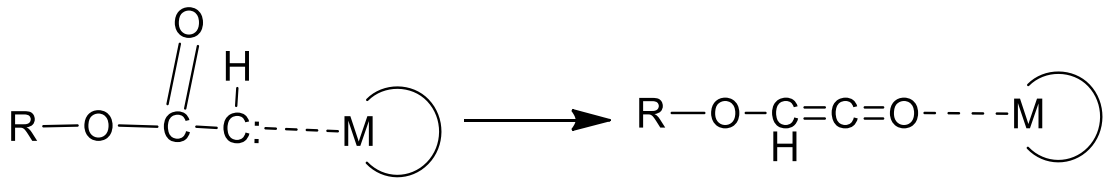

Covalent complex Coordination complex

Scheme 6: Ester rearrangement

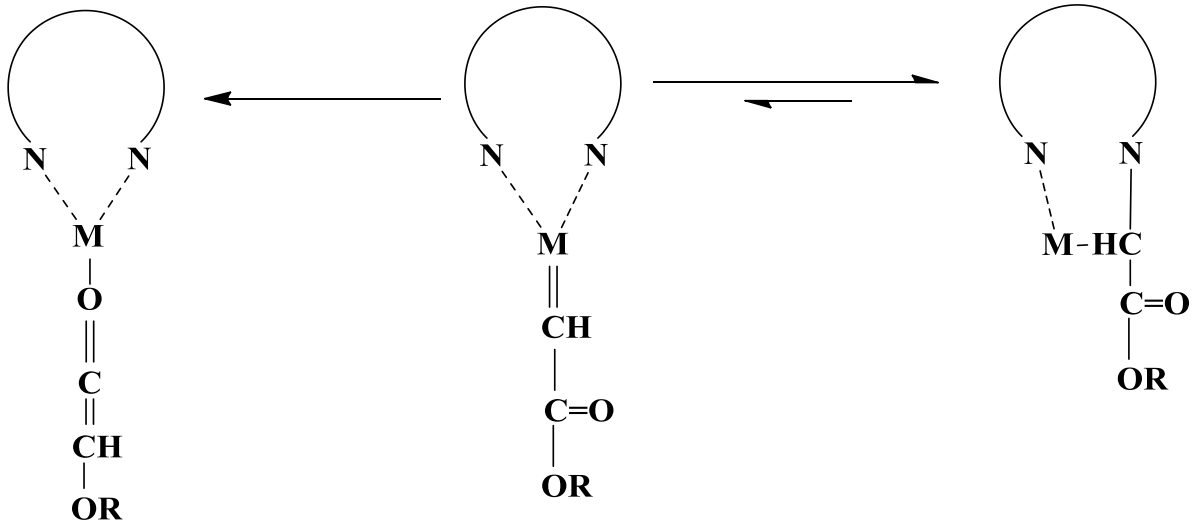

Wolff rearrangement product Bridging product

Scheme 7: Three possible bis-oxazolines products

In Scheme 7, the formal metal carbene is shown in the middle. This product can follow two rearrangement pathways: The first pathway is the Wolff rearrangement product, which is predicted to be the most favorable product in the Beauchamp study.[110] However, due to weak binding, this species could dissociate to form the original metal complex with the loss of a ketene. It can also lose CO to give an alkoxy carbene [M (CHOEt)]$^{+}$. The second pathway leads to a bridging carbene. This species,

similar to what was seen in the porphyrins, is expected to fragment to the metal cumulene [M (C=C=O)]$^+$ after alcohol elimination (see Schemes 4A, and 4B). Alternatively, metal carboxylic acids [M ($CHCO_2H$)]$^+$ could be formed after alkene elimination (see Scheme 3). In addition, the bridging carbene could go back to the formal carbene, and then give a Wolff rearrangement product (see Scheme 7). Dissociation would give back the original metal complex and ketene. Currently, we do not know the barrier between the Wolff rearrangement pathway and bridging products.

M+EDA	Initial Products $[M\ (CHCO_2Et)]^+$ At reaction time=5000 msec.	Fragmentation of $[M\ (CHCO_2Et)]^+$ At CID=35%	Subsequent Fragmentation of $[M\ (CHOEt)]^+$ OR $[M\ (CHCO_2H)]^+$ At CID=30%
A-complex+EDA Phenyl complex	$[M\ (CHCO_2Et)]^+$(13%) 2^{nd} addition (100%) 3^{rd} addition (45%) 4^{th} addition (20%)	$[M\ (CHOEt)]^+$ OR $[M\ (CHCO_2H)]^+$ (8%) A (15%) $[M\ (C=C=O)]^+$ (6%) 2^{nd} addition (22%) 3^{rd} addition (5%) $[M(CHCO_2Et)]^+$(100%)	A (20%) $[M\ (CH_2)]^+$ (100%) $[M\ (C=C=O)]^+$ (20%) $[M\ (CH)]^+$ (11%) M=C: (21%)
B-complex+EDA Isopropyl complex	$[M\ (CHCO_2Et)]^+$ (100%) $[M\ (CHOEt)]^+$ OR $[M\ (CHCO_2H)]^+$ (50%) $[M\ (C=C=O)]^+$ (4%)	$[M\ (CHOEt)]^+$ OR $[M\ (CHCO_2H)]^+$ (100%) $[M\ (CHCO_2Et)]^+$ (38%) B (66%) $[M\ (C=C=O)]^+$ (11%)	B (100%) $[M\ (C=C=O)]^+$ (2%) $[M\ (CHOEt)]^+$ OR $[M\ (CHCO_2H)]^+$ (95%)
C-complex+EDA tBu-complex	$[M\ (CHCO_2Et)]^+$ (100%) $[M\ (CHOEt)]^+$ OR $[M\ (CHCO_2H)]^+$ (13%) $[M\ (C=C=O)]^+$ (20%)	$[M\ (CHOEt)]^+$ OR $[M\ (CHCO_2H)]^+$ (65%) $[M(CHCO_2Et)]^+$(100%) C (2%) $[M\ (C=C=O)]^+$ (14%)	C very low intensity $[M\ (C=C=O)]^+$ (93%) $[M(CH_2)]^+$ very low intensity $[M\ (CH)]^+$ (6%) M=C: (50%) $[M\ (CHOEt)]^+$ OR $[M\ (CHCO_2H)]^+$ (100%)
D-complex+EDA Benzyl complex	$[M\ (CHCO_2Et)]^+$(100%)	$[M\ (CHOEt)]^+$ OR $[M\ (CHCO_2H)]^+$ (47%) $[M\ (CHCO_2Et)]^+$(80%) D (100%) $[M\ (C=C=O)]^+$ (10%)	D (17%) $[M\ (C=C=O)]^+$ (17%) $[M\ (CH_2)]^+$ (40%) M=C: (7%) $[M\ (CHOEt)]^+$ OR $[M\ (CHCO_2H)]^+$ (100%)

Table 6: List of products for the reactions of the copper bis-oxazolines complexes with ethyl diazoacetate (EDA), and also for the fragmentation of the single addition metal carbene, $[M\ (CHCO_2Et)]^+$ and the subsequent fragmentation of the product that has lost 28 mass units $[M\ (CHCO_2H)]^+$ or $[M\ (CHOEt)]^+$. Intensities are relative to the base peak.

4-3-C Fragmentation of the initial product $[M (CHCO_2Et)]^+$

In the 2nd column of Table 6, the products of CID on $[M (CHCO_2Et)]^+$ are listed (35% of maximum energy for all metal complexes).

There are three general pathways:

1- The first one is the loss of 28 mass units from $[M (CHCO_2Et)]^+$ to give $[M (CHCO_2H)]^+$ or $[M (CHOEt)]^+$. The complex $[M (CHOEt)]^+$ is related to the Wolff rearrangement product and involves a ketene intermediate (see Scheme 6). This ketene intermediate can dissociate to give the metal cation complex. After CO loss, the resulting complex $[M (CHOEt)]^+$ can rearrange to a coordination complex with an aldehyde (see Scheme 8). This complex could then dissociate to the metal cation complex.

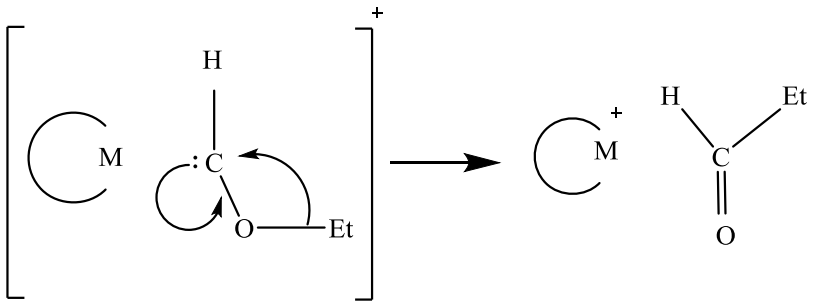

Scheme 8: Rearrangement of $[M (CHOEt)]^+$

Loss of 28 mass units can also give $[M (CHCO_2H)]^+$. This is likely come from the insertion (bridging) product. It can also potentially lose H_2O to give $[M (C=C=O)]^+$.

2- Loss of ethanol to give $[M (C=C=O)]^+$.

3- Loss of the entire adduction unit. The resulting bare metal complex can react again with ethyl

diazoacetate. The amount of the bare metal complexes observed reflect not only the amount of this fragmentation pathways, but also the subsequent rate of reaction of the bare complexes with ethyl diazoacetate.

All the complexes exhibit this general pattern, though (A) is complicated by multiple secondary reactions. The presence of the cumulene and metal cation complexes suggests that Wolff rearrangements and insertion products are formed in the initial reaction with ethyl diazoacetate.

4-3-D: Fragmentation of the secondary product $[M (CHCO_2H)]^+$ or $[M (CHOEt)]^+$

CID (30% of maximum energy) was used to investigate the fragmentation of the complex from the loss of 28 mass units $[M (CHCO_2H)]^+$ or $[M (CHOEt)]^+$. In general the fragmentation pattern of $[M (CHCO_2H)]^+$ in bis-oxazolines complexes is expected to be similar to the porphyrin complexes as described in Chapter 3 (Table 4). The insertion (bridging) complexes tend to fragment like esters and lose ethene (28 mass units) and possibly decaboxylate to give $[M (CH_2)]^+$ or $[M(CH)]^+$ products. The cumulene $[M (C=C=O)]^+$ can also form from the insertion product$[M (CHCO_2H)]^+$ and lead to M=C with CO loss. Formation of the bare metal bis-oxazolines complexes likely comes from Wolff rearrangements that lead to the ketene complex, which can dissociate, or CO loss products which can rearrange to an aldehyde complex and then dissociate to give the bare metal complex as we described in the previous section.

In looking at the data, we will assume that formation of the bare metal complex comes from the Wolff rearrangement and the other pathways (e.q. $[M (CH)]^+$, $[M (CH_2)]^+$ and [M

$(C=C=O)]^+$ are from the insertion products. With this approach it appears that (B) gives the greatest amount of Wolff rearrangement and the other complexes are dominated by insertion. The analysis is complicated because we are only looking at the subset of $[M\ (CHCO_2H)]^+$ and $[M\ (CHOEt)]^+$ complexes that survived the first fragmentation. However, the data clearly suggest a mix of Wolff rearrangement and insertion.

4-3-E: Kinetics:

The reaction of the phenyl copper complex (A) with the ethyl diazoacetate (EDA) is the fastest reaction, followed by tBu- copper complex (C) reaction with the ethyl diazoacetate and then isopropyl-copper complex (B) reaction with the ethyl diazoacetate, and finally the slowest reaction is the benzyl copper complex (D) reaction with the ethyl diazoacetate. All of them have good std. dev. values (see Table 7).

From the rate constant values in Table 7 we can recognize that there is a trend from the phenyl to the benzyl complexes commensurate with the expected steric demands of the substituents. The only exception of this trend is the isopropyl copper complex (B) which is not faster than the tert-butyl copper complex (C). We can explain this defect in the trend from the structures of the two copper complexes, B and C. In the isopropyl copper complex (B), there is an ethyl group attached to the carbon joining the two oxazolines rings that could sterically hinder the reaction, compared with the methyl groups attached to the carbon joining the two oxazolines rings in the tBu-copper complex (C).

The phenyl copper complex (A) is the fastest complex due to the smallest steric effects. The benzyl copper complex (D) is the slowest one due to steric effects with the benzyl groups and

potentially poor binding between the Cu and the diazoacetate, due to interference by the benzyl groups. It is possible that the benzyl groups coordinate to the Cu and deactivate the binding between the Cu and the reagent.

Copper bis-oxazolines+EDA	Rate Constant ±std. dev. % cc/molecule/sec.
(A+EDA)	4.47E-10 ±2.8%
(C+EDA)	3.43E-10 ± 3.0%
(B+EDA)	1.38E-10 ±1.1%
(D+EDA)	3.65E-11 ±1.9%

Table 7: Rate constant of the copper complexes reaction with ethyl diazoacetate.

4-3-F: Reactivity of metal complex [M ($CHCO_2Et$)]$^+$

To support our belief that the formal metal carbene ($M=CR_2$) is not stable and rearranges after formation, we allowed many alkenes such as ethyl vinyl ether, trichloroethylene, 3, 4-dihydro-2H-pyran and cyclohexene (purchased from Sigma-Aldrich St. Louis, MO, USA) to react with the metal complex [M ($CHCO_2Et$)]$^+$. There is no evidence of a reaction, and we reach a dead end with exactly the same fate as the porphyrin systems described in the previous chapter. It appears that these reaction products have all undergone insertion or a Wolff rearrangement.

4-3-G: Conclusions

Ligated Cu (1) species readily undergo reactions with ethyl diazoacetate (EDA). The main product is addition with loss of N_2, $[M (CHCO_2Et)]^+$. Multiple additions occur in some cases and these depend on steric factors in the copper ligand. Copper bis-oxazolines with a phenyl group (A) give multiple additions, while copper bis-oxazolines with a benzyl group (D) tend to have a single addition due to possible coordination between the benzene π-system and copper metal. The multiple additions trend for the complexes is A>B>C>D.

The fragmentation behavior of the single addition with loss of N_2, $[M (CHCO_2Et)]^+$ depends on the whether the carbene inserts to give a bridging product or undergoes a Wolff rearrangement. Applying CID energy to the $[M (CHCO_2Et)]^+$ with coordination-type binding (Wolff rearrangement) could lead to formation of the original complexes. From the intensities of the original complexes A, D, B, C in the second column of Table 6, the trend for the coordination product would be as D> B> A> C. However, these complexes can undergo reactions with ethyl diazoacetate in the ion trap and are unreliable for predicting yields. The fact the amounts are inversely proportional to the rate constants of the ethyl diazoacetate reaction supports this conclusion. The insertion product is expected to fragment like an ester.

From the fragmentation pattern of $[M (CHCO_2H)]^+$ or $[M (CHOEt)]^+$ complexes in bis-oxazolines complexes A, D, B, and C, we can estimate which product dominates. If the pattern of the fragmentation pathway of $[M (CHCO_2H)]^+$ complexes is similar to the porphyrin complexes as described at Chapter 3 than insertion (bridging) is assumed to be more favorable. This conclusion does not prevent or totally eliminate the formation of $[M (CHOEt)]^+$ complexes with the same m/z value of the complex $[M (CHCO_2H)]^+$.

$[M(CHOEt)]^+$complexes come from the loss of CO from a Wolff rearrangement product (see Scheme 6) and likely lead to the formation of the bare metal complexes during CID. The data suggests a mix of the two forms.

The phenyl copper complex (A) and tBu-copper complex (C) have high rate constants in their reactions with ethyl diazoacetate, but the phenyl copper complex (A) faster than the tBu-copper complex (C) due to the bulkiness of the tBu-group. The isopropyl copper oxazoline (B) is slower than the tBu-copper oxazolines complex (C) reaction due to the steric effect of the ethyl groups at the carbon bearing the oxazolines rings. Finally, the benzyl copper bis-oxazolines (D) is the slowest reaction due to the steric effect of the benzyl groups. The two possible products insertion (bridging) and Wolff rearrangement $[M(CHCO_2Et)]^+$ are not active when we tried to react an alkene with them, suggesting that they lack carbene character.

Chapter 5- Gas-Phase Synthesis of Copper 1, 10-phenanthroline Carbene Complexes and Evaluation of their Structure and Reactivity

5-1 Objective

Our objective in this study is to prepare copper carbene complexes, examine the mechanism of the copper carbene complex formation, and examine the reaction pathways of copper carbene complexes with alkenes. According to the generic catalytic cycle of metal-catalyzed reactions of diazo-compounds shown in Figure 5, there are two processes; the first process is the metal carbene complex formation, while the second process is the reaction with alkenes to obtain a cyclopropane and reform the copper cation complex.

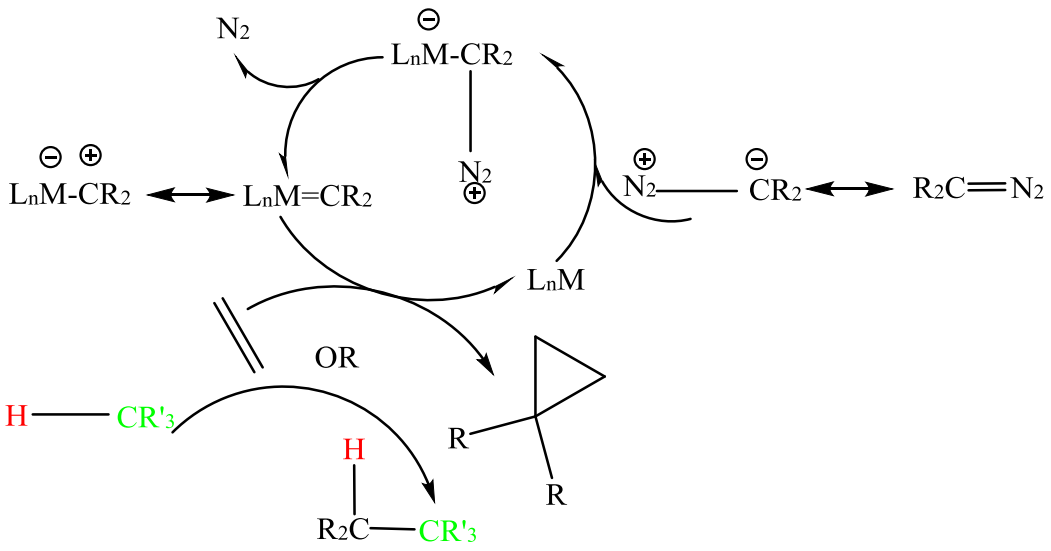

Figure 5: Generic catalytic cycle of metal-catalyzed reactions of diazo-compounds.

5-2 Introduction

Metal carbene complexes ($M=CR_2$) are important in organic synthesis, (particularly for cyclopropanations and C-H insertions) and are often part of catalyzed reactions. Many metal complexes have been used as catalysts. Copper is a very common metal for metal carbene formation, and is used in catalytic cycles with alkenes to form cyclopropanes.[111-114] However, as useful as these copper carbene complexes are, not much is known about the nature of the copper carbene intermediate that is part of the catalytic cycle. In this study, we explore the synthesis of copper carbene complexes in the gas phase in an ion trap mass spectrometer using several carbene precursors and 1, 10- phenanthroline (phen) as the copper ligand. It was used due to its rigid structure, which may prevent the insertion products found in the previous work with porphyrins and bis-oxazolines. 1, 10- phenanthroline is a bidentate ligand which allows vacant coordination sites for the alkene to coordinate to the copper carbene complex. Bis-oxazoline complexes are more flexible than 1, 10- phenanthroline complexes. In addition, a novel approach to carbene formation was developed using betaine as the carbene precursor. This pathway leads to a metal carbene and allows us to probe the reactivity of the copper carbene with several alkenes. This mechanistic gas-phase study brings a better understanding of metal-catalyzed transformations and complements information available in the condensed phase.

5-3 Experiment Design

1, 10- phenanthroline (phen) is a versatile ligand with many important properties for this study. It has a rigid structure imposed by the center ring, it is commercially available, and is soluble in most organic solvents, and it readily forms metal complexes.[115]

We formed the 1, 10- phenanthroline copper cation complex by addition of 1, 10- phenanthroline (purchased from Sigma-Aldrich St. Louis, MO, USA) at a concentration of 10^{-4} M in methanol (purchased from Fischer-Scientific, Fair Lawn, NJ, USA) to copper trifluoromethanesulfonate (purchased from Sigma-Aldrich St. Louis, MO, USA). At a concentration of 10^{-4} M in methanol at room temperature (see Figure 28). The ESI spectrum of the 1, 10- phenanthroline copper complexes is shown in Figure 29.

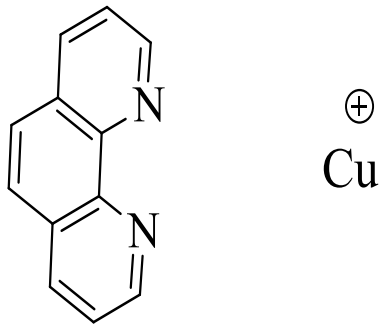

Figure 28: 1, 10- phenanthroline complex with copper complex.

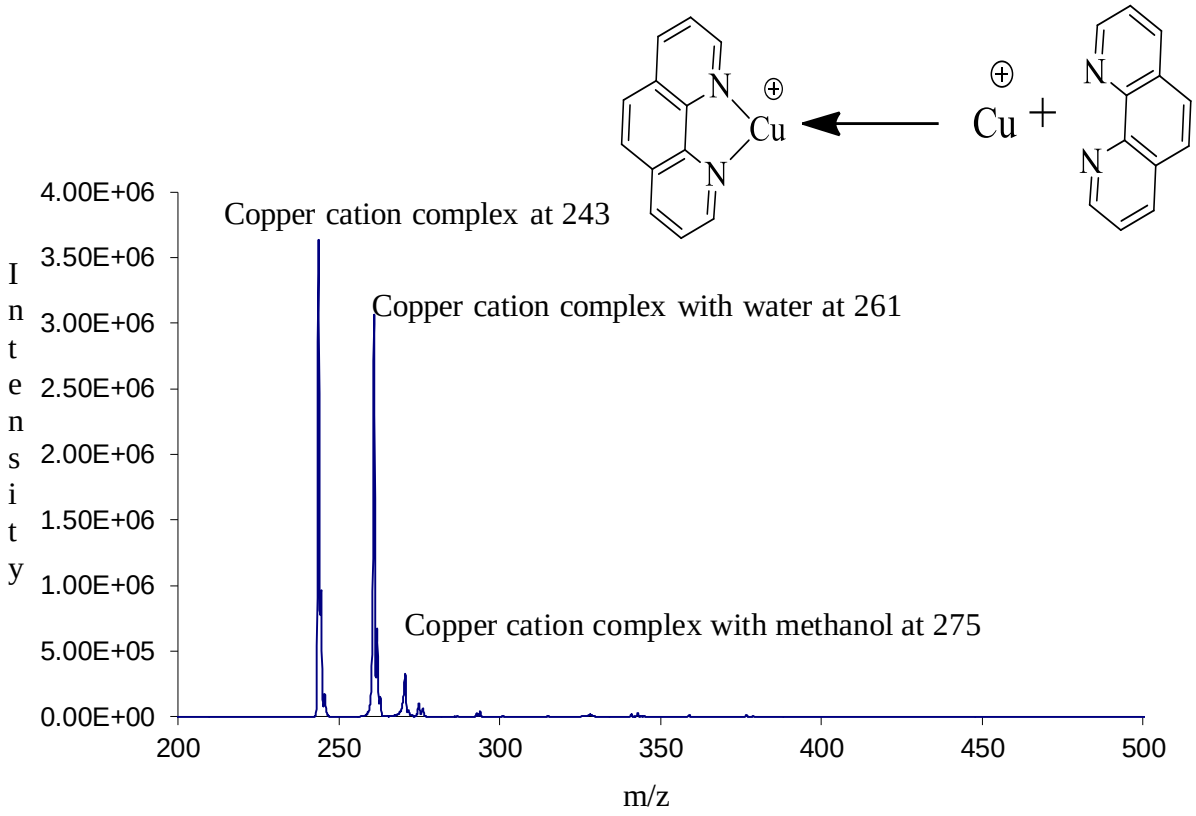

Figure 29: 1, 10- phenanthroline copper cation complex.

Note: In this spectrum, some complexation reactions with background water (m/z =261) and methanol (m/z =275) were observed.

5-4 Diazoacetate as carbene source

We allowed the 1, 10- phenanthroline copper cation complex (m/z =243) formed by electrospray ionization (ESI) to react in the ion trap with a 10% solution of ethyl diazoacetate in cyclohexane. Addition with loss of N_2 is seen at m/z =329 $[M\ (CHCO_2\text{-}Et)]^+$. Spontaneously, the $[M\ (CHCO_2\text{-}Et)]^+$ complex can lose 28 mass units, which we assume is CO in a Wolff

rearrangement, giving $[M (CHO-Et)]^+$ complexes as the major product at m/z =301 (see Figure 30). Support for this assumption is given in a subsequent section.

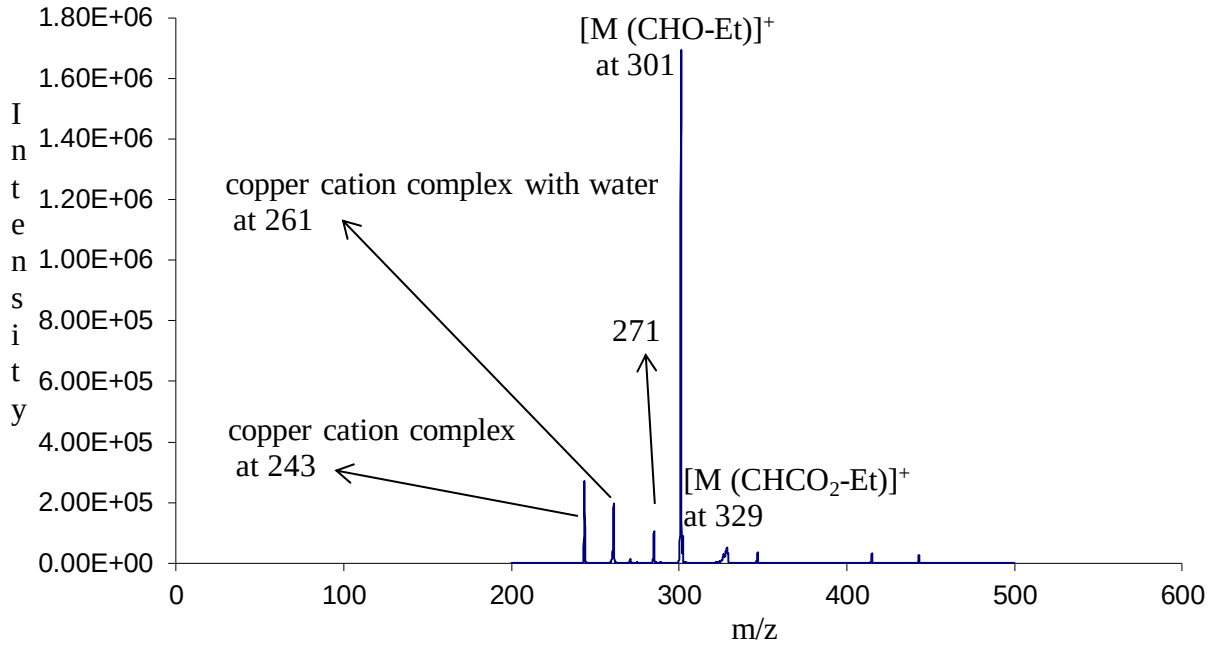

Figure 30: Spectrum of the 1, 10 phenanthroline cation complex + ethyl diazoacetate.

The peak at 271 could be either a copper cation complex coordinated with ethylene having lost formaldehyde as shown in Figure 36 or an $[M (C=O)]^+$ species having lost ethane as shown in Figure 31. We cannot distinguish these products because they have the same m/z at 271.

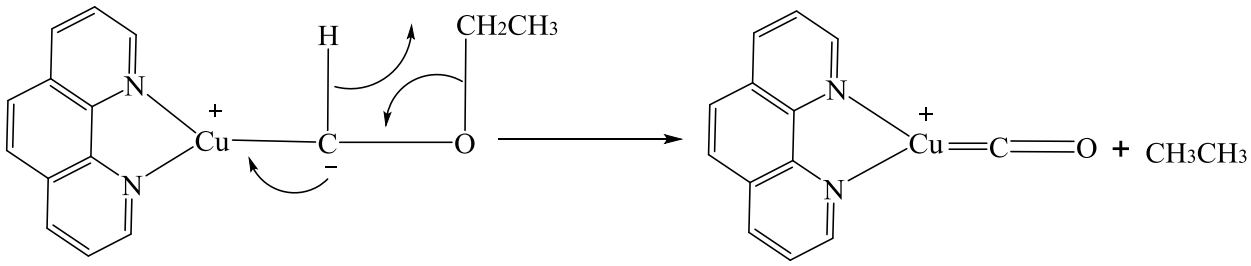

Figure 31: Proposed mechanism of the $[M (C=O)]^+$ species formation from $[M (CHO-Et)]^+$

When applying CID to the $[M (CHO-Et)]^+$ complex (m/z =301), thirty mass units are lost, giving the metal cation complex coordinated with ethylene or C=O at m/z =271; this is the same peak obtained spontaneously when the 1, 10 phenanthroline cation complex reacts with ethyl diazoacetate (see Figure 30). Under CID, the 1, 10- phenanthroline copper cation complex (m/z =243) coordinated with water at m/z =261 are detected also (see Figure 32). This pattern makes us more confident that the Wolff rearrangement product dominates because if the product was formed by insertion followed by ethene loss (i.e. ester cleavage), there is no route back to the 1, 10- phenanthroline copper cation complex (m/z =243).

There is no evidence for any reactions when we introduced a series of alkenes such as ethyl vinylether, trichloroethylene, 3, 4-dihydro-2H-pyran and cyclohexene (purchased from Sigma-Aldrich St. Louis, MO, USA) to react with the $[M (CHCO_2-Et)]^+$ complex. This is another reason to push us to believe that the product formed from the reaction of the 1, 10-phenanthroline cation complex with ethyl diazoacetate is a Wolff rearrangement form $[M (EtOCH=C=O)]^+$ which spontaneously loses CO to give $[M (CHO-Et)]^+$ (see Figure 36). Beauchamp found a similar conclusion that the Wolff rearrangement products are inactive toward reactions with alkenes.[110]

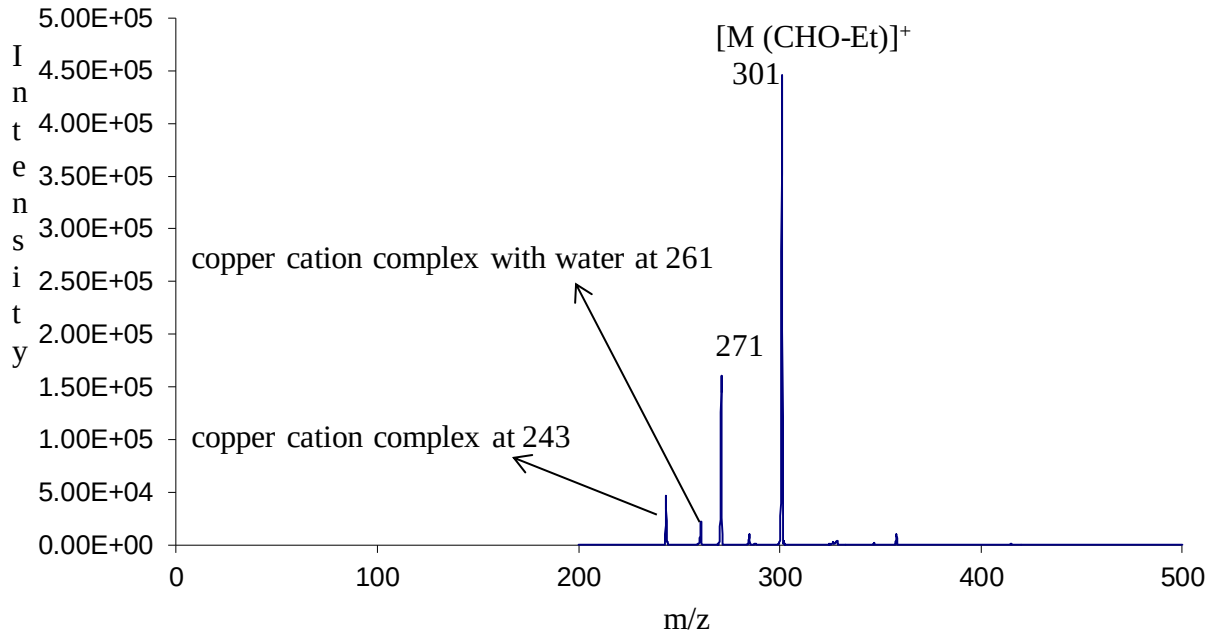

Figure 32: Fragmentation of Wolff rearrangement product $[M (CHO-Et)]^+$ at m/z =301 losing formaldehyde at m/z=271.

Similar reactions pathways are observed when the 1, 10 phenanthroline copper cation complex (m/z =243) reacts with a 10% solution of tert-butyl diazoacetate in cyclohexane. Here a significant yield of the addition with loss of N_2 product is formed at m/z =357 $[M (CHCO_2\text{-}tBu)]^+$. Spontaneously, the $[M (CHCO_2\text{-}tBu)]^+$ complex loses 28 mass units (CO as we assumed) giving $[M(CHO\text{-}tBu)]^+$ complexes as the major product at m/z =329. The 1, 10- phenanthroline copper cation complex (m/z =243) and 1, 10- phenanthroline copper cation complex coordinated with water at m/z =261 are also seen (see Figure 33). We do not see a peak for the loss of isobutene, which would be expected for on insertion followed by an ester fragmentation.

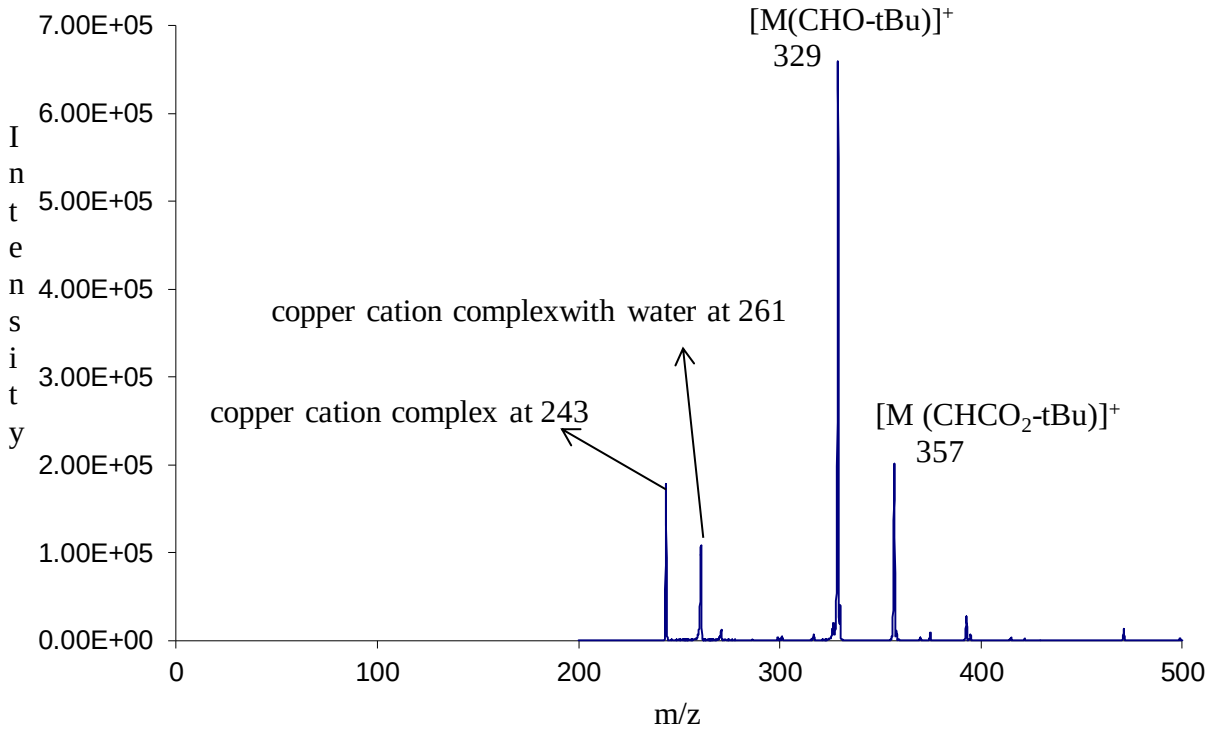

Figure 33: Copper 1, 10-phenanthroline cation complex + tert-butyl diazoacetate.

After applying CID to fragment the $[M\ (CHO\text{-}tBu)]^+$ complex (m/z =329), 30 mass units are lost, which we interpret as loss of formaldehyde, which forms a 1, 1 dimethyl ethylene $[(CH_3)_2C{=}CH_2]$ complex with the copper cation at m/z =299 (see Figure 34).

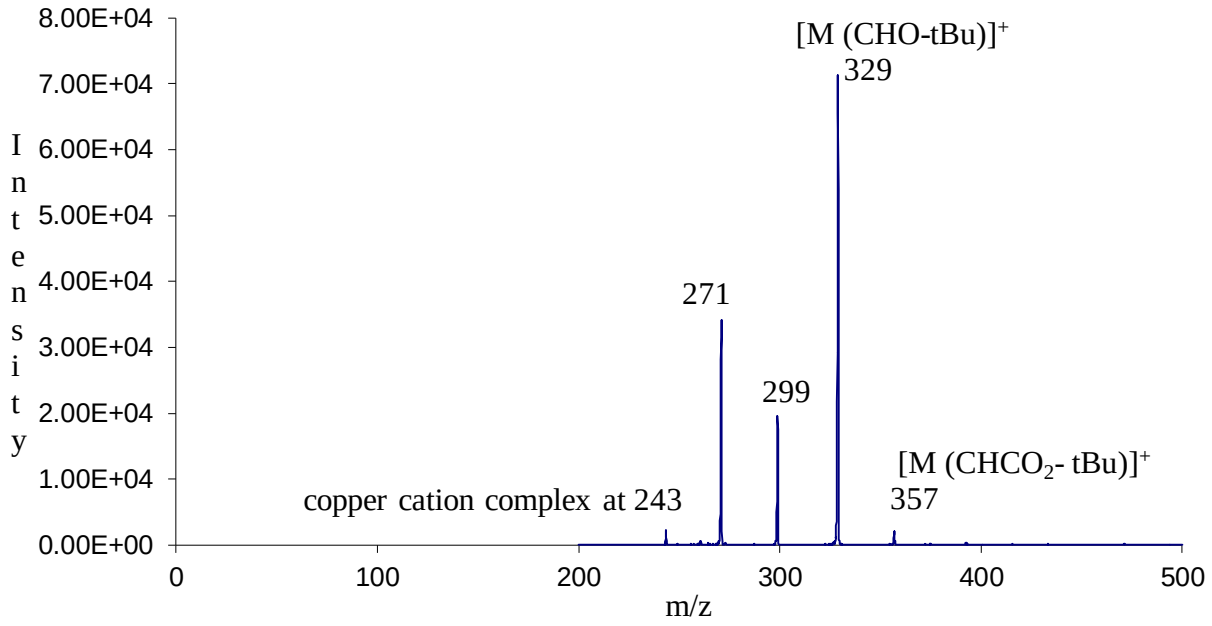

Figure 34: Fragmentation of Wolff rearrangement product $[M (CHO\text{-}tBu)]^+$ at m/z=329 losing formaldehyde at m/z=299.

From the fragmentation patterns of $[M (CHO\text{-}Et)]^+$ at m/z=301 and $[M (CHO\text{-}tBu)]^+$ at m/z =329 as shown in Figures 32 and 34, we see that the former gives a peak at m/z=271 and the later gives two peaks, one at m/z =271 and one at m/z =299. The peak at m/z =299 can be explained by formaldehyde loss as shown in Figure 37.

This gives us confidence that the pathways involving formaldehyde loss as shown in Figures 36 and 37 are active for both diazoacetates.

The m/z =271 peak in Figure 34 can be explained by the formation of a $[M (C=O)]^+$ species (see Figure 35). This suggests that alkane loss is active here and likely also occurs with ethyl diazoacetate (see Figure 31).

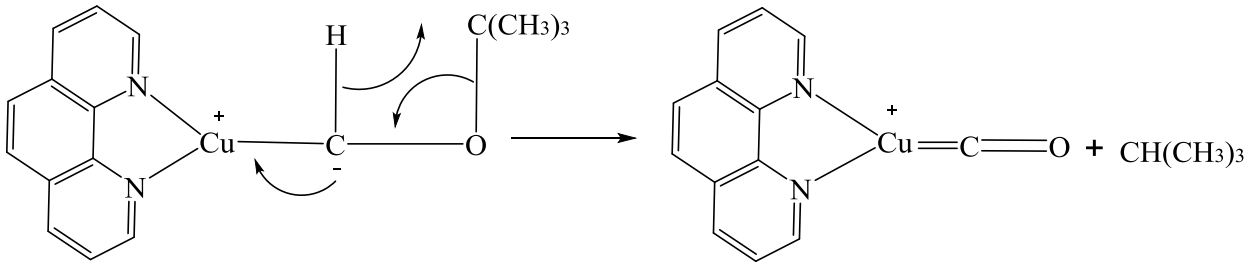

Figure 35: Proposed mechanism of the $[M (C=O)]^+$ species formation from $[M (CHO\text{-}tBu)]^+$

There is no evidence for any reaction when we introduced alkenes such as ethyl vinylether, trichloroethylene, 3, 4-dihydro-2H-pyran and cyclohexene (purchased from Sigma-Aldrich St. Louis, MO, USA) to react with the $[M (CHCO_2\text{-}tBu)]^+$ complex. This pushes us to believe that the product formed from the reaction of the 1, 10- phenanthroline cation complex with tert-butyl diazoacetate is a Wolff rearrangement form $[M (CH (OtBu)=C=O)]^+$ which spontaneously loses CO to give us a $[M (CHO\text{-}tBu)]^+$ complex (Figure 37). Beauchamp found the same conclusion we reached that the Wolff rearrangement products are inactive toward the reaction with alkenes.[110] In general we interpret the loss of CO from $[M (CHCO_2\text{-}Et)]^+$ and $[M (CHCO_2\text{-}tBu)]^+$ complexes giving $[M (CHO\text{-}Et)]^+$ and $[M (CHO\text{-}tBu)]^+$ complexes respectively, as the major products, most likely from a Wolff rearrangement.[110] Pathways to the products observed in Figures 30, 32, 33 and 34 are summarized in Figures 36 and 37.

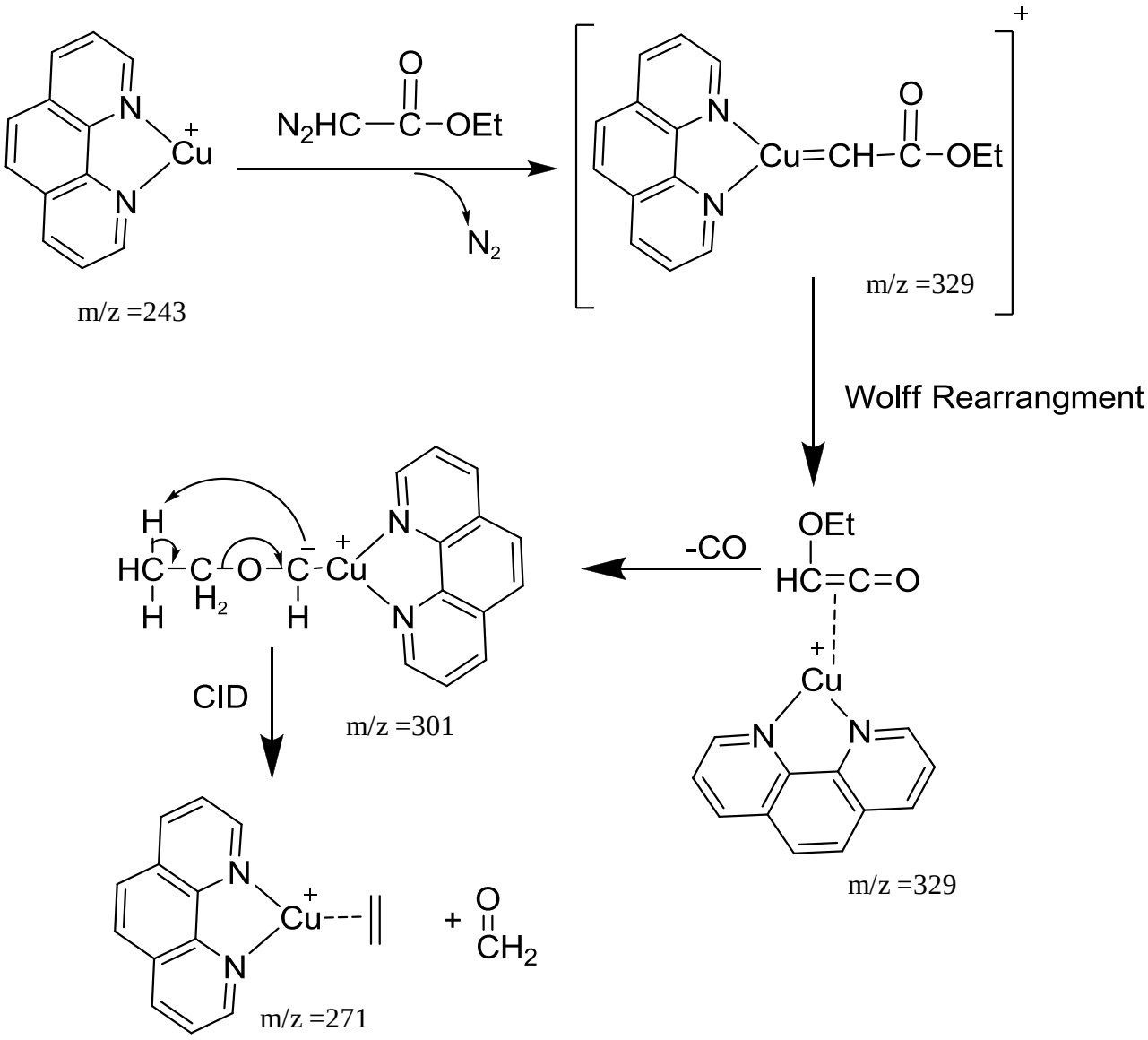

Figure 36: Proposed mechanism of the copper cation complex reaction with ethyl diazoacetate, giving a Wolff rearrangement product $[M\ (CHCO_2Et)]^+$ and subsequent fragmentations

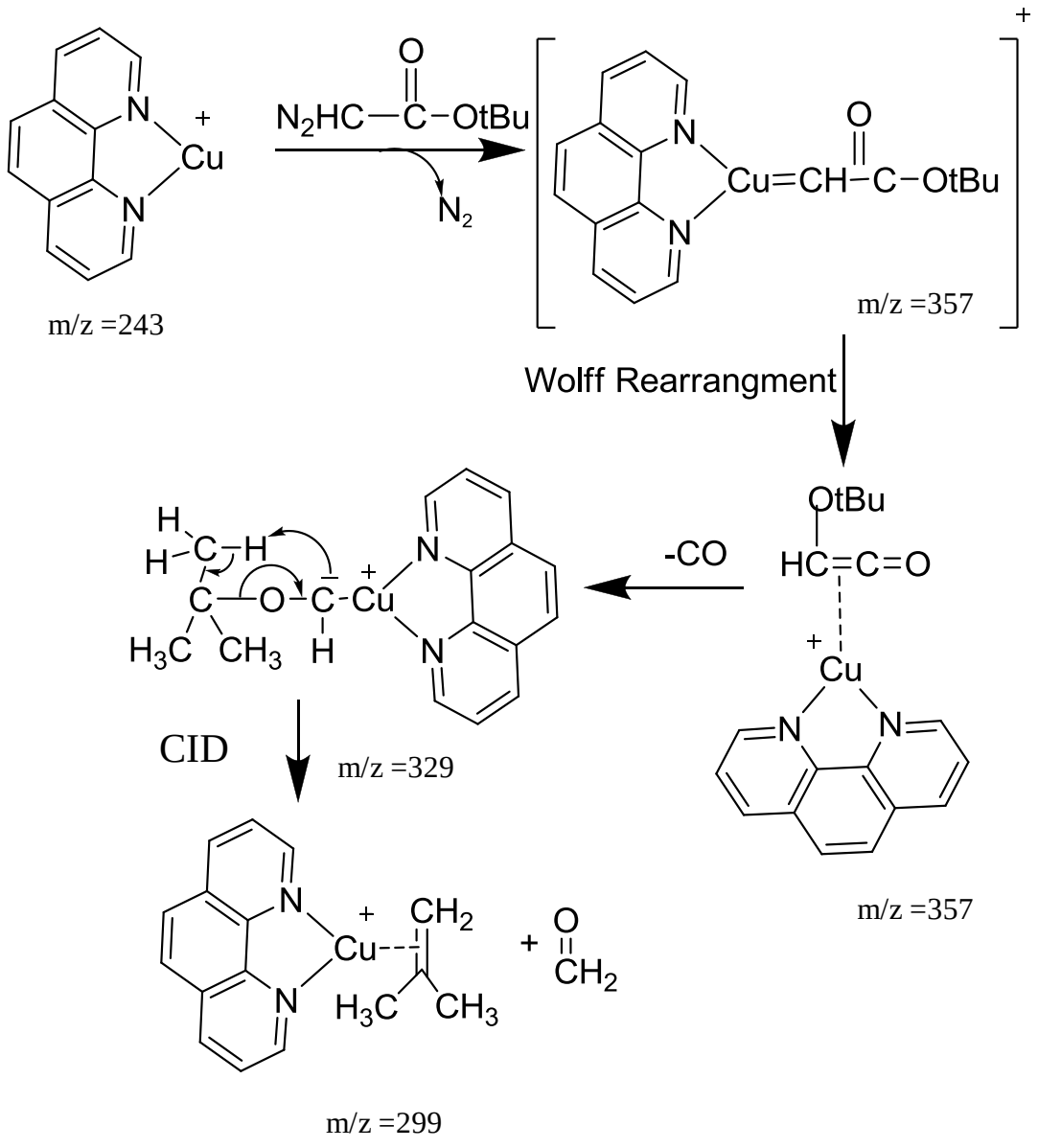

Figure 37: Proposed mechanism of the copper cation complex reaction with tert-butyl diazoacetate, giving a Wolff rearrangement product $[M\ (CHCO_2\,tBu)]^+$ and subsequent fragmentations.

5-5 Trimethylsilyldiazomethane as carbene source

To avoid the Wolff rearrangement products, we turned to trimethylsilyldiazomethane (Si $(CH_3)_3CHN_2$) (purchased from TCI America Portland, OR, USA), as a carbene precursor. Trimethylsilyldiazomethane (m/z =86) reacts with the copper 1, 10- phenanthroline cation complex (m/z = 243) by addition with loss of N_2, giving a product at m/z 329. Because the reaction is slow, water competes with trimethylsilyldiazomethane in the reaction and coordinates with water is the base peak (see Figure 38).

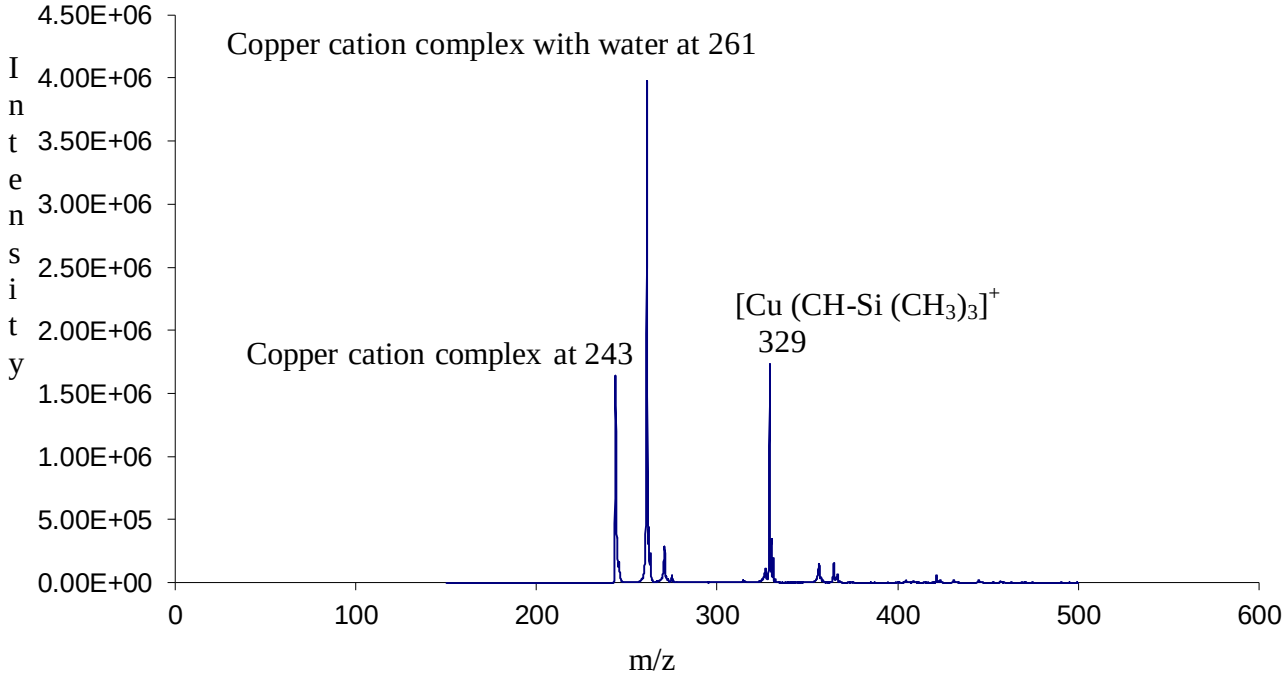

Figure 38: Reaction of copper 1, 10- phenanthroline complex with trimethylsilyldiazomethane.

To explore the reaction cycle (see Figure 5) with the copper carbene product [Cu (CH-Si $(CH_3)_3]^+$,we allowed it to react alkenes. Many alkenes, including ethyl vinylether, cyclohexene, trichloroethylene and 3, 4-dihydro-2H-pyran (purchased from Sigma-Aldrich St. Louis, MO. USA), were introduced into the ion trap and allowed to react with [Cu (CH-Si $(CH_3)_3]^+$, but there was no evidence of a chemical reaction. The carbene should be highly reactive, so the lack of reaction with this set of alkenes suggests that it rearranged. A 1, 2 methyl migrations is another type of rearrangement that destroys the carbene and prevents the cycle shown in Figure 5. Analogies to free carbene chemistry, as well as computational modeling, suggest that a 1, 2 methyl migrations can take place to give a silaethene. Modeling data from the research group indicate that the barrier to rearrangement is low, 3.5 kcal/mol at the M06/6-311+G** level, and would occur rapidly. A proposed mechanism can be seen in Figure 39.

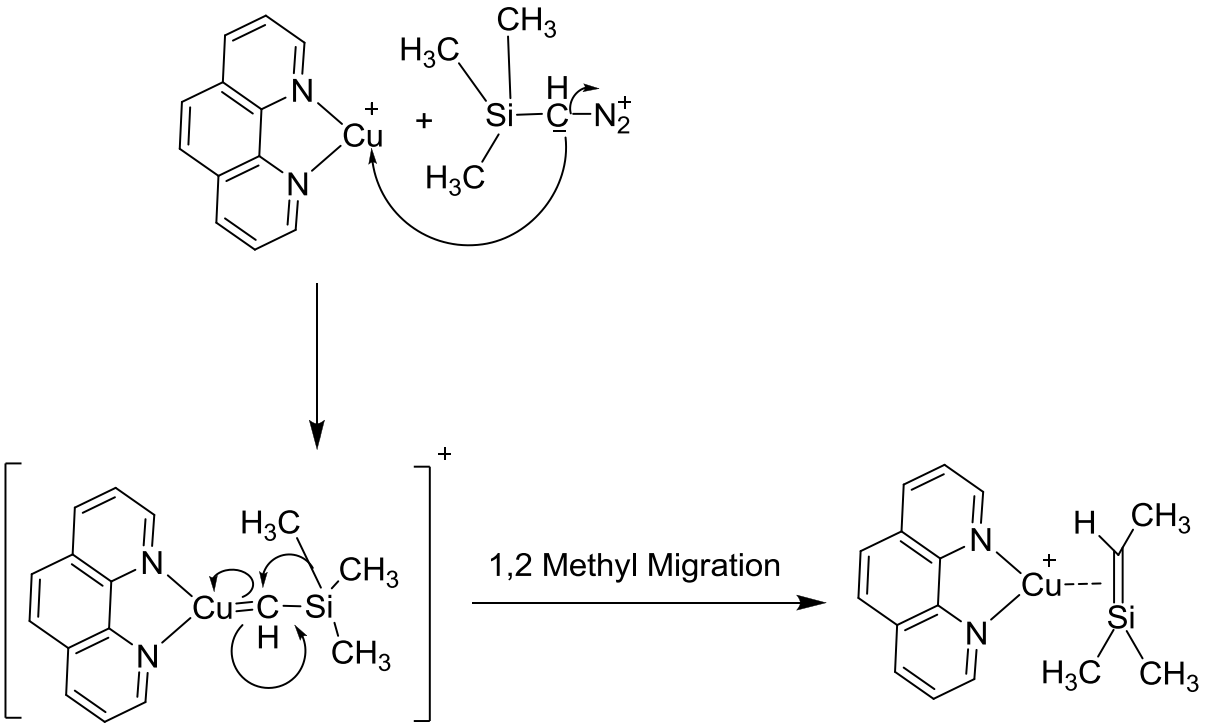

Figure 39: Proposed mechanism of the reaction of copper 1, 10- phenanthroline complex with trimethylsilyldiazomethane.

5-6 Betaine as ylide precursor

It is not easy to form ligated metal carbenes ($M=CR_2$) in the gas phase due to the formation of the insertion products[109] and rearrangents[110]. The insertion product is common with ligands like the porphyrins and bis-oxazolines.[109]Ligated copper carbenes cannot be formed from ethyl diazoacetate and tert-butyl diazoacetate reactions with copper 1, 10 phenanthroline complexes because, after losing N_2, the carbene can rearrange to a ketene form (Wolff rearrangement).[110]

Trimethylsilyldiazomethane also gave a product that rearranged and destroyed the carbene. The parent carbene, CH_2, is an attractive option because it cannot rearrange, but diazomethane as carbene sources is a dangerous material and the exothermicity of the reaction can potentially lead to an insertion product.

Previous work by Chen showed that an ylide complex could be used to form a gold carbene complex[116] by using CID to dissociate the PPh_3 group as shown in Figure 40. Chen demonstrated alkene reactions with the gold carbenes he obtained.

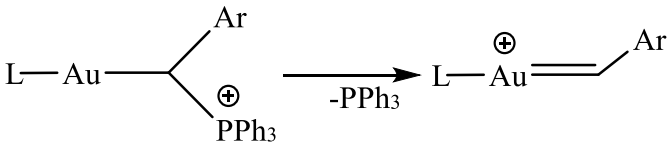

Figure 40: Gold carbene complex formation from gold ylide complex.

Inspired by Chen's work, we turned to betaine as an ylide source. Reacting 1, 10-phenanthroline copper cation complex with betaine (purchased from Fischer-Scientific, Fair Lawn, NJ, USA) 1:1 ratio, we obtained the copper complex as shown in Figure 41.

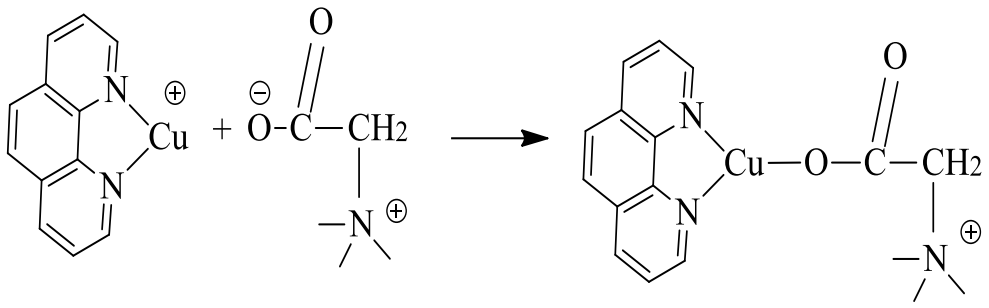

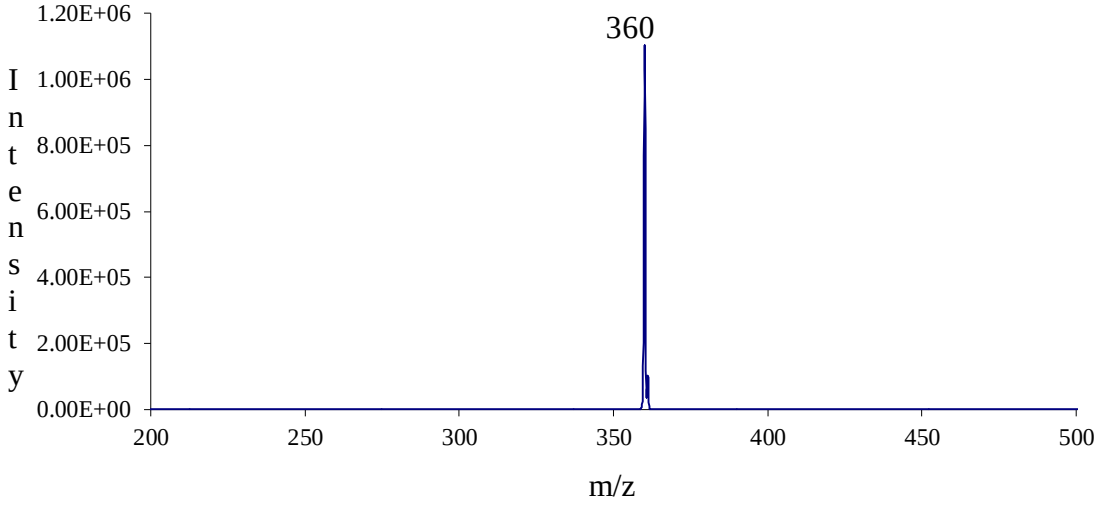

Figure 41: Reaction of the copper 1, 10- phenanthroline cation complex with betaine.

From here we thought we could prepare a copper ylide complex by decarboxylation. CID of the betaine complex led to CO_2 loss and formation of the described ylide (see Figure 42).

This process is well known and O'Hair gives many examples. Double decarboxylation of a copper dicarboxylate [$CH_3CO_2CuO_2CCH_3$] via CID has been used by O'Hair to obtain the dimethyl cuprate anion [CH_3CuCH_3]$^-$.[117] O'Hair also studied the catalytic cycle of the dimetylcuprate anion [CH_3CuCH_3]$^-$ reaction with allyl acetate ($C_3H_5OCOCH_3$) forming [$CH_3CuO_2CCH_3$]$^-$, followed by decarboxylation via multistage mass spectrometry.[118]

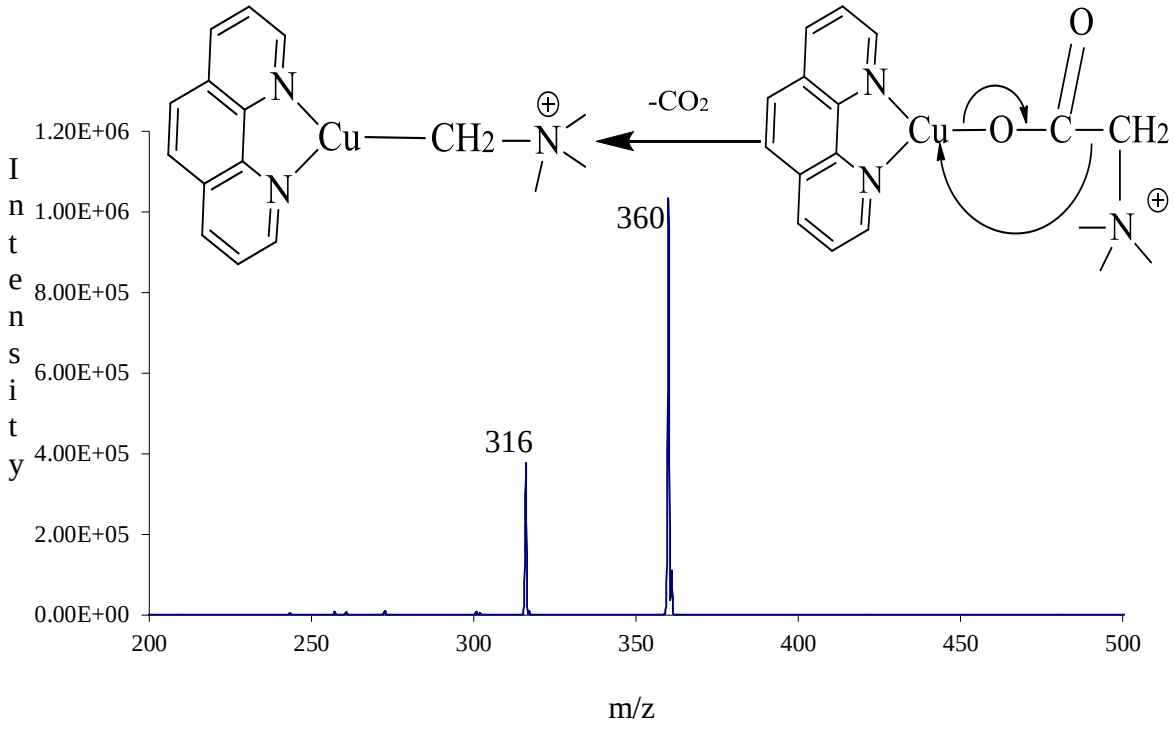

Figure 42: First fragmentation leading to decarboxylation and ylide formation.

This first step is followed by isolation of the ylide product peak at m/z =316, and a second application of CID energy, which results in the loss of the trimethylamine group to potentially give the copper carbene $[M\ (CH_2)]^+$ (see Figure 43).

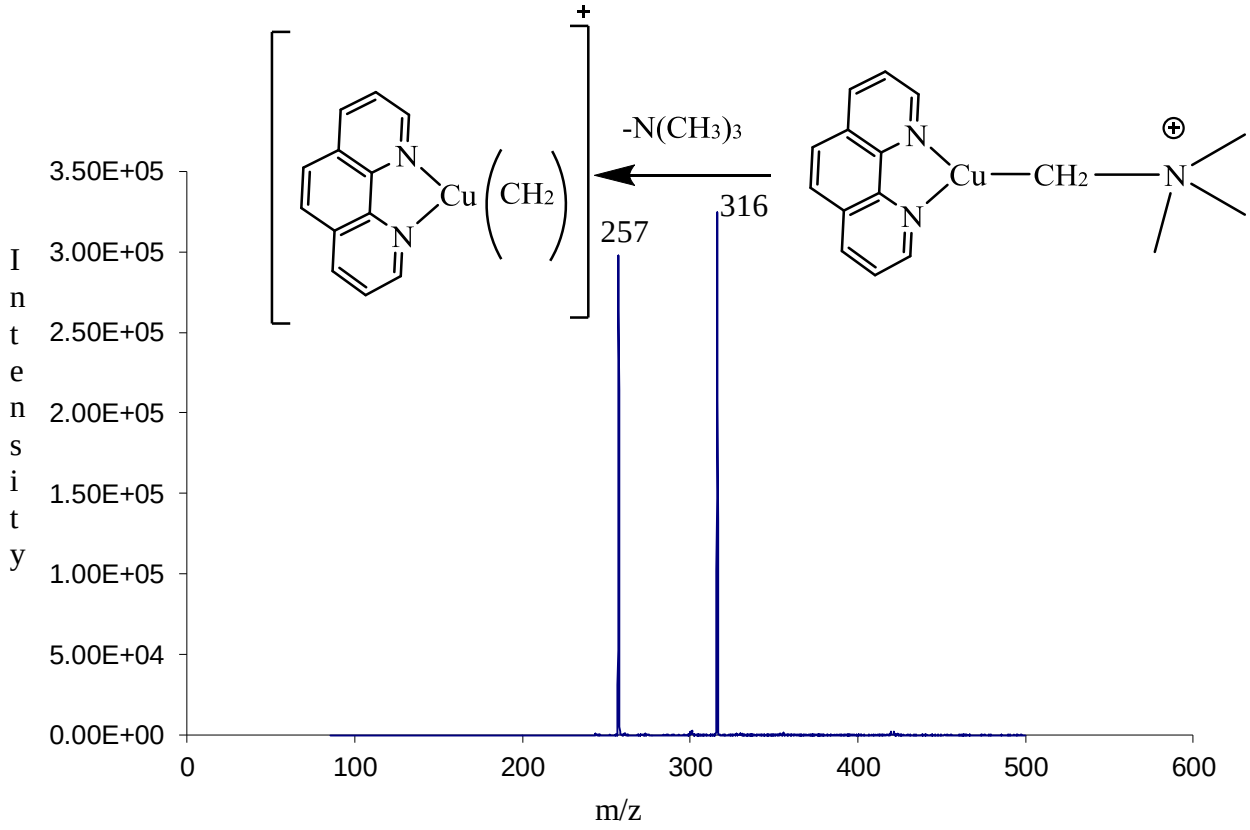

Figure 43: Second fragmentation causing loss of trimethylamine group.

5-7 Forming copper "carbene" $[Cu(CH_2)]^+$ from ylide

Copper "carbene" complexes were generated via a multistage mass spectrometry pathway involving controlled CID energy sequences.[119] Two sequence steps of controlled fragmentation as shown in Figure 44 were used; decarboxylation followed by expulsion of a trimethylamine group (see Figures 42 and 43).

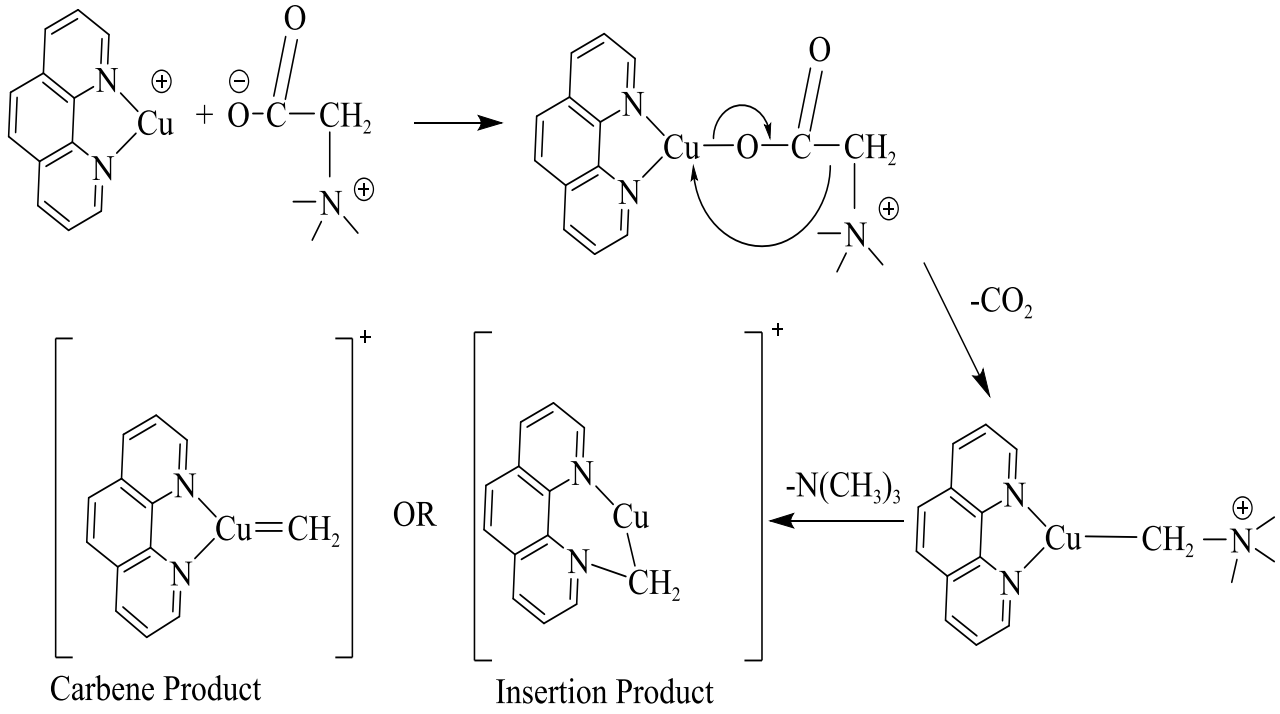

Figure 44: Two steps to form copper 1, 10 phenanthroline "carbene".

5-8: Distinguishing between copper carbene complexes

When we isolate the $[M\ (CH_2)]^+$ complex at m/z =257, there are two possible forms of the copper carbene complex. It could be the true $Cu{=}CH_2$ species or an insertion product involving the Cu-N bond to the phenanthroline.

Under hard conditions, where we applied high CID energy (40%) and a short activation time (40 ms), we formed the copper carbene complex $[M{=}CH_2]^+$ at m/z =257 as the major product along with the insertion product $[M\ (CH_2)]^+$. A spectrum of the peak isolated at m/z=257, under these conditions is shown in Figure 45.

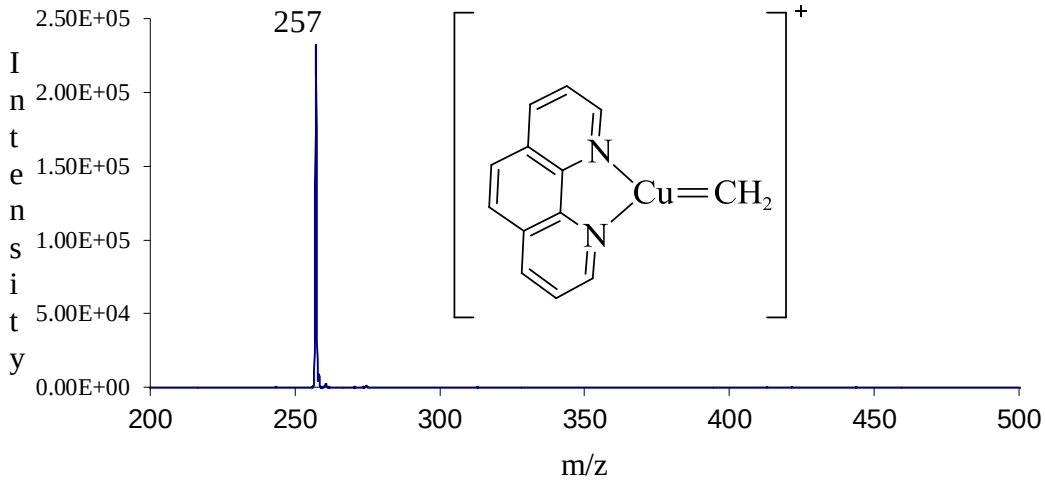

Figure 45: High CID energy and short reaction time (hard conditions) for fragmentation of ylide.

Under soft conditions, where we applied lower CID energy (20%) and a longer activation time (120 ms), we obtained mainly the insertion product $[M(CH_2)]^+$ at m/z =257. Isolation of m/z = 257 obtained under soft conditions gives the spectrum shown in Figure 46.

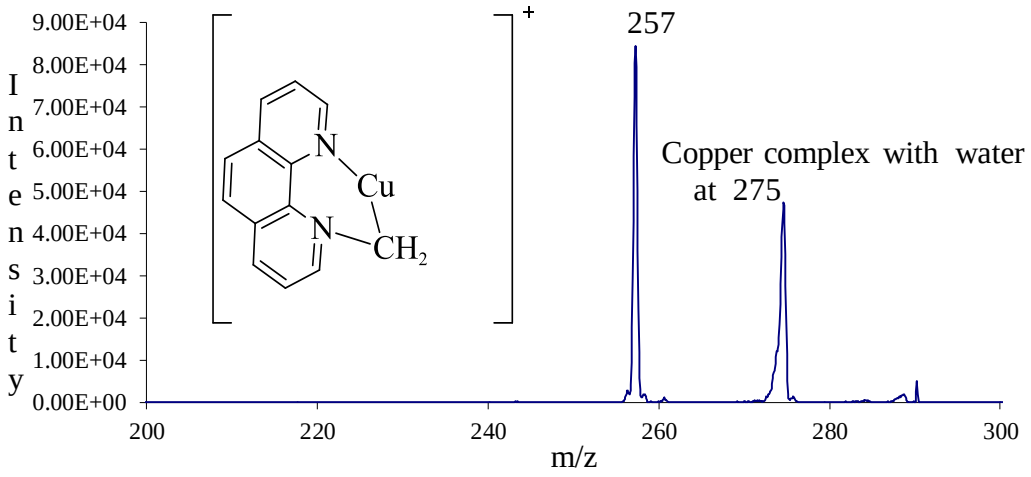

Figure 46: Low CID energy and long reaction time (soft conditions) for fragmentation of ylide.

There are two reasons to lead us to believe that the complex obtained in soft conditions is the insertion product. The first reason is the copper cation complex readily coordinates with water giving a peak at m/z =275 (see Figure 46). This peak is not obtained under hard conditions, and we have previously observed that copper, when it has only two coordination sites, readily forms adducts with water (see Figure 29).

The second reason behind our belief that the complex obtained in soft conditions was the insertion product and the complex obtained in hard conditions is the copper carbene comes from their reactivity with alkenes. The species mainly formed under the hard conditions reacts with alkenes in what appears to be a cyclopropanation process (Scheme 9). This is discussed in more detail below.

The preference in the fragmentation can be rationalized. Under the hard conditions, direct C-N cleavage to release the N $(CH_3)_3$ is favored entropically. Under the soft conditions, it is possible that the phenanthroline nitrogen assists in the deplacement of the N $(CH_3)_3$. This is enthalpically more favorable and leads directly to insertion, but would be much less favorable entropically, especially at the higher internal energiew of the hard CID.

5-9 Reaction of copper carbene $[Cu=CH_2]^+$ with alkenes

In chapters 3 and 4, we have a valuable understanding of the reaction pathways of the diazoesters with transition metal catalysts (metal porphyrin and copper bis-oxazoline systems), which lead to "metal carbene" intermediates that undergo insertions and Wolff rearrangements (see Figure 21 and Scheme 9) respectively. We also studied their kinetics and the fragmentation pathways of the products, but none were related to a true metal carbene. After the success in forming the formal copper 1, 10-phenanthroline carbene complex $[Cu=CH_2]^+$ as shown in Figure 45, we investigated the cycle analogous to the general catalytic cycle shown in Figure 5.

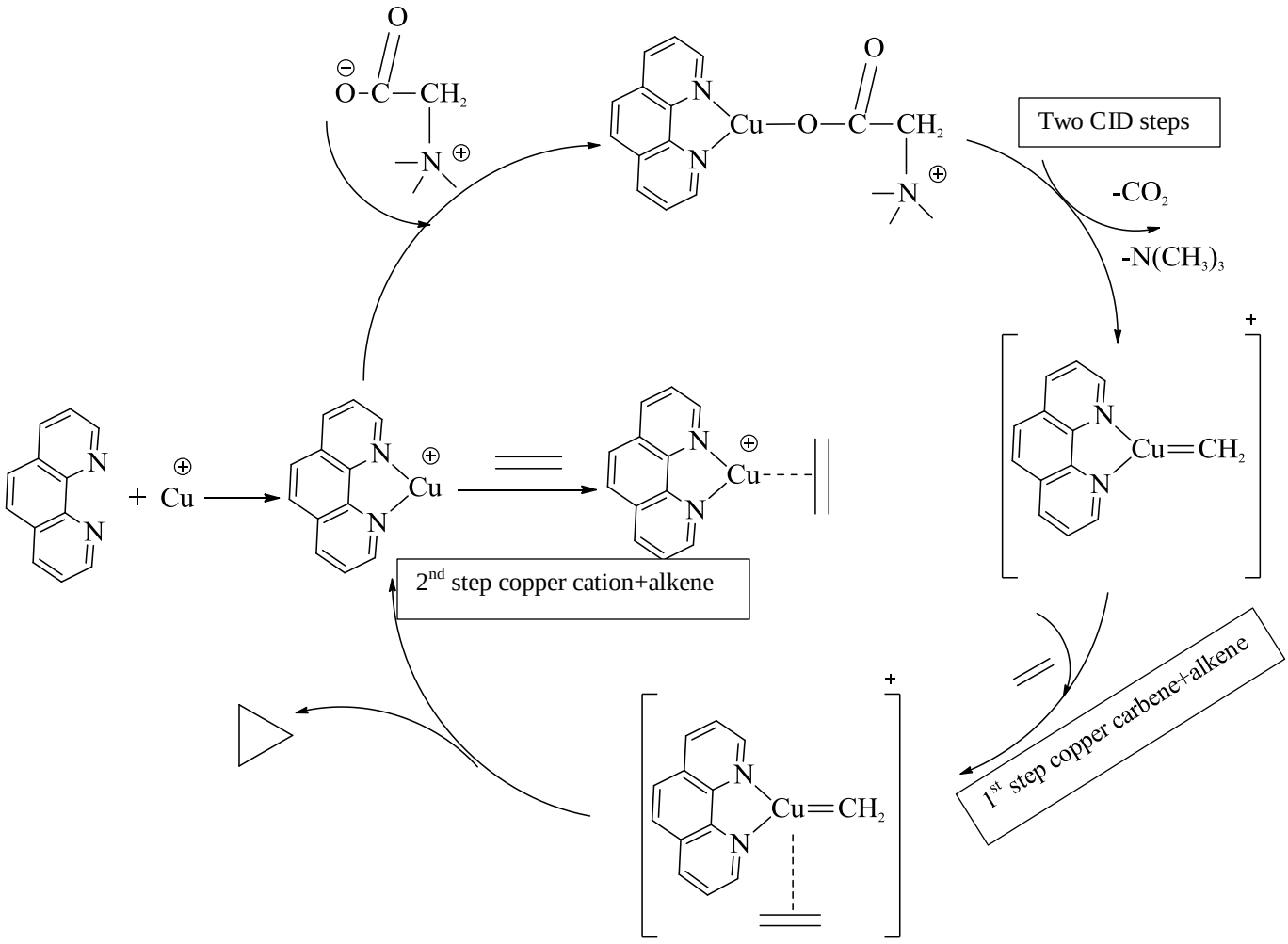

Scheme 9: Cycle involves Cu-carbene.

Based on the cycle shown in Scheme 9, we screened the reactivity of the 1, 10-phenanthroline copper carbene complex with many alkenes such as ethyl vinylether, cyclohexene, trichloroethylene and 3, 4-dihydro-2H-pyran (purchased from Sigma-Aldrich St. Louis, MO. USA). This step leads to the formation of a cyclopropanation and release the copper phenanthroline cation complex.

The 1, 10-phenanthroline copper cation complexes reacts very fast with alkenes forming an alkene complex; therefore, a successful cyclopropanation will lead to the copper cation complex, which will in turn be converted into a copper cation alkene complex.

5-9-A: Soft conditions:

The $M{=}CH_2$ species formed with low CID energy (20%) and a long activation time (120 ms) was allowed to react with many alkenes (Figures 47, 48, 49 and 50). In these spectra, we notice that adducts with alkenes are the major products for all the alkenes we used. This is logical because the formation of the insertion product allows extra space (see Figure 46) for the alkene to coordinate with the copper. We also note that for all the alkenes we used, the complex of the copper cation with the alkene is less intense than the complex of the copper carbene species with the alkene. This pattern is consistent for all the alkenes (Figures 47, 48, and 49).

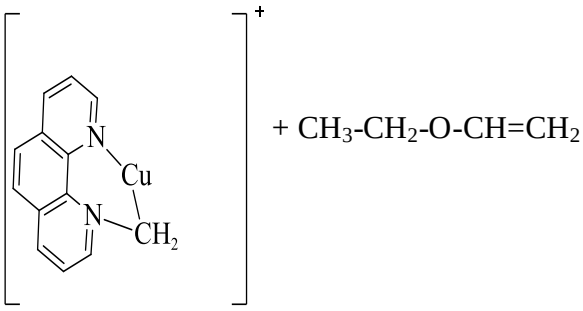

+ CH_3-CH_2-O-CH=CH_2

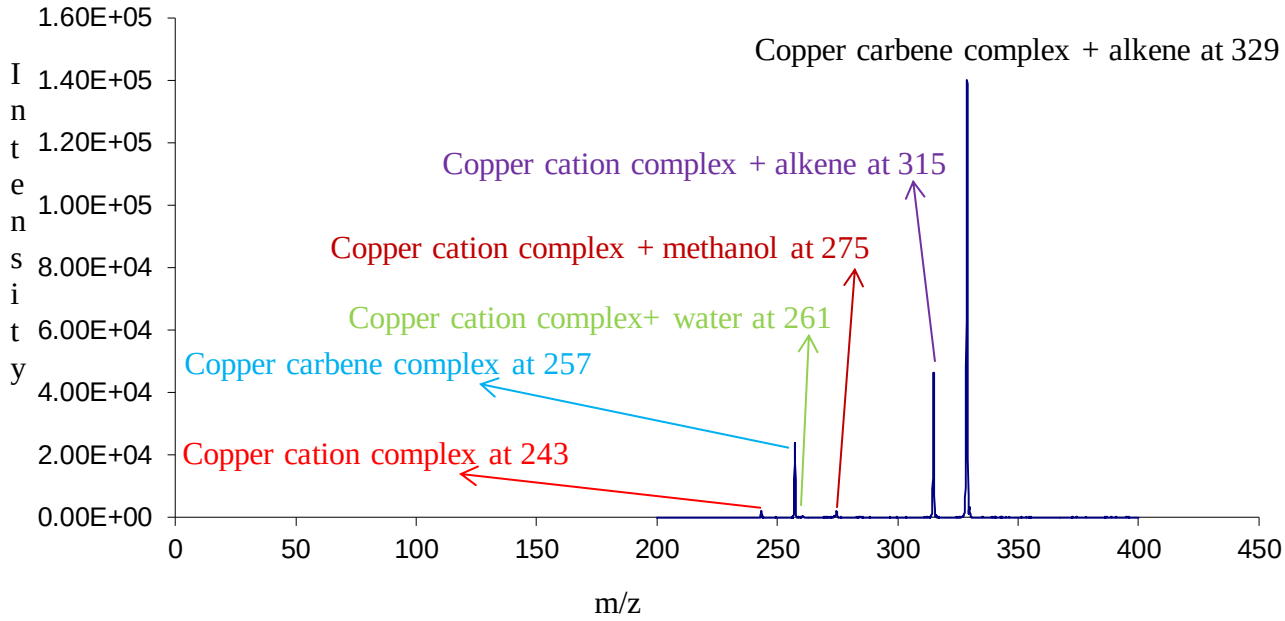

Figure 47: Copper carbene complex formed under soft conditions (insertion product) reacting with ethyl vinylether.

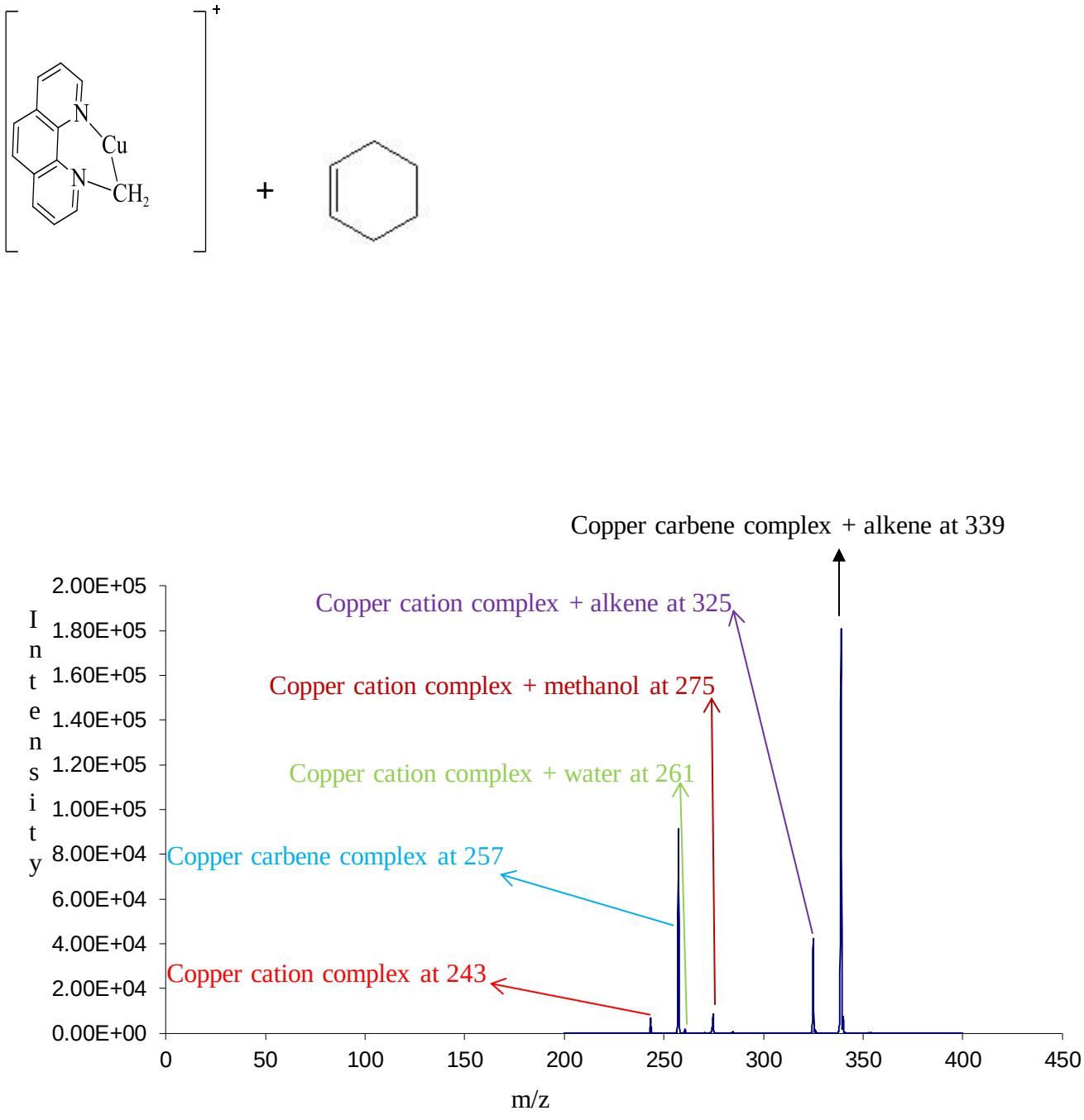

Figure 48: Copper carbene complex formed under soft conditions (insertion product) reacting with cyclohexene.

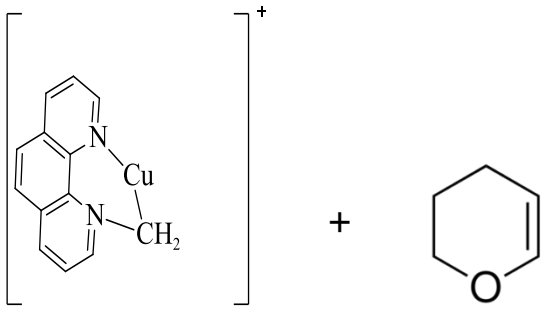

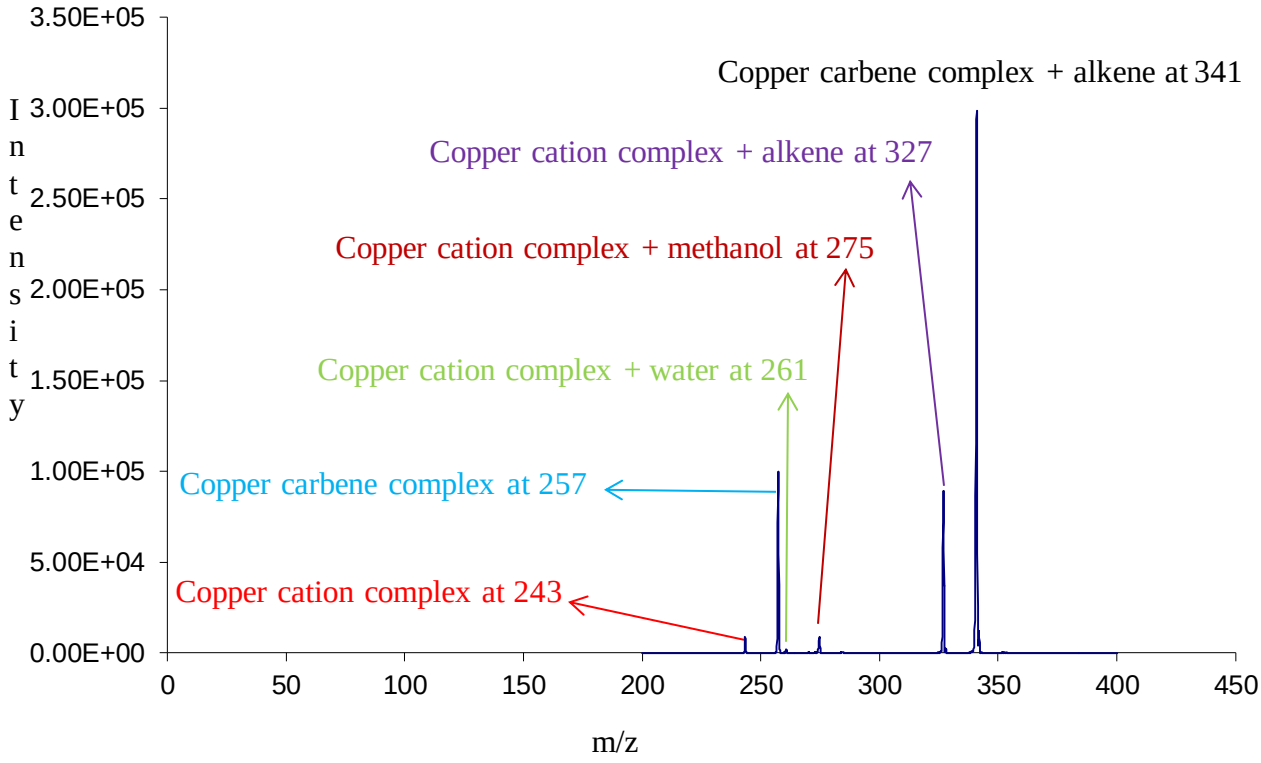

Figure 49: Copper carbene complex formed under soft conditions (insertion product) reacting with 3, 4-dihydro-2H-pyran.

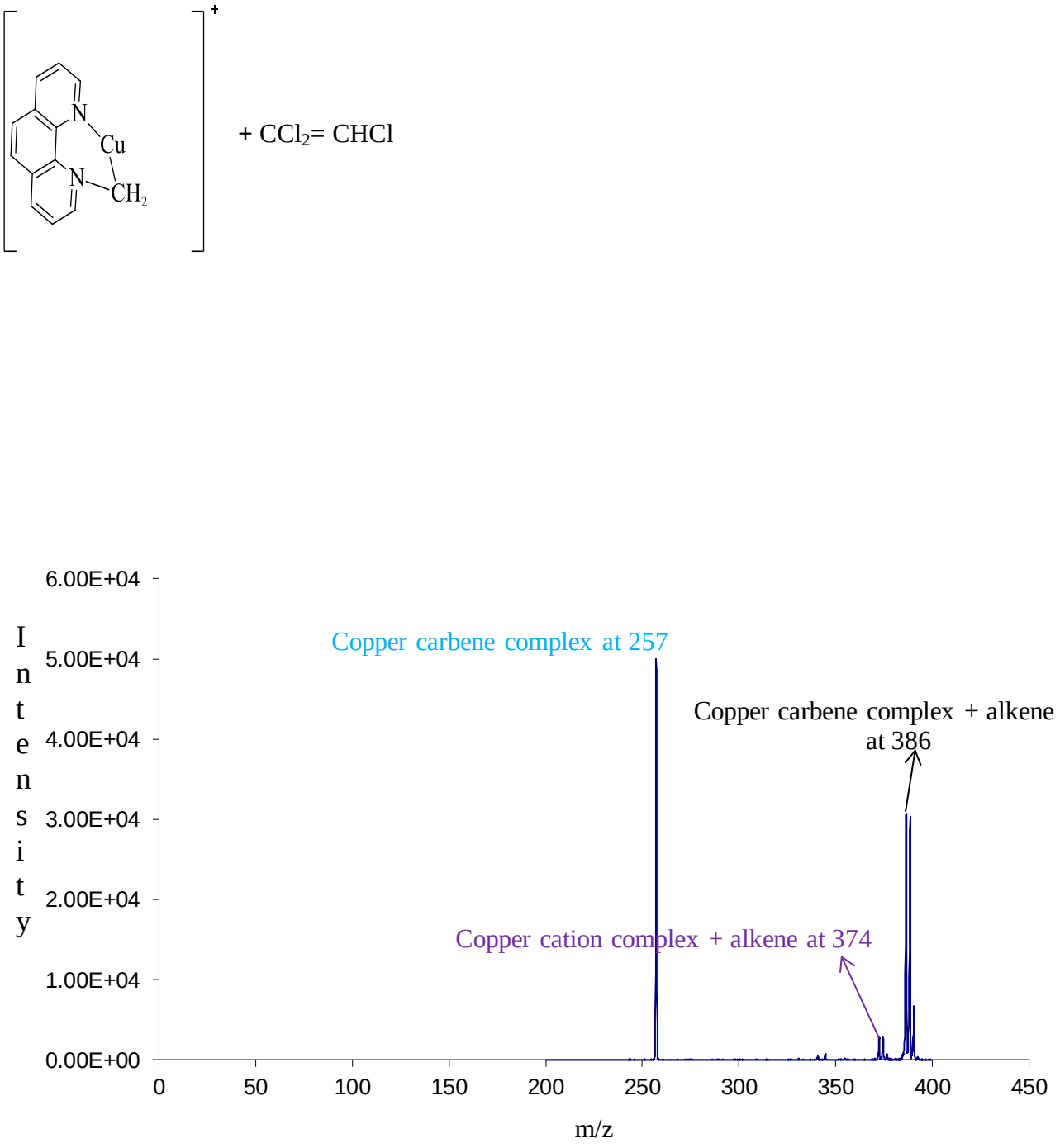

Figure 50: Copper carbene complex formed under soft conditions (insertion product) reacting with 100% trichloroethylene.

5-9-B: Hard conditions:

The $[M{=}CH_2]^+$ species formed under hard conditions with high CID energy (40%) for a short time (40 ms) was allowed to react with four alkenes (Figures 51, 52, 53 and 54). Turning to Figures 51, 52, 53 and 54, we notice that complexes of the copper cation with alkene are the major products for all the alkenes. This is the opposite pattern than we found when we used the soft conditions, where the complex with the carbene dominates. The only explanation for forming the copper cation complexes with the alkenes is that the $[M{=}CH_2]^+$ species formed under hard conditions (see Scheme 9) undergoes cyclopropanation followed by alkene addition to the released copper cation complex.

The copper carbene complex does not give copper cation with alkene complexes because it reacts to give cyclopropane. This path is not possible with the insertion product (soft conditions), so the copper carbene with alkene complex is formed with high intensity.

At soft conditions as well as at hard conditions, the formation of the copper carbene complex with alkenes peaks are related to the insertion product while the copper cation complex with alkenes peaks are related to the formal carbene product. At soft conditions the ratio between the insertion products to the formal carbene is roughly 4:1, while at hard conditions the ratio between the copper cation complexes with alkenes to the copper carbene complex with alkenes is roughly more than 9:1. In conclusion both products are formed in both conditions.

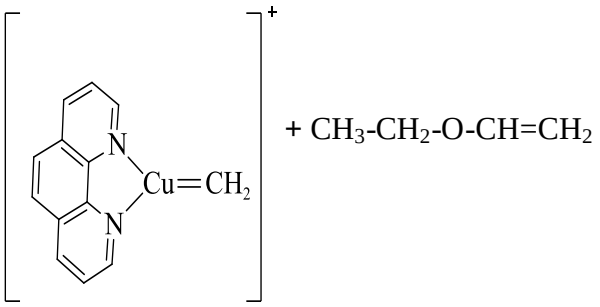

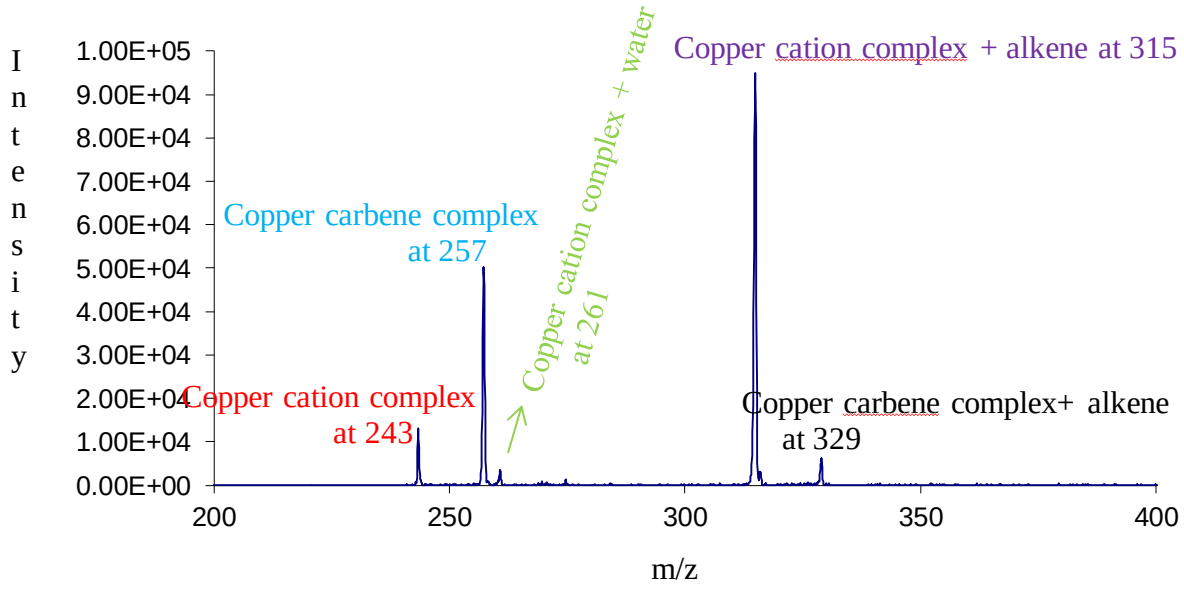

Figure 51: Copper carbene complex formed under hard conditions (formal product) reacting with ethyl vinylether.

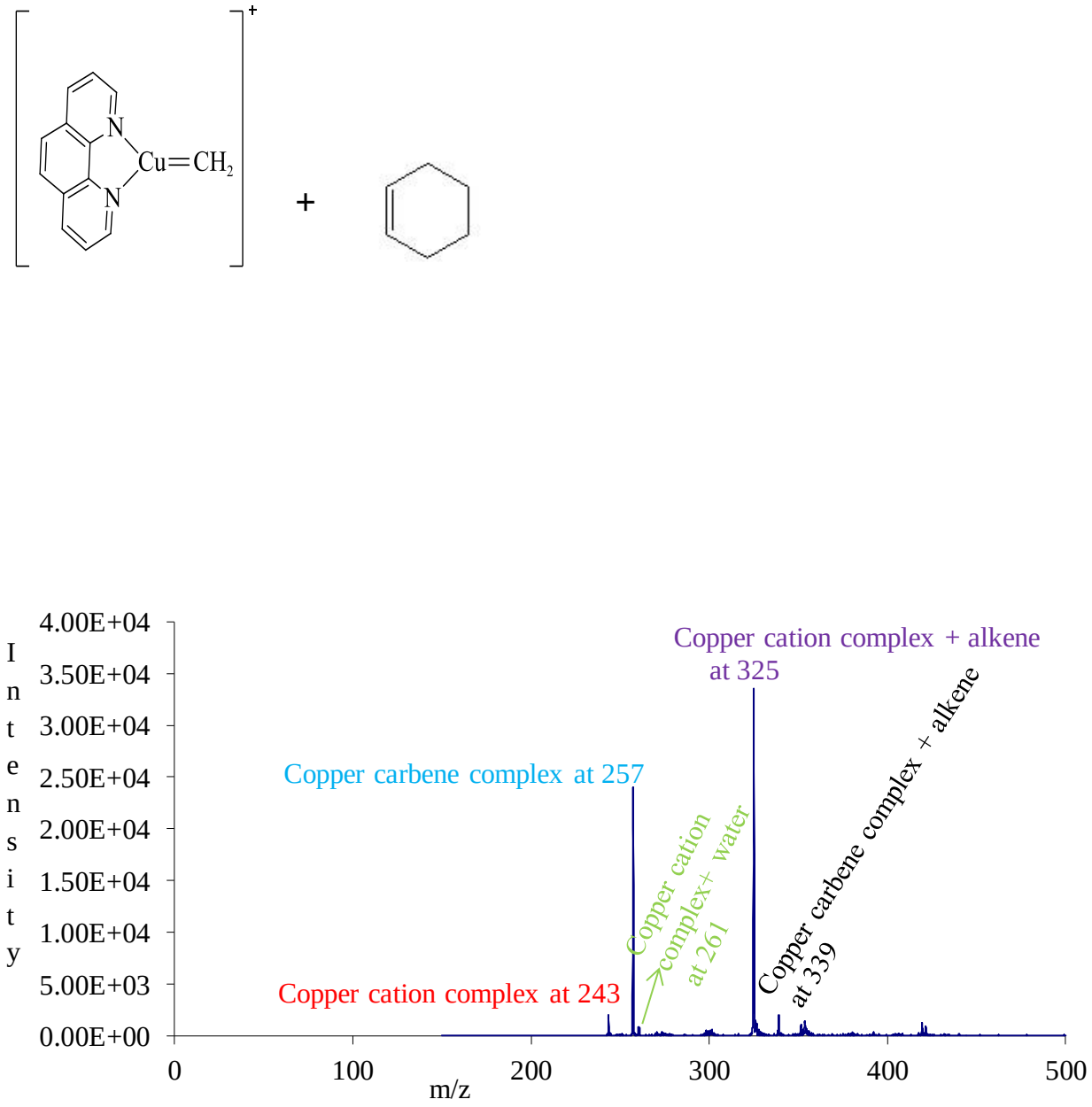

Figure 52: Copper carbene complex formed under hard conditions (formal product) reacting with cyclohexene.

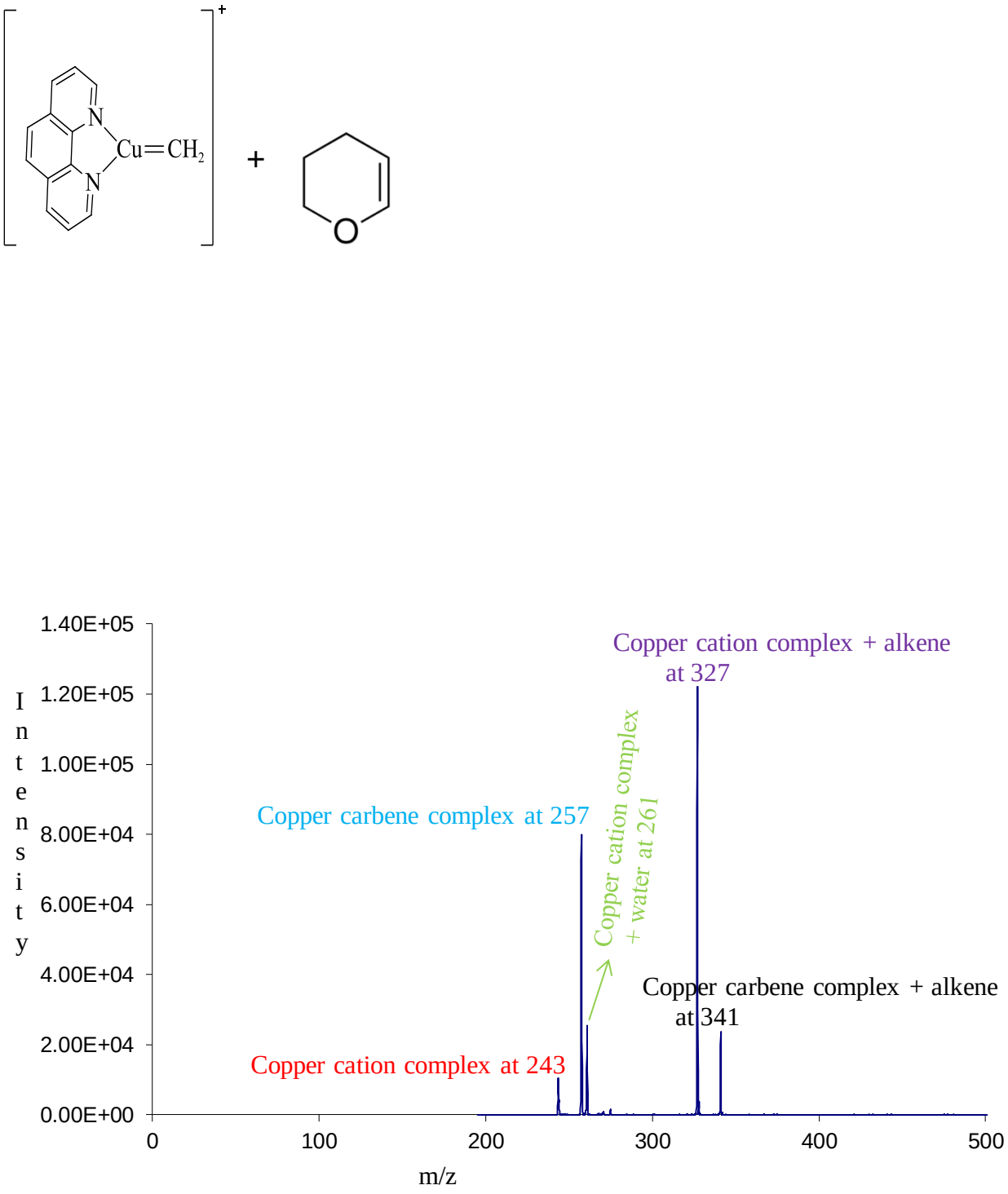

Figure 53: Copper carbene complex formed under hard conditions (formal product) reacting with 3, 4-dihydro-2H-pyran.

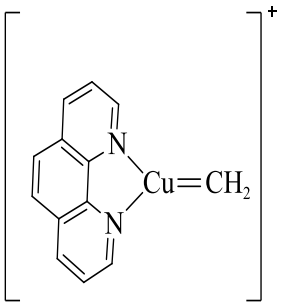

+ CCl_2= CHCl

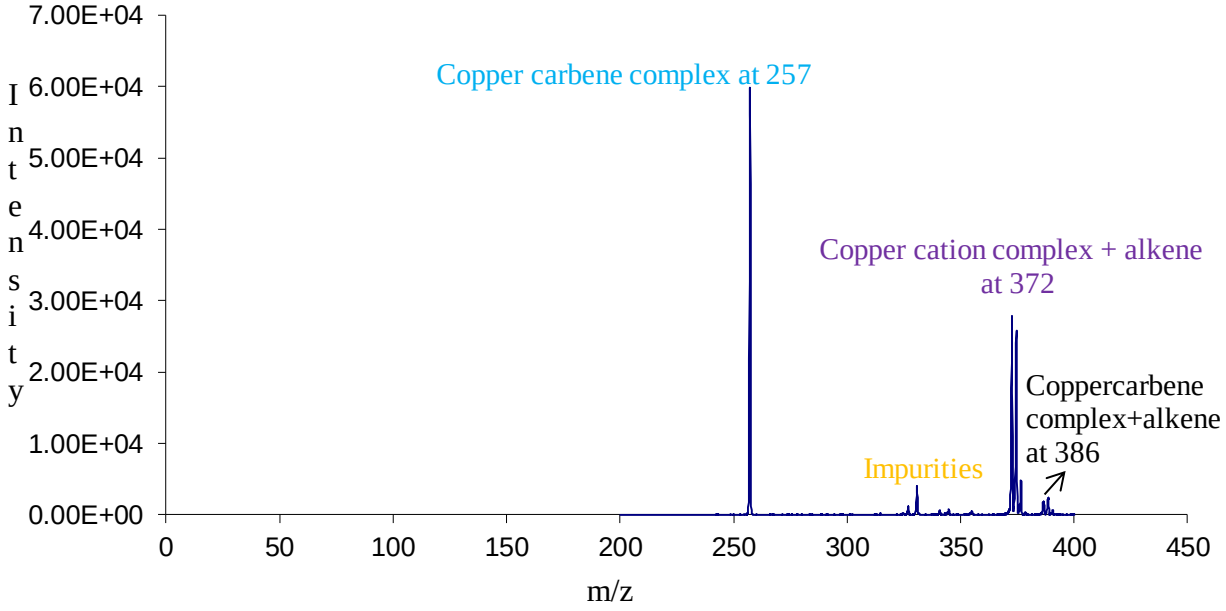

Figure 54: Copper carbene complex formed under hard conditions (formal product) reacting with trichloroethylene.

Notes: 1- Because the reaction as shown in Figure 54 is very slow, the copper carbene complex reacted with the impurities in the ion trap.

2- The peaks are not sharp due to the chlorine isotope pattern.

5-10 Rate Measurement

Because the densities of the ions are extremely small compared to the concentrations of the neutral reagents, we analyze the reactions with a pseudo first-order equation (slope = -k). We measure the absolute rates at three different reagent pressures and monitor reactions for at least three half-lives.

We determined the rate constants for the two steps shown in Scheme 9 so that we could model and understand the overall product distributions that were observed in the reactions with alkenes.

Copper cation+Alkene	Rate Constant cc/molecule/sec. ±std. dev. %
Cu-Cation+ Pyran	2.20 E -09 ± 2.3 %
Cu-Cation+ Cyclohexene	6.51 E-10 ± 3.1 %
Cu-Cation+ Ethylvinyl ether	3.91 E-10 ± 1.8 %
Cu-Cation+ Trichloroethylene	7.66 E-12 ± 2.9 %

Table 8: 1, 10-phenanthroline Cu-cation reaction with alkenes (2^{nd} step of the cycle)

Looking to the results in Table 8, the slowest reaction is between the copper cation complex and trichloroethylene due to the three chlorines, which are the electron-withdrawing group and decrease the alkene electron density. This makes it less nucleophilic to react with the copper cation. The fastest reaction is between the copper cation complex and pyran because there is added electron density (oxygen lone pair) in the pyran π-system. Cyclohexene is next due to lower electron density and nucleophilicity than the pyran. Ethyl vinyl ether comes before trichloroethylene; it is clear because of the electron-donating group in ethyl vinylether, compared to the three withdrawing-groups in trichloroethylene. Pyran and cyclohexene are more rigid and faster than ethyl vinyl ether, where rotation of the ethyl group might interfere with complexation.

Copper carbene +Alkene	Rate Constant cc/molecule/sec. ±std. dev. %
Cu-Carbene + Pyran	6.45E-10 ± 3.6 %
Cu-Carbene +Cyclohexene	3.77E-10 ± 0.5 %
Cu-Carbene +Ethylvinyl ether	9.38E-11 ± 0.7 %
Cu-Carbene + Trichloroethylene	8.49E-13 ± 3.8 %

Table 9: 1, 10-phenanthroline Cu-carbene formed under hard conditions reacting with alkenes (1st step of the cycle)

We saw the same trend in the reactivity for the copper carbene reactions with alkenes. However, all copper cations reactions with the alkenes (see Table 8) are faster than the copper carbene reactions with alkenes (see Table 9). This conclusion can explain the formation of the copper cation alkene complexes as the base peaks in the reactions of the carbenes with alkenes. The only route to form these complexes is through the fast reactions of the copper cations formed from the cyclopropanation process (see Scheme 9).

5-11 Reaction Profiles

Our results indicate when the copper cation complex is formed; it subsequently reacts with the alkene to give a copper-alkene complex or with adventitious water in the ion trap to give a copper-water complex. (This complex reacts with the alkene by a ligand swapping reaction to also give the copper-alkene complex).

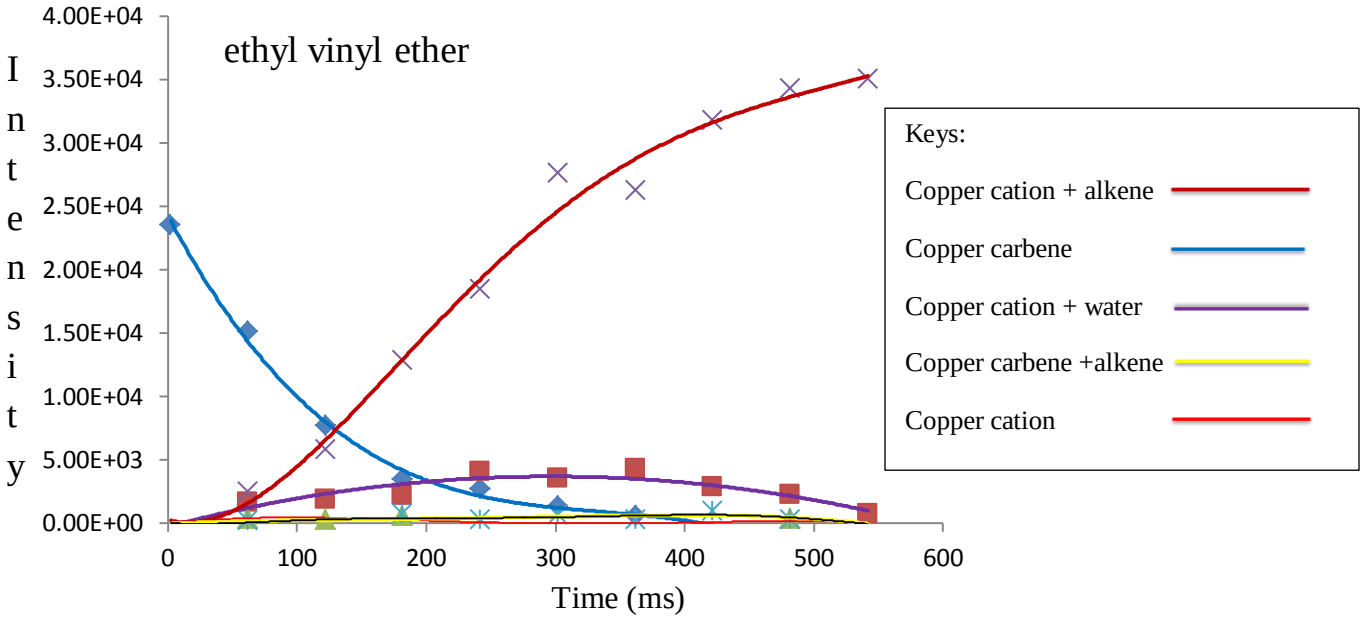

Figure 55: Reaction profile for ethyl vinylether with copper carbene.

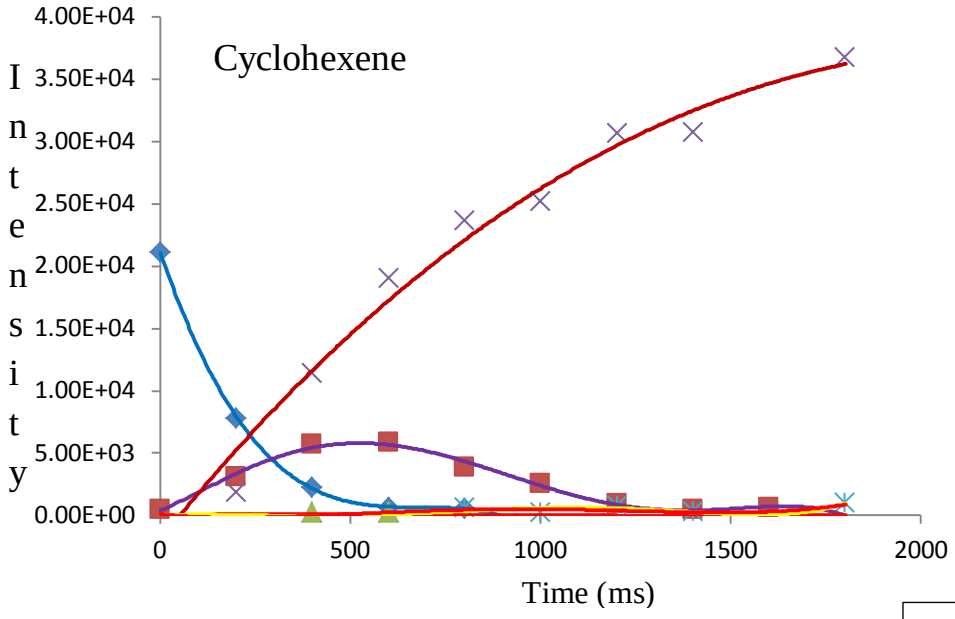

Figure 56: Reaction profile for cyclohexene with copper carbene.

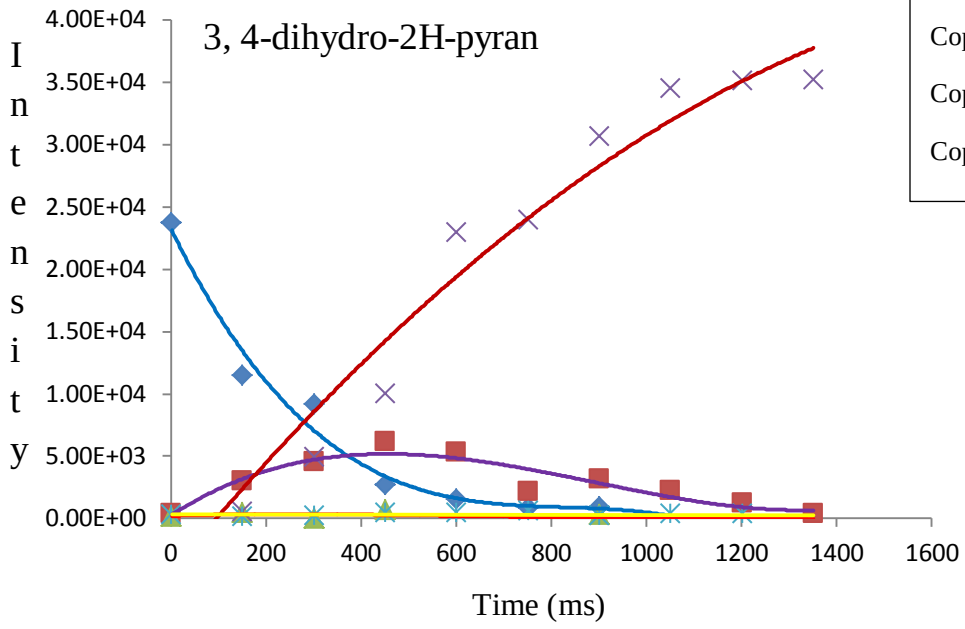

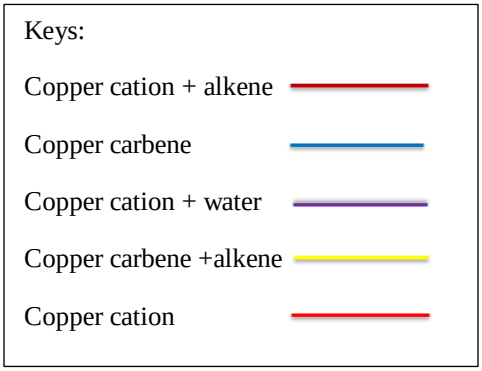

Figure 57: Reaction profile for 3, 4-dihydro-2H-pyran with copper carbene.

Looking to Figures 55, 56 and 57, we noticed the disappearance of the copper carbene complex (blue line) proportional with formation of the copper cation with alkene complex (red line). There is competition between the water (violet line) and alkene to react with the copper cation, which is re-formed according to the catalytic cycle (see Scheme 9). Alkenes will dominate (red line) due to their stranger binding to the copper. Also we noticed only a very low intensity of the copper cation complex (orange line) because the copper cation reacts rapidly with alkenes to form the copper cation with alkene complex (red line). Adduct of the alkene with the copper carbene is also found at low intensity due to the presence of the insertion product.

Chapert 6: Conclusions

The parent carbene, CH_2, is an attractive option, but diazomethane as a carbene source is a dangerous material and the exothermicity of the reaction can potentially lead to an insertion product. It is not easy to form ligated metal carbenes ($M=CR_2$) in the gas phase due to the formation of the insertion, Wolff rearrangement, and 1, 2 methyl migration products.

Allowing Mn, Fe, and Co porphyrin complexes to react with ethyl and tert-butyl diazoacetate in an ion trap mass spectrometer. The manganese porphyrin produces only adducts, but the iron and cobalt porphyrins give addition with loss of N_2 to produce insertion products. The porphyrin complexes prefer the bridging (M-N insertion) over the formal carbene. These results are supported by DFT calculation and the insertion products we formed are inactive toward the alkenes reactions.

Wolff rearrangement and insertion products are formed when we used diazoacetates as carbene precursors and a flexible ligand (bis-oxazolines). Studies by Beauchamp and Dzik support our results and confirm that these rearrangement products will not react with alkenes. We have turned to 1, 10-phenanthroline, a rigid aromatic ligand. Under ESI conditions, a copper (I) complex with 1, 10- phenanthroline can be formed. When treated with diazoacetate esters, the dominant product results from addition with loss of nitrogen followed by loss of CO. This appears to be the result of a Wolff rearrangement product of the “metal carbene” to give a metal ketene complex that spontaneously loses CO. There is no evidence of cyclopropanation when we reacting these products with alkenes.

Trimethylsilyldiazomethane was also used as a carbene precursor and reacts with the copper (I) phenanthroline complex to give addition with loss of nitrogen, but the product exhibits

no carbene reactivity with alkenes. Here computational modeling suggests that the metal carbene undergoes a 1, 2 methyl migration giving an exceptionally stable sila-alkene complex with the copper.

Chen[116] used an ylide as a carbene precursor and O'Hair[117,118] gives us many examples in his studies of multistage decarboxylations. Inspired by Chen and O'Hair, we turned to betaine $(CH_3)_3N^+CH_2COO^-$ as an ylide precursor. Betaine is safe to use and commercially available. As an alternative path to a metal carbene, we have used ESI to form a complex between the copper (I) phenanthroline and betaine (see Figure 41). Copper carbene ions were generated via a multistage mass spectrometry pathway involving controlled CID energy sequences. Under CID conditions the complex decarboxylates to give a copper ylide complex. Further CID leads to loss of trimethylamine and the formation of a complex between methylene and copper (I) phenanthroline. Depending on the CID conditions, two isobaric products are formed. One exhibits no carbene reactivity and the other readily gives carbene behavior with alkenes. The former is likely a metal-ligand insertion product $[M(CH_2)]^+$ and the latter is the true metal carbene species $[M{=}CH_2]^+$. The gas phase study with two simple controlled CID steps was a success; we formed the copper carbene species by using the multistage mass spectrometry experiments. All reaction steps and intermediates could be probed (see Figures 42 and 43) respectively.

Two CID conditions were used: (1) Hard conditions when we apply high CID enegy (40%) to fragment ylide compound at a short reaction time (40ms). The major product was the formal copper carbene $[M{=}CH_2]^+$. (2) Soft conditions when we apply low CID (20%) to fragment ylide compound at long reaction time (120ms). The major product was the insertion product $[M(CH_2)]^+$. We are explored reactions of the carbene with electron-rich alkenes such as

ethyl vinyl ether and 3, 4-dihydro-2H-pyran and electron-deficient alkenes such as trichloroethylene to see the differences in the reaction pathway with different alkenes.

Currently chemists present the carbeniods as a formal metal carbene $M=CH_2$, but this is not likely because we have shown that rearrangements occur readily. At long reaction times in the condensed phase, cyclopropanations have been observed with the copper carbenes and alkenes. Our data suggest that they would rearrange on that time frame. We suggest that the carbenes in the condensed phase coordinate with solvent to give weakly bound, but stable ylides that do not undergo insertions or other rearrangements.

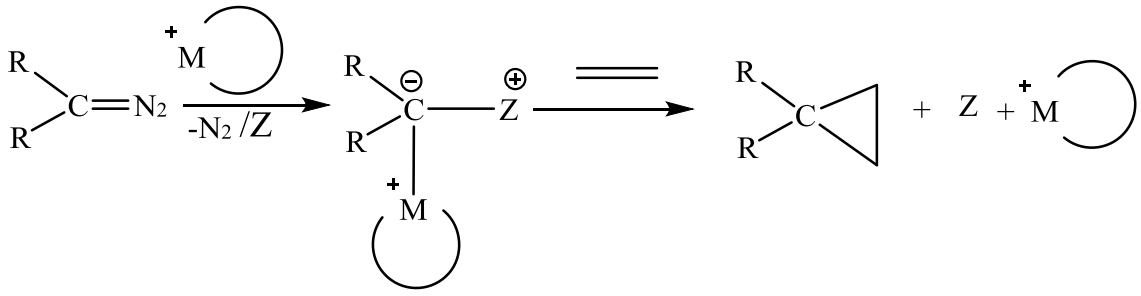

Z = Solvent

References

[1] Wong, F. M.; Wang, J.; Hengge. A. C.; Wu. W. *Org. Lett.* **2007**, *9*, 1663-1665.

[2] Fischer, E. O.; Maasböl, A.*Angew. Chem., Int. Ed* **1964**, *3*, 580-581.

[3] Fischer, E. O.; Maasböl, A. *Chem. Ber*.**1967**, *100*, 2445-2456.

[4] Mills, O. S; Redhouse, A. D. *Angew. Chem., Int. Ed.* **1965**, *4*, 1082-1082.

[5] Fischer, E. O. *Angew. Chem*., **1974**, *86*, 651-663.

[6] Dötz, K. H.; Fischer, H.; Hofmann, P.; Kreissl, F. R.; Schubert, U.; Weiss, K. *Transition Metal Carbene Complexes, VCH*: Weinheim **1983**.

[7] Schrock, R. R.; Guggenberger, L. J. *J. Am. Chem. Soc.* **1975**, *97*, 6578-6579.

[8] Geuther, A., *Eur. J. Org. Chem.***1862**, *123*, 121-122.

[9] Doering, W. v. E.; Hoffmann, A. K. *J. Am. Chem. Soc*. **1954**, *76*, 6162-6165.

[10] Fischer, E. O.; Maasbol, A. *Angew. Chem., Int. Ed. Engl*. **1964**, *3*, 580-581.

[11] Fischer, E. O.; Maasbol, A. *Angew. Chem. Int. Ed. Engl*. **1964**, *76*, 645.

[12] Fischer, E. O. ; Dötz, K. H.*Chem. Ber*.**1970**, *103*, 1273-1278.

[13] Fischer, E. O.; Dötz, K. H. *Chem. Ber*.**1972**, *105*, 1356-1367.

[14] The first cyclopropanation with a Fischer carbene complex was achieved with a group VIIIb metal: Jolly, P. W.; Pettit, R. *J. Am. Chem. Soc*.**1955**, *88*, 5044-5045.

[15] Schrock, R. R., *J. Amer. Chem. Soc*. **1975**, *97*, 6577-6578.

[16] Schrock, R. R., *Acc. Chem. Res*. **1979**, *12*, 98-104.

[17] Doyle, M.P; *Chem. Rev*. **1986**, *86*, 919-939.

[18] Perez, P.J; Diaz-Requejo, M.M. *Organometallic chem*.**2005,** *690*, 5441-5450.

[19] Dotz, K. H.; Jahr, H. C. In Carbene Chemistry.; Guy Bertrand.; Marcel Dekker, Inc. New York, **2002**; pp 241-244.

[20] Davies, H.M.L.; Beckwith, R.E.J. *Chem. Rev*.**2003**, *103*, 2861-2904.

[21] Davies, H.M.L.; Hansen, T.; Churchill, M.R. *J.Am. Chem. Soc***. 2000,** *122*, 3063-3070.

[22] Pirrung, M.C.; Morehead Jr, A. T.; *J.Am. Chem. Soc***. 1994,** *116*, 8991-9000.

[23] Davies, H.M.L.;Beckwith, R.E.J. *Chem. Rev*.**2003,** *103*,2861-2904.

[24] Davies, H.M.L.; Hansen, T.; Churchill, M.R. *J.Am. Chem. Soc***. 1997,** *119*, 9075-9076.

[25] Doyle, M.P.; Hu,W. *J.Org.Chem*.**2000,** *65*, 8839-8847.

[26] Muller, P. Tohill, S. *Tetrahedron* **2000,** *56*, 1725-1728.

[27] Pirrung, M.C.; Morehead Jr, A. T.; *JACS***. 2002,** *124*, 1014-1023.

[28] Gronert, S. *Chem, Rev.* **2001**, *101*, 329-360.

[29] Gronert, S.; Depuy,C.H.; Bierbaum,V.M. *J.Am.Chem.Soc*.**1991,** *113*,4009-4010.

[30] Canty, A. J.; Traill, P. R.; Colton, R.; Thomas, I. M., *Inorg. Chem. Acta* **1993**, *210* (1), 91-97.

[31] Vicent, C.; Viciano, M.; Mas-Marza, E.; Sanau, M.; Peris, E., *Organometallics* **2006**, *25* (15), 3713-3720.

[32] Bonchio, M.; Licini, G.; Modena, G.; Bortolini, O.;Moro, S.; Nugent, W. A., *J. Am. Chem. Soc.* **1999**, *121* (26), 6258-6268.

[33] Li, Z.; Tang, Z. H.; Hu, X. X.; Xia, C. G., *Chem. Eur. J.* **2005**, *11* (4), 1210-1216.

[34] Gilbert, B. C.; Lindsay Smith, J. R.; Mairata i Payeras, A.; Oakes, J.; Pons i Prats, R., *J. Mol. Cat. A: Chem*. **2004**, *219* (2), 265-272.

[35] Chen, H.; Tagore, R.; Olack, G.; Vrettos, J. S.; Weng, T. C.; Penner- Hahn, J.; Crabtree, R. H.; Brudvig, G. W., *Inorg. Chem*. **2007**, *46* (1), 34-43.

[36] Dyson, P. J.; Russell, K.; Welton, T., *Inorg. Chem. Commun*. **2001**, *4* (10), 571-573.

[37] Pelagatti, P. J.; Carcelli, M.; Calbiani, F.; Cassi, C.; Elviri, L.;Pelizzi, C.; Rizzotti, U.; Rogolino, D., *Organomettallics* **2005**, *24* (24), 5836-5844.

[38] Daguenet, C.; Scopelliti, R.; Dyson, P. J., *Organometallics* **2004**, *23* (21), 4859-4857.

[39] Wilson, S.R.; Wu, Y., *Organometallics* **1993**, *12* (4), 1478-1480.

[40] Raminelli, C.; Prechtl, M. H. G.; Santos, L. S.; Eberlin, M. N.; Comasseto, J. V., *Organometallics* **2004**, *23* (16), 3990-3996.

[41] Chevrin, C.; Le Bras, J.; Henin, F.; Muzart, J.; Pla-Quintana, A.; Roglans, A.; Pleixats, R., *Organometallics* **2004**, *23* (20), 4796-4799.

[42] Roglans, A.; Pla-Quintana, A., Palladium intermediates in solution. In *Reactive Intermediates: MS Investigations in Solution*, Santos, L. S., Ed. Wiley-VCH Verlag GmbH & Co. KGaA: **2010**; PP 229-275.

[43] O'Hair, R. A. J., Gas phase ligand fragmentation to unmask reactive metallic species. In *Reactive Intermediates: MS Investigations in Solution*, Santos, L. S., Ed. Wiley-VCH Verlag GmbH & Co. KGaA: **2010**; PP 199-227.

[44] McIndoe, J. S., Mass spectrometry in organometallic chemistry. In Spectroscopic Properties of Inorganic and Organometallic Compounds, Yarwood, J.; Douthwaite, R.; Duckett, S., *Eds. Royal Society of Chemistry*: **2010**; *Vol. 41*, pp288-308.

[45] Kebarle, P.; Tang, T.; *Anal. Chem*. **1993**, *65*, 972A-986A.

[46] Rohner, T. C.; Lion, N.; Girault, H. H.; *Phys. Chem*. **2004**, *6*, 3056-3068.

[47] Kebarle, P.; *J. Mass Spectrom*. **2000**, *35*, 804-817.

[48] Cole, R. B.; *J. Mass Spectrom*. **2000**, *35*, 763-772.

[49] Hayes, R. N.; Gross, M. L.; *Methods Enzymol* **1990**, *193*, 237-263 and references cited therein.

[50] Hoffmann, E. D.; Stroobant, J. C.; *Mass Spectrometry Principles and Applications*. **1996** and references cited therein. 3rd addition. John Wiley & sons. LTD NY.

[51] Reid, G. E.; O'Hair, R. A. J.; Styles, M. L.; McFadyen, W. D.; Simpson, R. J.; *Rapid Commun. Mass Spectrom*. **1998**, *12*, 1701-1708.

[52] Gronert, S.; *Chem. Rev*. **2001**, *101*, 329-360.

[53] Fisher, K. J.; *Prog. Inorg. Chem*. **2001**, *50*, 343-432.

[54] Eller, k.; Schwarz, H.; *Chem. Rev*. **1991**, *91*, 1121-1177.

[55] Damrauer, R.; *Organometallics* **2004**, *23*, 1462-1479.

[56] Plattner, D. A.; *Int. J. Mass Spectrom*. **2001**, *207*, 125-144.

[57] Plattner, D. A.;*Top. Curr. Chem*. **2003**, *225*, 153-203.

[58] Green, M. K.; Lebrilla, C.B.; *Mass Spectrom Rev*. **1997**, *16*, 53-71 and references cited therein. John Wiley & sons. LTD NY.

[59] Brodbelt, J. S.; *Mass Spectrom Rev*. **1997**, *16*, 91-110 and references cited therein. John Wiley & sons. LTD NY.

[60] O'Hair, R. A. J.; *Annu. Rep. Prog. Chem., Sect. B*, **2001**, *97*,393.

[61] Waters, T.; O'Hair, R. A. J.; *Annu. Rep. Prog. Chem., Sect. B*, **2002**, *98*,433 and references cited therein.

[62] Paul,W.; Steinwedel,H., *Zeitschrift für Naturforschung*, **1953**, *8A*.448.

[63] Paul, W.; *Angew. Chem. Int. Ed. Engl*., **1990**, *29*, 739-748.

[64] Cooks, R. G.; Glish, S.A. McLuckey; Kaiser, R.E.; *Chem. Eng. News*. **1991**, *69*, 26-39.

[65] March, R.E.; Hughes, R.J.; *Quadrupole Storage Mass Spectrometry*. Wiley, New York **1989**.

[66] Fischer, H.; Orth, H. *Die Chemie Des Pyrrols*; Akademische Verlagsgesellschaft: Leipzig, **1934**; *Vol. 1*.

[67] Fischer, H.; Orth, H. *Die Chemie Des Pyrrols*; Akademische Verlagsgesellschaft: Leipzig, **1937**; *Vol. 2A*.

[68] Fischer, H.; Stern, A. *Die Chemie Des Pyrrols*; Akademische Verlagsgesellschaft: Leipzig, **1940**; *Vol. 2B.*

[69] Rothemund, P., *J. Am. Chem. Soc.*, **1936**, *58*, 625-627.

[70] Rothemund, P., *J. Am. Chem. Soc.*, **1935**, *57*, 2010-2011.

[71] Rothemund, P.; Menotti. A. R., *J. Am. Chem. Soc.*, **1941**, *63*, 267-270.

[72] Nakazono, T.; Rene Parent, A.; Sakai, K., *Chem. Commun.***2013,** *49*, 6325-6327.

[73] Machado, G.S.; Lima, O.; Ciuffi, K.J.; Wypych, F.; Nakagaki, S., *Catal. Sci. Technol.***2013,** *3*, 1094-1101.

[74] Maraval, V.; Ancel,J.; Meunier, B.,*J.Cat.* **2002,** *206*, 349-357.

[75] Waters, T.; Wedd, A. G.; O'Hair, R. A. *J. Chem. Eur. J.* **2007**, *13*, 8818-8829.

[76] Plattner, D. A. *Int. J. Mass Spectrom.* **2001**, *207*, 125-144.

[77] Chen, P.; Chisholm, M. H.; Gallucci, J. C.; Zhang, X. Y.; Zhou, Z. P. *Inorg. Chem.* **2005**, *44*, 2588-2595.

[78]Gronert, S.; Koehn, S.; Aldajaei, J. *Org. Lett*. **2010**, *12*, 676-679.

[79] Faust, D. *Angew. Chem. Int. Ed.* **2001**, *40*, 2251-2253.

[80] Donaldson, W. A. *Tetrahedron* **2001**, *57*, 8589-8627.

[81] Reissig, H. ; Zimmer, R. *Chem. Rev*. **2003**, *103*, 1151-1196.

[82] Gnad, F. ; Reiser, O. *Chem. Rev*. **2003**, *103*, 1603-1624.

[83] Maxwell, J. L., Brown, K. C., Bartley, D. W., Kodadek, T.*Science*, **1992,** *256,* 1544-1547.

[84] Huang, L.;Chen,Y.;Gao,G.;Zhang, X.P.,*J.Org.Chem,***2003,** *68,*8179-8184.

[85] Lai,T.; Chan, F.; So, P.;Ma, D.;Wong,K.;Che,C.,*Dalton.Trans,***2006,** 4845-4851.

[86] Wang,P.;Liao,S.;Wang,S.R.;Gao,R.;Tang,Y.,*Chem.Commun.***2013,** *49,*7436-7438.

[87] Wong, F. M.; Wang, J.; Hengge, A. C.; Wu, W. *Org. Lett*. **2007**, *9*, 1663-1665.

[88] Scheidt, W. ; Reed, C. A. *Chem. Rev*. **1981**, *81*, 543-555.

[89] Hill, C. L. ; Williamson, M. *Inorg. Chem.***1985**, *24*, 2836-2841.

[90] Rovira, C. ; Kunc, K. ; Hutter, J. ; Parrinello, M. *Inorg. Chem*. **2001**, *40*, 11-17.

[91] Saunders, W.H.; Cockerill, A.F. In *Mechanisms of Elimination Reactions*.; Wiley & Sons, New York, 1973; pp 60-68.

[92] Dzik, W.I.; Xu, X.; Zhang, X.P.; Reek, J.N.H. ; De Bruin, B. *J. Am. Chem. Soc*. **2010**, *132*, 10891-10902.

[93] Johnson, A.W.; Batten, P.; Hamilton, A.; Shelton, G.; Ward,D. *J.Chem. Soc.Chem. Commun.***1974,** 550-551.

[94] Nozaki, H.; Moriuti,S.; Takaya, H.; Noyori,R. *Tetrahedron. Lett.* **1966,** 5239-5244.

[95] Nozaki, H.; Moriuti,S.; Takaya, H.; Noyori,R. *Tetrahedron.***1968,** *24,*3655-3658.

[96] Aratani, T.; Yoneyoshi, Y.; Nagase, T. *Tetrahedron. Lett.***1975,** *16,* 1707-1710.

[97] Aratani, T; Yoneyoshi, Y.; Nagase, T. *Tetrahedron. Lett.***1982,** *23,* 685-688.

[98] Fritschi, H; Leutenegger, U.; Pfaltz, A. *Angew. Chem. Int. Ed. Engl.***1986,** *25,* 1005-1006.

[99] Denmark, S.E.; Stavenger, R.A.; Faucher, A.; Edwards, j.p., *J.Org. Chem.***1997,** *62,* 3375-3389.

[100] Evans, D.A.; Kleinbeck, F.; Rueping, M. In *Asymmetric Synthesis-The Essentials*; Wiley-VCH Weinheim, Germany, **2007**; pp 72-77.

[101] Fritschi, H; Leutenegger, U.; Pfaltz, A. *Helv. Chim. Acta.* **1988,** *71,*1553-1565.

[102] Fritschi, H.; Leutenegger, U.; Siegmann, K.;Pfaltz, A.; Keller, W.; Kratky, C. *Helv. Chim. Acta.* **1988,** *71,* 1541-1552.

[103] Lowenthal, R.E.; Abiko, A.; Masamune, S. *Tetrahedron Lett.***1990,** *31,*6005-6008.

[104] Lowenthal, R.E.; Masamune, S. *Tetrahedron Lett.***1991,** *32,*7373-7376.

[105] Evans, D.A.; Woerpel, K.A.;Hinman,M.M.; Faul, M.M. *J. Am. Chem. Soc.***1991,** *113,*726-728.

[106] Evans, D. A. ; Miller, S. J. ; Lectka, T. ; Matt.P. *J. Am. Chem. Soc.* **1999**, *121,* 7559-7573.

[107] Evans, D. A; Woerpel, K. A.; Scott, M. S. *Angew. Chem. Int. Engl.* **1992**, *31,* 430-432.

[108]Kanemasa, S. ; Hamura, S. ; Harada, E. ; Yamamoto. H. *Tetrahedron Lett*. **1994**, *35,* 7985-7988.

[109] Gronert, S.; Aldajaei, J.T. *Int.J.Mass.Spect.***2012,** *316,* 68-75.

[110] Beauchamp, J. L.; Julian, R.R.; May, J. A.; Stoltz, B. M. *J. Am. Chem. Soc*. **2003**, *125*, 4478-4486.

[111] Lebel, H.; Davi, M.; Díez-Gonzlez, S.; Nolan,S. P. *J. Org. Chem*. **2007**, *72*, 144-149.

[112] Pfaltz, A. *Acc. Chem. Res*, **1993**, *26*, 339-345.

[113] Evans, D. A.; Miller,S. J.; Lectka,T.; von Matt, P. *J. Am. Chem. Soc*. **1999**, *121*, 7559-7573.

[114] Doyle, M.P. *Chem. Rev*. **1986**, *86*, 919-939.

[115] Sammes,P.G.; Yahioglu, G.*Chem.Soc.Rev*.**1993,** *23*, 327-334.

[116] Fedorov, A.; Batiste, L.; Bach, A.; Birney, D.M.; Chen, P. *J.Am.Chem.Soc*.**2011**, *133*,12162-12171.

[117] James,P.F.; O'Hair, R. A. J. *Org. Lett.* **2004,** *6*, 2761-2764.

[118] Rijs, N.J.; O'Hair, R. A. J. *Organometallics* **2012,** *31*,8012-8023.